Variability and trends in rainy season characteristics of the Eastern Cape

Precious Mahlalela

Thesis presented for the degree

of Doctor of Philosophy

Department of Oceanography

Faculty of science

University of Cape Town

September 2022

I dedicate this work to my parents (Bagezile Claudia Mahlalela and Phineas Lomabinda Mahlalela), sisters (Vumile and Phetsile), nephews and niece (Melokuhle, Okuhle and Wenzokuhle). In memory of my aunt (Lomasontfo Mabuza).

This work has been supervised by:

Primary Supervisor

Prof. Chris Reason

Department of Oceanography

University of Cape Town Cape Town

South Africa

Co-supervisor

Dr Ross Blamey

Department of Oceanography

University of Cape Town Cape Town

South Africa

Plagiarism declaration

I understand what plagiarism is and declare that, with the exception of work properly acknowledged, all of the work in the thesis is my own. This thesis contains less than 80,000 words, including references and footnotes, and less than 150 figures, including appendices.

Signature: Signed by candidate Date: September 2022

Abstract

Forming part of south-eastern South Africa, the Eastern Cape province has been prone to extreme weather events such as floods and droughts. The region also displays considerable interannual rainfall variability with a tendency towards prolonged dry periods in recent decades. There is generally a poor understanding of the factors contributing to this rainfall variability. This is concerning considering the recent prolonged (2015 – 2020) drought, that has had major socio-economic effects particularly on the large impoverished rural population as well as on some urban areas where supplied water services have broken down in several cases. Even with some rainfall relief in the province during 2022, water shortages persist, particularly in the largest metropolitan area of Nelson Mandela Bay.

The region is influenced by both midlatitude and tropical systems leading to a complex regional meteorology that hitherto has not been much studied compared to other parts of South Africa. Here, variability and trends in rainfall characteristics for the Eastern Cape are examined. Focus is placed on the spring (September–November) and summer (December– February) as these seasons contribute the largest proportion to annual totals. The spring season contributes between about 25–35% of the annual rainfall total, while the summer season contributes about 40–45%. Due to limited available station data, the Climate Hazards Infrared Precipitation with Stations (CHIRPS) data set is used. Comparisons with the available station data, provides confidence in the CHIRPS-derived results.

On interannual time scales, the results indicate that dry (wet) springs over the Eastern Cape are associated with a cyclonic (anticyclonic) anomaly southeast of South Africa as part of a shift in the zonal wavenumber 3 pattern in the midlatitudes. Over the landmass, a stronger (weaker)

Botswana High is also apparent with increased (decreased) subsidence over and near the Eastern Cape which is less (more) favourable for cloud band development and hence reduced (enhanced) rainfall during dry (wet) springs. The summer season shows significant El Niño Southern Oscillation (ENSO) and Southern Annular Mode (SAM) influences as well as from the Botswana High. Composites show that dry (wet) summers tend to be associated with a negative (positive) SAM pattern superimposed with a wave number 4 anomaly.

According to CHIRPS data, the spring season has shown a significant decreasing trend in total rainfall as well as the number of light, moderate, and heavy rainfall days over most of the province since 1981. The summer signal is less consistent, with a significant increase in rainfall in some inland areas but a decrease in rainfall near the coast which is not found to be statistically significant. The observed summer trends are attributed to an increase in light and moderate rainfall days inland and a decrease in heavy rainfall days near the coast. An examination of the regional rainfall features suggests that the observed decrease in spring rainfall may be related to an observed decrease in the number of cloud bands during the spring while, the observed increase in rainfall inland during the summer might be associated with increased ridging along the south coast.

Analysis of mid-century (2040–2060) CMIP5 rainfall projections suggests that there may be a flattening of the annual cycle over the Eastern Cape with the winter becoming wetter and parts of the summer drier. There is a large spread in CMIP5 model projections over the region with the multi-model mean projecting a very slight drying in both seasons. It is suggested that existing climate models may find representing the Eastern Cape region particularly challenging given its sharp gradients in land surface and ocean conditions and its complex meteorology.

Acknowledgements

Firstly, I would like to thank the National Research Foundation for funding my PhD studies through the South African National Antarctic Programme (SANAP). Professor Mamokgethi Phakeng for additional funding through the Vice Chancellor Scholarship and the University of Cape Town Doctoral Research Scholarship.

I would also like to express my sincere gratitude to my supervisors Prof. Chris Reason and Dr Ross Blamey for their continuous support throughout my Ph.D. research journey. Thank you for your patience, motivation, and sharing your extensive knowledge. Your advice was invaluable throughout the research and writing of this thesis. Thanks to Dr Neil Hart for providing the cloud bands dates used as part of the analysis for this research.

This journey has not been an easy one, but it has been made endurable by the many people who have contributed to my personal and research development. I thank the staff and fellow post-graduate students in the Department; I cannot mention everyone, but a special thanks goes to Cashifa for always lending a listening ear and being willing to assist. Thank you to my friends Bellinda (you've been part of every beginning and end *mfazi*), Wade (always), Mathabo, Jesse, Ramontsheng, Mhlangabezi, João, Natalie, Sika, and Victor for your support. To my pseudo family (Aunty Hilly and Uncle Sharlon) thank you for giving me home away from home, may God bless you.

Finally, I am grateful to my parents for allowing me to pursue my PhD. I know it wasn't easy and you didn't always understand what I was going through, but your unwavering support and love got me through it. To my sisters *ngiyidlalile indzima yami!!*

Contents

List of Figures

List of Tables

Chapter one: Introduction

1.1 Background

South Africa is facing severe pressure with respect to water security due to an increased water demand with increasing population, poor planning and management of water resources, limited investment into water reservoir infrastructure, and recurring droughts over the past decade. Although droughts often happen in South Africa, in recent decades there has been a tendency for more multi-year droughts to occur. For example, summer rainfall time series for various parts of South Africa, including the Eastern Cape and adjoining KwaZulu-Natal (KZN) Province show more multi-year droughts during late 1970s – 2017 than during the late 1950s – 1970 (**Fig. 5** of Blamey et al. 2018). In February 2018, the Western Cape Province was declared a disaster area after a severe drought which occurred between 2015 and 2018 (Sousa et al., 2018, Mahlalela et al., 2019, Burls et al., 2019, Pienaar and Boonzaaier, 2018). In October 2019, the Eastern Cape Province (see **Fig. 1.1** for its location in South Africa) was declared a drought disaster region following pronounce water shortages in many urban and rural areas. The Eastern Cape is of interest not just because of the recent severe drought but also because its western parts lie near the transition zone between the summer (most of southern Africa) and winter rainfall regions (southwestern South Africa, Reason et al. 2002, Blamey et al. 2018) and because it is a region of sharp vegetation, soil moisture and topographic gradients (**Fig. 1.1**). As a result, the meteorology here is complex and often involves interactions with the regional topography or the neighbouring warm Agulhas Current (e.g., Rouault et al. 2002, Singleton and Reason 2006).

In addition to drought events, the region, and indeed most of southern Africa, sometimes experiences severe flood events during the extended summer (September to February) of the year. Recent floods in April 2022 affecting the KwaZulu-Natal and Eastern Cape Provinces highlight the devastating socio-economic and environmental impacts of these extreme weather

events. The flooding in these provinces resulted in fatalities, infrastructure damage, and inundated cropland. It is estimated that the KwaZulu-Natal province will require R 1.9 billion for disaster relief interventions (Gov't of South Africa, 26 Apr 2022). This vulnerability to severe events results from southern Africa having a highly variable climate on intraseasonal, interannual, and decadal time scales (e.g. Tyson et al., 1975, Lindesay 1988, Mason 1995, Mason and Jury 1997, Todd and Washington 1998, Reason 1998, 1999, Reason and Mulenga 1999, Reason et al. 2000, 2005, Behera and Yamagata 2001, Reason and Roaualt 2002, Rouault et al. 2002, Cook et al. 2004, Usman and Reason 2004, Washington and Preston 2006, Malherbe et al. 2014, Dieppois et al. 2016). To date, however, relatively little work has been done on the climate of the Eastern Cape region compared to other parts of South Africa despite it being an important agricultural part of the country with a sizeable rural population. The region is also one of the least developed of South Africa's nine provinces with many impoverished rural settlements which are particularly vulnerable to severe weather events such as floods and droughts.

1.2 Thesis objectives and structure

The overall objective of this thesis is to determine the variability and trends in rainfall characteristics during the spring and summer rainy seasons in the Eastern Cape. This research is motivated by the increased threat to water security and susceptibility to severe weather events in the Eastern Cape and, more broadly, South Africa, in recent decades. To investigate the potential mechanisms underlying observed interannual variability as well as the projected changes in local rainfall. Understanding rainfall inputs into the rainfall catchment areas of the Eastern Cape is crucial for effective planning and management of water resources. The results chapters address the following questions after the Literature Review (**Chapter 2**) and Data and Methodology (**Chapter 3**):

❖ **Chapter 4**

- What are characteristics of rainfall variability for spring and summer rainfall?
- How do rain days of different intensity categories contribute to seasonal totals?
- What are the observed trends in seasonal rainfall and rainfall characteristics?
- Are there any statistical relationships between rainfall characteristics in the Eastern Cape and large-scale climate modes?

❖ **Chapter 5**

- What are the potential mechanisms behind observed interannual variability in the region?
- Are there any relationships between seasonal rainfall and climate modes of variability such as ENSO, SAM and the SIOD?
- Are there any observed trends in regional circulation which might influence rainfall over the Eastern Cape?

❖ **Chapter 6**

- How well can CMIP5 models represent regional rainfall?
- What are the CMIP5 model projections for future spring and summer rainfall?
- What are the projected changes in regional circulation patterns from CMIP5 models?

It should be noted that some of the results (parts of **Chapter 4** and **5**) have been published in: Mahlalela, P.T., Blamey, R.C., Hart, N.C.G. and Reason, C.J.C., 2020. Drought in the Eastern Cape region of South Africa and trends in rainfall characteristics. *Climate Dynamics*, *55*(9), pp.2743-2759.

Following the results, **Chapter 7** discusses the main findings of this work, highlights some of the limitations, and provides future directions for this research.

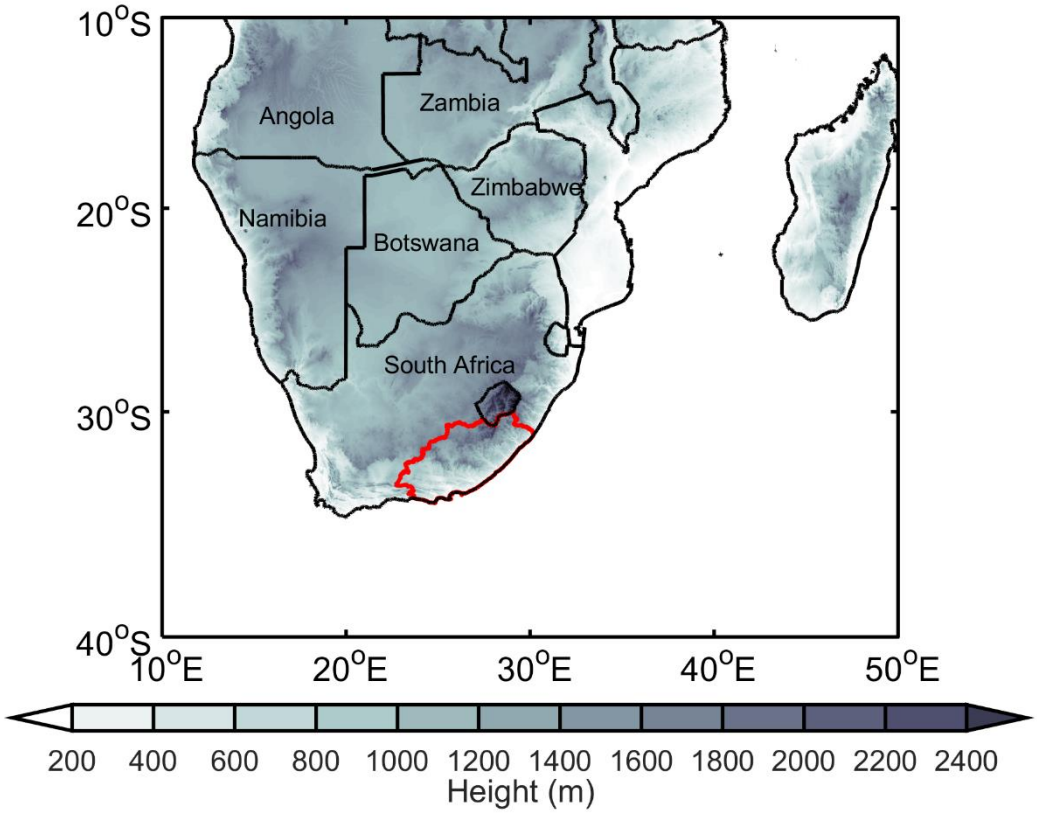

Figure 1.1: Topography map (shaded: m) highlighting topographic gradients across Southern Africa. The red polygon indicates the Eastern Cape province.

Chapter two: Literature review

This chapter presents a review of South African climate to help better understand the diverse climatic conditions in the Eastern Cape. The literature review will concentrate on the typical spatial rainfall patterns across the country, regional circulation and rain bearing systems, and the drivers of the regional climate variability.

2.1 Spatial rainfall patterns across South Africa

Rainfall and temperature patterns of South Africa are generally moderated by the surrounding oceans and topography. The country is surrounded by a strong western boundary current to the east and south (Agulhas Current) and an intense eastern boundary current upwelling system (Benguela Current) to the west leading to strong SST differences at the same latitude on either coast. Generally, eastern South Africa experiences warm and rainy austral summers (December-February; DJF) and cool and dry winters (June-August; JJA). Although DJF is the main rainy season over most of southern Africa, substantial rains can occur in the preceding two or three months with onset of the rainy season typically sometime in October-November; (ON). This corresponds with a southward shift in the Inter-Tropical Convergence Zone (ITCZ), a weakening of the winter high over the subcontinent, and early summer rainfall over tropical and, to a lesser extent, subtropical southern Africa (Reason, 2017). There are variations in timing in which different parts of subtropical southern Africa experience maximum summer rainfall. For instance, the southern interior and western interior has maximum rainfall in March; and the central interior, KwaZulu-Natal and north-eastern interior receives a maximum rainfall in January (Rouault and Richard, 2003).

The southwestern tip of South Africa experiences a Mediterranean climate characterised by rainy winters (June-August; JJA) (Reason et al., 2002, Reason and Rouault, 2005, Philippon et

al., 2012, Pohl et al., 2014, Mahlalela et al., 2019) and dry summers. North of this region, the west coast quickly becomes semi-arid and merges into the southern margins of the hyper-arid Namib Desert near the South African / Namibian border. On the south coast rainfall, can occur throughout the year (Weldon and Reason, 2014, Engelbrecht et al., 2015a, Engelbrecht and Landman, 2016) due to ridging anticyclones and topographic uplift of moist marine air by the coastal mountains (Engelbrecht et al., 2015a, Weldon and Reason, 2014, Reason, 2017). The contrast in rainfall between the summer and winter rainfall regions is also notable in the different time scales of variability and potential factors contributing to rainfall variability. As a result, each rainfall region should be considered separately when considering weather events, as different systems contribute to rain formation and its variability. This south coast region forms a transition zone between the summer and winter rainfall regions, making the meteorology more complicated.

2.2 Regional circulation

The main circulation features that control the climate of South Africa are semi-permanent anticyclonic circulation over the subtropical South Atlantic and South Indian Oceans (see **Fig. 2.1**), the tropical convergence zones, including the Inter-Tropical Convergence Zone and the South Indian Ocean convergence zone, and far to the south, the Circumpolar Trough (Midgley et al., 2005, Reason et al., 2006). The South Atlantic High Pressure (SAHP) and South Indian High Pressure (SIHP) shifts 5 – 6° meridionally between summer and winter with the later also shifting about 13° zonally between the two seasons (Tyson and Preston-Whyte, 2000). Subsidence over the subcontinent occurs during the winter due to the equatorward shift in both anticyclones; additionally, during this season the SIHP is centred westward around 60° E, and a winter anticyclone becomes established over the interior with increased subsidence there. These conditions are unfavourable for rain-bearing weather over the interior and eastern coast

of South Africa (Reason, 2017). However, the SAHP's northwestward shift away from western South Africa allows for midlatitude frontal systems to track towards the southwestern parts of South Africa. Although these seasonal changes are well established, it should be noted that recent decades have seen a southward shift in the anticyclones associated with a positive tendency in the Southern Annular Mode (SAM) (Sousa et al., 2018, Mahlalela et al., 2019). These changes in the position of the anticyclones have implications for winter rainfall systems reaching the southwestern Cape. In contrast, more poleward-located anticyclones ridging south of South Africa have been identified as promoting moisture transport into the south coast, thereby increasing rainfall over this region during the summer (Weldon and Reason, 2014, Engelbrecht and Landman, 2016, Engelbrecht et al., 2015a). The anticyclones are located 5 or 6° poleward of the mean winter location in the summer. This increases ridging and rainfall over the south coast (Taljaard, 1996, Favre et al., 2012, Weldon and Reason, 2014, Engelbrecht and Landman, 2016, Engelbrecht et al., 2015a). The subcontinent's position relative to the SAHP and low-pressure systems of the circumpolar trough also contribute to rainfall seasonality over South Africa's west and, to a lesser extent, south coast (Midgley et al., 2005). During the winter season, the westerly wind belt shifts equatorward, and the associated circumpolar trough in the Southern Ocean shifts northward, bringing rain to the country's southwestern tip. However, during the summer, the westerlies retreat poleward as the SAHP shifts south-eastward. This shift in the position of these circulation systems causes dry conditions in the southwestern and interior of South Africa during the summer (December to February).

The southward shift in anticyclones occurs as the ITCZ moves across the equator and over the South Indian Ocean in early summer. The ITCZ migrates from about 20°N in the spring to 15 – 20°S over the western South Indian Ocean in the summer, with its southernmost position in February over central Madagascar and northern Mozambique. While there is a strong

meridional shift in the ITCZ over the western Indian Ocean, this is not the case over the Atlantic with the ITCZ never moving south of the equator. The ITCZ migrates north between March and April, with the northward shift being slower than the southward shift in austral spring (Nicholson and Grist, 2003, Suzuki, 2011, Reason, 2017). During the austral summer, the ITCZ in the Atlantic sector is found over West Africa slightly inland of the Gulf of Guinea coast (Reason et al., 2006).

Other important convergence zones during summer are the South Indian Ocean convergence zone (SICZ) extending southeastwards from southern Mozambique into the South West Indian Ocean (Cook, 2000) and a convergence zone stretching northeastwards from the Angola low (AL) to the eastern Congo Basin (Howard et al., 2019). The Angola low is a lower to mid-troposphere cyclonic feature that develops over southeastern Angola and northeastern Namibia (**Fig. 2.1**) (Mulenga, 1999, Mulenga et al., 2003, Reason et al., 2006, Crétat et al., 2019) which forms as a heat low in early summer before evolving into a tropical low in mid-summer (Munday and Washington, 2017). The contrast between strong surface heating over the AL region and the cooler adjacent ocean leads to moisture inflow from the tropical South East Atlantic where it converges with moisture emanating from the western Indian Ocean. The latter is generally the most important low level moisture source over subtropical southern Africa (d'Abreton and Lindesay, 1993, Reason et al., 2006, Rapolaki et al., 2021, Rapolaki et al., 2019). As a result, the Angola Low is significant for the development of tropical extratropical cloud bands (Harrison, 1984, Hart et al., 2010, Hart et al., 2013), the major synoptic summer rainfall-producing system over subtropical southern Africa. Variability in the strength of the AL determines the moisture available for cloud bands. This suggests that when the Angola Low is stronger (weaker), more (less) low level moisture is available in the source region of cloud bands (Reason et al., 2006, Ndarana et al., 2021) leading to wetter (drier) summers in

central and eastern South Africa (Cook et al., 2004). Another important near-surface low is also visible over the Mozambique Channel, most likely as a result of the adjustment of the easterly low-level winds due to Madagascar's topography (Barimalala et al., 2018), termed the Mozambique Channel Trough. Barimalala et al. (2018) showed evidence that a weaker (stronger) Mozambique Channel Trough leads to increased (reduced) moisture advection into southern Africa and enhanced (reduced) precipitation over the southern African interior.

The Botswana High (BH) is another important regional circulation system in the mid-level troposphere during the spring, summer, and early autumn. It forms in August, strengthens, and moves southward over southern Africa during the spring and summer, reaching a peak in February. The system is part of the circulation response to heat released by high precipitation areas, such as the Congo Basin and the Amazon (Reason, 2016). Its impact on rainfall in southern Africa has been highlighted by Driver and Reason (2017), and for Zimbabwe by Matarira (1990). A composite analysis of 500 hPa geopotential height for anomalously wet (dry) summers in Zimbabwe were found to be associated with a negative (positive) height anomaly over the southern parts of the subcontinent suggesting influence of the Botswana High (Matarira, 1990). During El Niño (La Niña) events, the high is typically stronger (weaker), but there are also a number of neutral El Niño Southern Oscillation (ENSO) summers with large anomalies in the Botswana High (Driver and Reason, 2017). In general, a stronger BH is associated with more subsidence and suppresses convection and cloud band formation while summers with a weaker or displaced Botswana High are more favourable for convective rainfall development (Reason, 2016, Driver and Reason, 2017).

2.3 Rainfall Systems

Summer rainfall is mostly dependent on convective processes, resulting in thunderstorms being a predominant feature owing to the strong influence of diurnal heating and atmospheric instability (Tyson and Preston-Whyte, 2000). Such thunderstorms can occur as random air mass storms or as organised convection in particular weather systems such as tropical-extratropical cloud bands (also known as Tropical Temperate Troughs -TTTs) or mesoscale convective complexes (MCC). The former are the major rain-bearing synoptic system over southern Africa during the summer (Tyson and Preston-Whyte, 2000, Hart et al., 2010, Harrison, 1984) and are characterized by the presence of convection, rainfall, and diagonal cloud bands in the north-west – south-east direction (see **Fig 2.1**) that links upper tropospheric frontal system of the mid-latitude westerly circulation with tropical disturbances over the subcontinent (Harrison, 1984, Todd and Washington, 1998, Reason et al., 2006, Hart et al., 2010, Crétat et al., 2012). They are known to produce heavy rainfall events (Tyson and Preston-Whyte, 2000, Hart et al., 2010).

In the northern parts of South Africa, tropical cyclones (denoted as TC in **Fig. 2.1**) can make important contributions to rainfall in a few summers (Dyson and Van Heerden, 2002, Reason and Keibel, 2004, Malherbe et al., 2013, Rapolaki et al., 2019). On average, between six and twelve tropical cyclones are recorded in the South Indian Ocean between November and April (Mavume et al., 2009, Malherbe et al., 2013, Rapolaki and Reason, 2018). Although some tropical cyclones form in the Mozambique Channel, few of them make landfall; instead, they more usually track south through the channel (Reason, 2007). Approximately 5% of those generated in the southwest Indian Ocean make landfall on the southern African mainland (Reason and Keibel, 2004, Nash et al., 2015). Over northeastern South Africa, tropical cyclones

contribute up to 10% of January-February rainfall on average with the contribution increasing to 30 – 40% over central and northern coastal Mozambique (Mawren et al., 2022).

During particularly the late summer, tropical lows are also important for rainfall in southern Africa. Taljaard (1953) was the first to describe tropical lows over southern Africa, noting that these lows are quasi-stationary in the Angola region and are associated with low-level convergence. In seasonal and climatological terms, these systems, along with dry and shallow heat lows, combine to form the Angola Low (Munday and Washington, 2017, Howard and Washington, 2018, Howard et al., 2019, Rapolaki et al., 2019). They have a significant impact on local rainfall during December to February (Howard et al., 2019, Rapolaki et al., 2019). Rapolaki et al. (2019) showed that tropical low-pressure systems were responsible for 48% of summer extreme rainfall events over the Limpopo River Basin.

The mesoscale convective complex (MCC) is another important convective system during the summer season. They are large, long-lived convective cloud systems with a quasi-circular cloud shield (Blamey and Reason, 2012). MCCs are the largest of the mesoscale convective systems (MCSs; **Fig. 2.1**), which are defined by an organized group of thunderstorms acting as coherent systems, which include mesoscale convective complexes (MCCs) and squall lines (Blamey and Reason, 2012). Blamey and Reason (2012) found that MCCs contribute up to 20% of summer rainfall between November and March in southeastern Africa, but less than 6% in the western interior. During the summer, a single MCC event can produce roughly one-third of the monthly total rainfall on the southern parts of southern Africa. Morake et al. (2021) found that MCSs over eastern South Africa mainly occur between November and March with a peak in December with most systems occurring along the eastern escarpment and northern Agulhas Current. A relative hot spot in MCS occurrence was in southern KZN / eastern Lesotho

but due to the 30°S limit of the Huang et al. (2018) source data, systems slightly further south over the Eastern Cape could not be assessed. Based on Morake et al. (2021), it seems however likely that the northern Eastern Cape province could also often experience MCSs in summer.

Over southern South Africa, Cut-Off Lows (COLs; illustrated in **Fig 2.1**) have been found to be responsible for almost all the severe flooding events experienced in this region, including the Eastern Cape (Tyson and Preston-Whyte, 2000, Singleton and Reason, 2006). These systems are most common during the austral spring and autumn (Taljaard, 1985, Singleton and Reason, 2007a, Molekwa et al., 2014). Cut-Off Lows are middle/upper tropospheric features produced when pre-existing cold troughs extending equatorward are cut off from their high-latitude source region, leaving a closed cyclonic vortex. When a COL is confined in the middle and upper troposphere (cold pool) it causes strong instability and hence thunderstorms, strong winds and heavy precipitation may occur. Cut-Off Lows can also be produced from deep lows extending towards the lower troposphere where there may be a meso-low with an onshore low level jet across the Agulhas Current which can produce strong winds and heavy rainfall on the windward side of the coastal mountains (Singleton and Reason, 2006, Singleton and Reason, 2007b, Favre et al., 2012). Cut-Off Lows are quasi-stationary in nature which could lead to two to three days of heavy rainfall over the same region, increasing chances of flooding. Favre et al. (2012) suggest that they contribute between 25 – 35% of the annual rainfall accumulation over the transition zone between the summer and winter rainfall domains making them a vital part of the climate of the region. Furthermore, Favre et al. (2012) presents evidence of a 25% increase in the frequency of COLs rainy days over the last three decades (1979 – 2006). While the spring-summer seasons are characterised by strong temperature/pressure meridional gradients between the tropics and the midlatitudes which may favour COL development, on longer time scales, variability in COL frequency over South Africa has been linked to ENSO

and the semiannual oscillation (Singleton and Reason, 2007a). Molekwa et al. (2014) suggested that the contribution of COLs to annual rainfall totals over Eastern Cape is smaller over the northeastern and southwestern parts compared to the transition zone along the south coast which includes the western areas of the Eastern Cape. Furthermore, these authors noted that over the Eastern Cape, COL frequency has a winter maximum with associated heavy rainfall. In contrast, the summer season records a minimum frequency in COLs here (Molekwa et al., 2014).

The occurrence of COLs is often associated with a banana-shaped ridging anticyclone south of the south coast of South Africa. More generally, anticyclones ridging along the south coast often leads to rainfall over the south of the country (Weldon and Reason, 2014, Engelbrecht and Landman, 2016, Engelbrecht et al., 2015a). Ridging highs promote moisture transport from the southwest Indian Ocean (SWIO) into South Africa (Engelbrecht et al., 2015a, Ndarana et al., 2021). Wet spells have been associated with increased moisture flux from the SWIO together with positive low-level geopotential height anomalies over the eastern part of the country (Cook et al., 2004, Ndarana et al., 2021). The exact location and intensity of ridging high pressure systems determines where rainfall occurs (Taljaard, 1996, Engelbrecht et al., 2015a, Ndarana et al., 2021). Ridging located further southward are more conducive to rainfall along the south coast than ridges located more equatorward even if the pressure distribution is otherwise similar. Ridging highs along the south coast have been identified as contributing to a spring rainfall peak (Jury, 1993, Levey and Jury, 1996, Jury et al., 1996, Engelbrecht et al., 2015a) there. Increased rainfall occurs on the windward sides of the mountains due to orographic uplift of moist, unstable air.

Cold fronts, associated with extratropical cyclones typically tracking well south of South Africa, are particularly important for winter rainfall in western South Africa. Such fronts can

also contribute to occasional winter rain along the south and east coasts and sometimes to summer rainfall in these regions. However, in the summer half of the year, their most important role is providing the midlatitude input into the cloud bands discussed earlier. The location and orientation of baroclinic zones in the mid- and high latitude troposphere, as well as Sea Surface Temperature (SST) gradients (Trenberth, 1998) determine the distribution of extratropical cyclones in the Southern Hemisphere. The climatology of extratropical cyclones over the Southern Hemisphere derived by Jones and Simmonds (1993) highlights the southwest (SW) Atlantic as a key area for cyclogenesis (Reason et al., 2002). This region shows strong SST gradients associated with the confluence between the warm poleward flowing Brazil Current and the cold equatorward flowing Malvinas Current. Anomalous warm (cold) SSTs in this region might favour an increase (decrease) in cyclogenesis which can then impact downstream on the South Western Cape region if other factors are favourable (Reason et al., 2002, Reason and Jagadheesha, 2005). In the central South Atlantic cool (warm) SST anomalies reduce (enhance) the tropical-midlatitude meridional gradient, thereby weakening (strengthening) weather systems moving towards western South Africa (Reason et al., 2002). Further east, warm (cool) SST anomalies near the coastal areas of Western Cape are favourable (unfavourable) for local storm intensification leading to increased (decreased) rainfall (Reason et al., 2002).

2.4 Climate variability

Rainfall variability in South Africa is known to be influenced by various climate modes as well as anomalies in regional circulation systems and SST in the neighbouring oceans. The ENSO phenomenon accounts for approximately thirty percent of rainfall variability over eastern South Africa, with El Niño events typically associated with drought over the summer rainfall region

and La Niña associated with wet conditions (Tyson and Preston-Whyte, 2000, Blamey et al., 2018, Gosling, 2011). However, the relationship between ENSO and precipitation over southern Africa has long been known to be nonlinear (Reason et al., 2002, Mulenga et al., 2003, Reason and Jagadheesha, 2005, Meque and Abiodun, 2015). El Niño droughts essentially occur due to modulations in the Walker circulation which modulates regional circulation patterns over southern Africa as well as SST in the neighbouring tropical Indian and Atlantic oceans (Lindesay, 1988, Reason et al., 2000, Mulenga et al., 2003, Lindesay et al., 1986). During El Niño summers, the South Indian Convergence Zone (SICZ) is weakened displaced (Cook, 2000) and cloud bands tend to form more offshore than over the land (Fauchereau et al., 2009, Hart et al., 2018). Subsidence increases over the land, often associated with a stronger mid-level Botswana High (Driver and Reason, 2017, Blamey et al., 2018), which suppresses convection and cloud band development.

By contrast, ENSO does not have the same influence over the winter rainfall region. At this time of year, ENSO SST anomalies are far weaker in the equatorial Pacific than they are during the mature phase (austral summer). Thus, teleconnections to South Africa such as through the Pacific South America pattern (Kiladis and Mo, 1998, Colberg et al., 2004) are not yet as well developed as later in the ENSO episode. Some studies have suggested that El Niño events might be associated with positive anomalies in winter (May-July) rainfall due to a northward shift of storm tracks over the mid-latitude South Atlantic (Philippon et al., 2012).

While ENSO is the dominant climate mode globally on interannual time scales, over the extra-tropical Southern Hemisphere, the Southern Annular Mode (SAM) is the leading mode (Hartmann and Lo, 1998, Thompson and Wallace, 2000). SAM involves a large-scale oscillation of atmospheric mass between the mid- and high latitudes and hence affects large

scale wind, temperature and rainfall patterns over many parts of the Southern Hemisphere. The SAM is barotropic in nature, revealed as being the leading empirical orthogonal function (EOF) in many atmospheric fields, including surface pressure, geopotential height, surface temperature, and zonal wind over the Southern Hemisphere south of about 20°S (Marshall, 2003). It is characterized by opposing pressure anomalies of different signs between the Antarctic and midlatitudes near 40° – 50°S. The positive phase of the SAM is associated with negative pressure anomalies over the polar cap, positive pressure anomalies over the midlatitudes, resulting in the strengthening and poleward shift in storm tracks (Gillett et al., 2006). During a negative SAM phase there is an expansion in the westerly wind belt towards the equator, which allows storm passage and increased winter rainfall over western South Africa (Reason and Rouault, 2005). Conversely, the eastern and southern parts of the country may experience abnormally wet (dry) conditions during the positive (negative) phase of the SAM (Gillett et al., 2006, Mahlalela et al., 2019).

The SAM and ENSO have been shown to have interactions at the interannual scale, with El Niño (La Niña) events sometimes corresponding to negative (positive) SAM phase (Pohl et al., 2010). L'Heureux and Thompson (2006) show that 25% of the SAM variance linearly relates to the ENSO state, the SAM variability is also shown to be forced by ENSO anomalies (Pohl et al., 2010). Yu et al. (2015) found that ENSO forcing only became significant after the 1990s and suggested it to be related to the change in the ENSO type from being mostly of the eastern Pacific (EP) to a central Pacific (CP) type. The two types differ in their longitudinal position; CP ENSO develops and decays in the central equatorial Pacific, while the EP develops near the South American coast and has its SST anomalies centred over the eastern equatorial Pacific (Yu et al., 2015). The shift in the longitudinal position of ENSO SST variability therefore has implications on the observed climate over the adjacent land masses. CP ENSO is suggested to

induce the SAM through an eddy-mean flow interaction mechanism in the stratospheric and tropospheric mechanism pathways (Yu et al., 2015). During an El Niño event, an increased meridional temperature gradient associated with tropospheric warming produces a strengthening and equatorward displacement in the subtropical jet. This strengthening affects the propagation of transient eddies due to changes in the location of eddy momentum flux convergence (Yu et al., 2015). An acceleration of westerly (easterly) anomalies occurs on the equatorward (poleward) side inducing a negative SAM phase (Yu et al., 2015). Silvestri and Vera (2003) found that the relationship between SAM and ENSO was only significant during austral spring. Thompson and Wallace (2000) suggest that this is associated with the significant cooling (warming) of the tropopause at polar (tropical) regions which trigger SAM fluctuations during the spring season.

Another climate mode of importance for the summer rainfall region is the South Indian Ocean subtropical Dipole (SIOD) (Behera and Yamagata, 2001, Reason, 2001b, Reason, 2002). During its positive phase, warm SST anomalies occur south of Madagascar, while cool SST anomalies occur off western Australia, intensifying summer rainfall over southern Africa due to the weakening of the intertropical convergence zone (ITCZ) over the Indian Ocean and enhanced moisture transport towards the land and hence wetter conditions (Reason, 2001a). Roughly the opposite conditions occur during a negative SIOD event, which is associated with less rainfall over parts of subtropical southern Africa. Hoell et al. (2017) provide additional evidence that this mode of variability can either oppose or reinforce the ENSO signal if they occur at the same time. When a La Niña and a positive SIOD phase co-occur, the precipitation anomaly over southern Africa increases relative to when a La Niña co-occurs with a negative SIOD phase.

While the SIOD is a particular type of SST mode in the South Indian Ocean, there is a long history of research associating increased summer rainfall over eastern South Africa with warm SST anomalies in the greater Agulhas Current region (Walker, 1990, Reason and Mulenga, 1999, Reason, 2001a). Similar mechanisms are involved to those associated with the positive SIOD; namely, warmer SST east of South Africa lead to an increase in the transport of moist unstable air towards the land mass which is favourable for convective development there as well as intensifying cloud bands approaching from the west.

2.4 Summary

This literature review has shown that both the regional meteorology as well as the variability of rainfall over South Africa are complex and that the responses of the summer and winter rainfall regions to ENSO and SAM are different. Although much research has been done on rainfall variability in these two main rainfall regions, far less has been done on the transition region along the south coast between these two regions (Weldon and Reason, 2014, Engelbrecht and Landman, 2016, Engelbrecht et al., 2015a, Blamey et al., 2018). Thus, the climate of this part of South Africa, and more generally the Eastern Cape, is less well understood which makes it challenging to understand the mechanisms underlying extreme weather events like droughts and floods here. Furthermore, the influence of large-scale modes of variability, as well as the mechanisms by which they influence rainfall over this region, remains to be fully explored, which motivates the need for the work presented in this thesis. Because the Eastern Cape is prone to protracted dry periods (e.g., Fig 5 in Blamey et al., 2018) with intermittent flooding occurrences (Tyson and Preston-Whyte, 2000, Singleton and Reason, 2006), there is a need to revisit and update understanding on the region's rainfall variability and trends. As a result of these events, surrounding communities, may face severe water shortages. This is particularly true in the greater Nelson Mandela Bay municipality which

has been under threat of "Day Zero" water restrictions during 2021-22. Part of this severe water shortage is due to long periods of below average rainfall (discussed in this thesis) and part is due to mismanagement of available water resources by various levels of government as well as insufficient reduction in water consumption by users (aspects which are not discussed in any detail in this thesis).

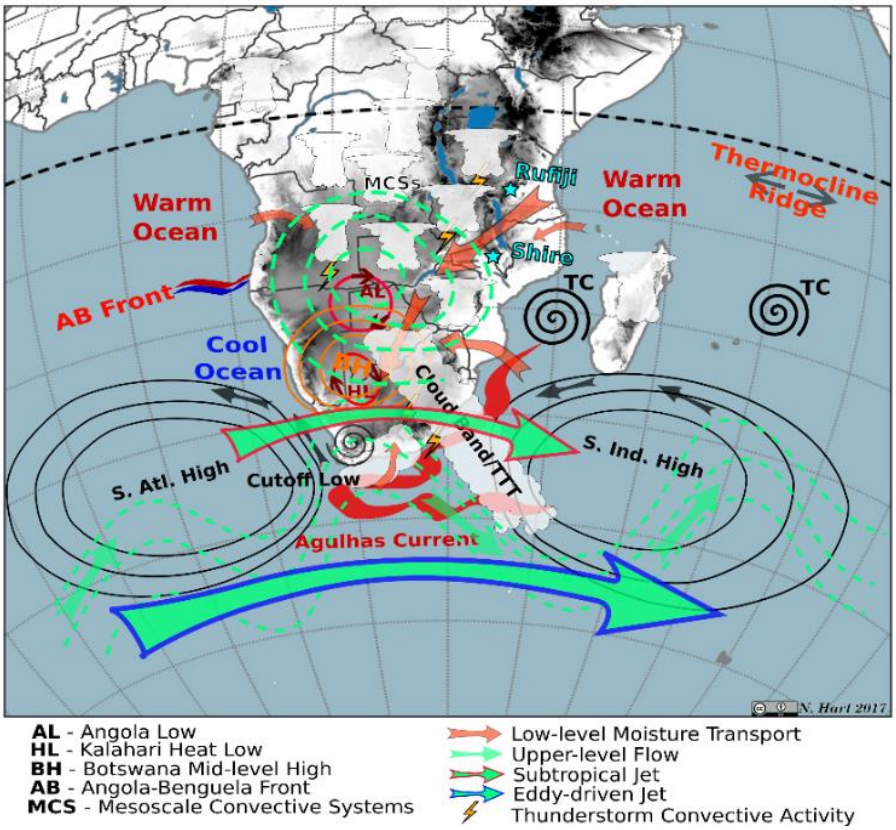

Figure 2.1: The figure depicts the location of key regional circulation features influencing the weather and climate of southern Africa during the summer season as described in the text © Dr Neil Hart, 2021.

Chapter three: Data and methodology

3.1 Rainfall Analysis

3.1.1 Station rainfall data

Daily rainfall station data over the Eastern Cape were provided by the South African Weather Service (SAWS) for January 1981–December 2018. The data was reduced to only the stations with 90% data available for the full period, and for which the station location has stayed more or less the same, which resulted in 11 stations being available (see **Fig 3.1** for location). Daily data was converted to monthly data, and this was used to compute standardized anomalies of seasonal (spring-SON, and summer-DJF) rainfall for the period 1981–2018. Rainfall characteristics and trends are also investigated from daily data for the 11 available SAWS stations. As evident in **Figure 3.1** the available station data comprises of mostly coastal stations there was therefore a need to supplement available stations for better spatial coverage.

3.1.2 Climate Hazard Infrared Precipitation with Station

Due to the limited available station data the Climate Hazard Infrared Precipitation (CHIRPS) with station product was used to supplement available station data. CHIRPS is a merge of different products including satellite imagery and station values available at 0.05° (5 km) spatial resolution on a quasi-global (50° S–50° N) grid, for the period 1980 to present (Funk et al. 2015). A correlation analysis was done between CHIRPS and available station data to assess confidence in the ability of CHIRPS to represent the regions rainfall (**Chapter 4**). Trends in various seasonal rainfall characteristics such as the number of dry days (1 mm/day), light (2–9 mm/day), moderate (10–30 mm/day), and heavy (> 30 mm/day) were evaluated using a non-parametric Mann–Kendall test (Mann, 1945, Kendall, 1975) over the analysis period 1981–2018. This test was used as it makes no assumption about the data distribution and is insensitive

to outliers. The magnitude of the trend is calculated using the Sen's slope estimator (Theil, 1950, Sen, 1968). This method uses the median of all possible slopes for the given series making it statistically robust. The probability of the trend occurring was measured at a 5% significance level.

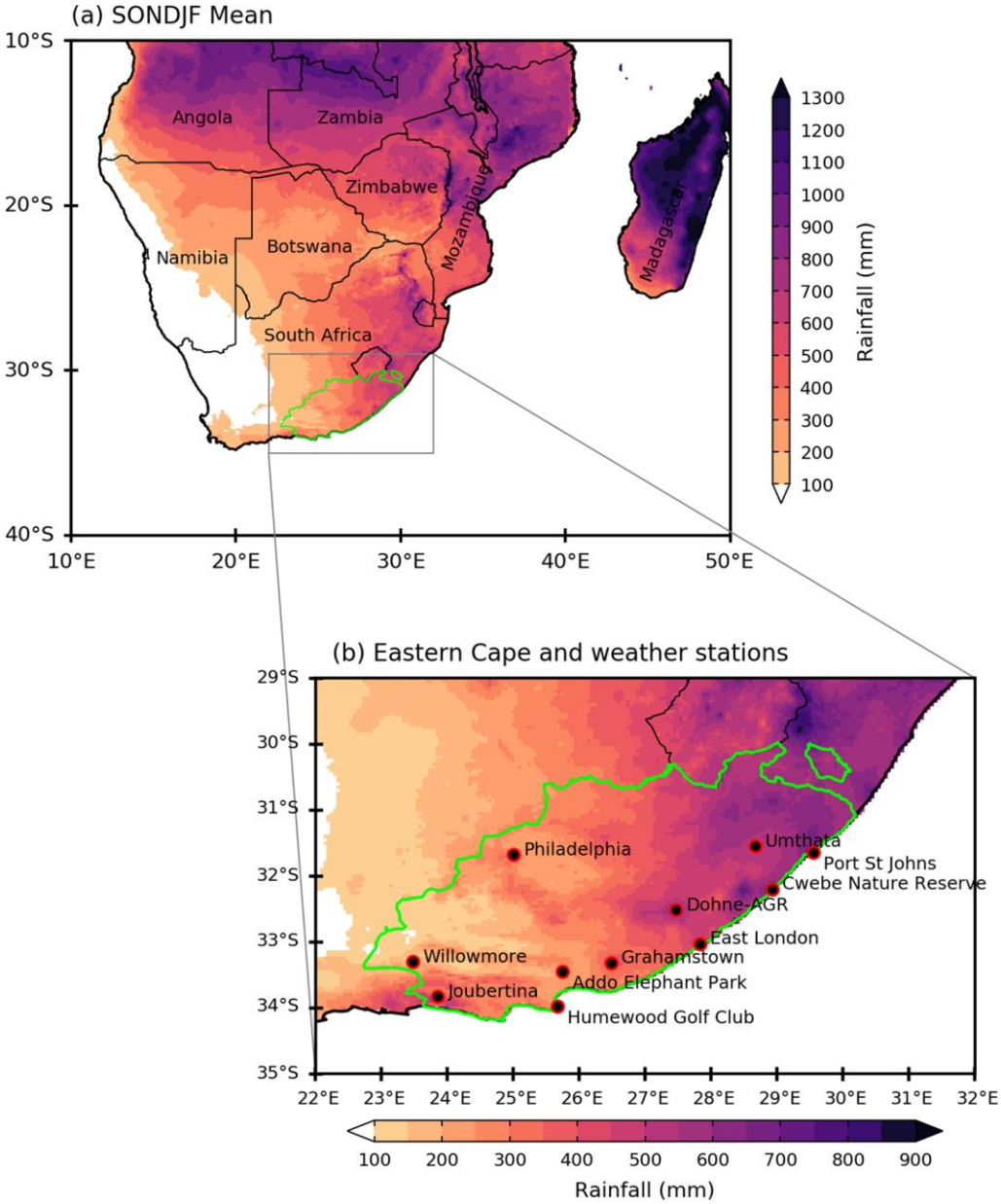

Figure 3.1: **(a)** The mean austral spring and summer (September– February) rainfall (shaded; mm) across southern Africa based on CHIRPS data from 1981 to 2018. **(b)** A zoomed in version of the mean spring and summer rainfall for the southeast region of the domain. The green polygon in both panels illustrates the location of the Eastern Cape Province in South

Africa. Also shown in panel (**b)** are the locations of the South African Weather Service rain-gauges used in the study.

3.2 Regional circulation analysis

3.2.1 National Centers for Environmental Prediction (NCEP) reanalysis data

National Centers for Environmental Prediction (NCEP)-Department of Energy (DOE) Second Atmospheric Model Intercomparison Project (AMIP-II) reanalysis data (Kanamitsu et al., 2002), at a spatial resolution here of 2.5° and on monthly time scale for the period 1979–2017, are used to determine circulation anomalies. Variables that are used here include monthly mean of zonal and meridional winds, geopotential height at 850 and 500 hPa, vertical velocities (omega), and outgoing longwave radiation (OLR). Moisture fluxes were computed from the horizontal winds and specific humidity. To analyses global SSTs, the National Oceanic and Atmospheric Administration (NOAA) 0.25° Optimum Interpolation Sea Surface Temperature (OISST) product is used. The variables are plotted to represent anomalous conditions in order to understand circulation patterns associated with wet and dry seasons.

The zonal wavenumber 3 (ZW3) index such as that proposed by Raphael (2004) is derived from NCEP II 500 hPa geopotential height. Raphael (2004) suggests using 500 hPa zonal anomaly which is constructed by removing zonal means from each grid point at three selected grid points namely, 45°–60° E (South Indian Ocean), 161°–171° E (South Pacific) and 71°–81° W (South West Atlantic) over the latitude range of 45°–50° S. The ZW index (ZW_i) is an average of the anomaly from all three regions and is calculated as follows:

$$ZW_i = \frac{(X_{monthly} - \overline{X}_{monthly})}{\sigma_{monthly}} \qquad (1)$$

Where X_{monthly} represents the three-monthly geopotential height value, $\overline{X}_{\text{monthly}}$ the three-monthly climatological mean and $\sigma_{monthly}$ the standard deviation of the three-monthly mean. The ZW3 index and seasonal rainfall are correlated using a Pearson's correlation and a Student t-test was used to test for statistical significance.

NCEP II reanalyses are also used to plot features of semi-permanent anticyclones in the Indian and Atlantic Oceans. For the purpose of this study, the northern, southern, eastern and western extension of the anticyclones is determined as the outer boundary of the 1020 hPa contour in the mean sea level pressure field (MSLP). This contour level is chosen as it is easily identified as closed contour level around the anticyclones, which is not intersected with the neighbouring land masses in either the early or late summer periods. The South Indian Ocean High's latitude and longitude are defined here as the location with the maximum in the MSLP field within the climatological mean area (40°–110° E; 15°–40° S). The latitude and longitude of the centre of the South Atlantic High is defined here as the location with a maximum in the MSLP field within the climatological mean area (40° W–15° E; 0°–45° S and values over land were masked).

3.2.2 ECMWF Reanalysis v5 (ERA5)

The Botswana High index is calculated using 500 hPa ERA5 [1]reanalysis data (Hersbach et al., 2020) with a 0.25° x 0.25° resolution for the period 1979 – 2019. For each season, the index represents geopotential height anomalies extracted at the core of the 5870m contour. This

[1] NCEP II was used for large scale circulation analysis because ERA5 only became available at a later stage due to computational constraints and therefore is only used for the Botswana High which required higher resolution to capture a realistic index.

method was adopted from Munday and Washington (2017) who defined the Angola Low as the minimum in the 850hPa geopotential height across Africa. The 5870m contour was found to be the highest well-defined contour which would allow for the tracking of the Botswana High in different seasons.

To analyse extratropical cyclone activity over the South Atlantic storm track dataset by Gramcianinov et al. (2020) available at Mendeley Data was used. This dataset, which is based on ERA5 reanalysis and is available from 1979 – 2019. The influence of ridging on storm tracking into the southeast of South Africa is investigated. Ridging days are classified according to Ndarana et al. (2021), who defined ridging as when a high pressure crosses the 25 °E line. Here we averaged wind across 1000 and 850 hPa at 35 °S and along 15 and 30 °E to determine ridging days over the south coast. Ridging days were defined as days with winds of more than 10 m/s.

3.3 Large scale modes of variability

The Southern Annular Mode (SAM) and El Niño Southern Oscillation (ENSO) are used to assess the influence of large-scale modes of variability. The Niño 3.4 index is used for the ENSO analysis, and it can be obtained from the Climate Explorer website available from 1856 to present. The Niño 3.4 index is based on the Extended Reconstructed Sea Surface Temperature (ERSST) dataset from the domain 5°N – 5°S, 120°– 170° W in the equatorial Pacific Ocean. The Marshall (2003) SAM index is used for SAM analysis. This index uses monthly mean differences between the mean sea level pressure (MSLP) anomaly at six stations close to 40°S and six stations close to 65°S. Since this index is based on station data, it eliminates the influence introduced by changes in observational coverage, which causes

spurious trends to be observed in indices based on reanalysis data. The Marshall index is developed using Gong and Wang (1999)'s empirical definition shown in equation (2) and was also obtained from the Climate Explorer available from 1957 to present.

$$SAM = P^*_{40^oS} - P^*_{65^oS} \qquad (2)$$

Where $P^*_{40°S}$ and $P^*_{65°S}$ are normalized monthly zonal MSLP at 40° and 65°S, respectively (Marshall, 2003). The study assumes that both indices (SAM and Niño 3.4) and rainfall are normally distributed making it possible to conduct a Pearson correlation between the de-trended series (i.e., SAM and rainfall).

3.4 Future climate projections

To see whether some insight may be obtained about future rainfall scenarios, a topic of great interest to both the public and the government, future rainfall projections in the region are considered using 36 models from the Coupled Model Intercomparison Project Phase 5 (CMIP5) ensemble (Taylor et al., 2012). A 21-year mid twenty-first century future period (2040–2060), under the high energy intensive scenario, Representative Concentration Pathway (RCP) 8.5, was chosen. The RCP 8.5 scenario was chosen because it corresponds to a high greenhouse gas emissions pathway and thus the upper bound of the RCPs. It is also a baseline scenario with no specific climate mitigation target (IPCC, 2008). Only one ensemble member (r1i1p1) per model is included in the analysis. For ease of comparison, precipitation (atmosphere variables) in the models is regridded using bilinear interpolation to a common 1.5° × 1.5° (2.5° × 2.5°) grid. Rainfall from the models is compared with satellite-based estimates from the Global Precipitation Climatology Project (GPCP) monthly precipitation data set (Adler et al., 2003) and Climate Prediction Center Merged Analysis of Precipitation (CMAP)

(Xie and Arkin, 1997). Instead of CHIRPS, the GPCP and CMAP datasets are used for model comparison because they provide a longer time period that is more comparable to the period available for models used in future climate projections. GPCP and CMAP are also more appropriate because they have similar spatial resolutions to the models, whereas CHIRPS has a much finer grid. Changes in regional circulation are also examined using 500 hPa GPH and MSLP. The data for circulation analysis came from Climate Explorer and represents the multi-model mean along the same Representative Concentration Pathway as rainfall. Although CMIP6 models are now available, computational constraints meant that only CMIP5 could be used for this study.

Chapter four: Rainfall analysis and trends

4.1 Introduction

This chapter examines rainfall patterns from September to February to better understand rainfall variability and trends in Eastern Cape, which is located in the southeast of the country. Although a significant amount of work has gone into understanding rainfall characteristics over most of South Africa, our knowledge of the Eastern Cape remains limited (Jury, 1993, Jury and Levey, 1993, Weldon and Reason, 2014, Engelbrecht and Landman, 2016). This is concerning given the fact that this region is prone to extreme climate events which have devastating socio-economic impacts. For example, two flood events of March 2003 and August 2006, which were both associated with COLs, had massive damage on infrastructure and regional agriculture, with estimated losses over ZAR 100 million for the 2006 event (Singleton and Reason, 2007a, Weldon and Reason, 2014, Engelbrecht and Landman, 2016). Droughts are also common in this area, with the most recent being the 2015 – 2020 dry period. Following severe water shortages in many urban and rural areas, the Eastern Cape Province, which encompasses majority of the southeast of South Africa, was declared a drought disaster region in October 2019. In recent decades there has been a tendency for more multi-year droughts to occur. For example, summer rainfall time series for six domains across South Africa's summer rainfall region, including one in the Eastern Cape and two in the adjoining KwaZulu-Natal Province, show that there were more multi-year droughts from the late 1970s to 2017 than from the late 1950s to the late 1970s across all domains (Blamey et al. 2018).

Figure 4.1a shows the catchment areas of the main dams supplying the largest municipality (Nelson Mandela Bay) over the southeast coast which contains the major coastal city of Port Elizabeth (located near 34°S) (termed the “west” basin) as well as those for rivers draining the wetter northeastern part of the province (termed the “east” basin). Water levels (**Fig. 4.1b**) at

two large supply dams (Impofu and Kouga) are being studied to determine the impact of drought and flood events on water availability. Both dams were close to full capacity during the 1993 – 1998 and 2012 – 2016 time periods, with the former being the dam's full capacity for the longest period. After being close to full in 2015, both dams fell to their lowest levels since 1985 with the decline during 2017–2019 being especially sharp. The Kouga dam was at 7% capacity in June 2020, and the combined supply dam capacity for the Nelson Mandela Bay metro had fallen below 20%. Understanding the variability and trends in rainfall characteristics is critical for effective regional water management and planning.

Rainfall patterns in Eastern Cape are highly variable. **Figure 4.2** depicts the annual rainfall cycle from the two rainfall basins used to highlight rainfall differences across the province. The west basin forms part of the south coast, which receives rainfall throughout the year (Weldon and Reason, 2014, Engelbrecht et al., 2015, Engelbrecht and Landman, 2016). Monthly rainfall totals averaged from 1981 to 2018 show rainfall peaks in February and November, with the February peak being the highest at 50 mm. The northeastern region, where the warm Agulhas Current hugs the coast and where summer rainfall is more common due to the increasing influence of moist, unstable air masses than further south, experiences highest rainfall between December and February, with a maximum in January. An examination of the seasonal contributions to annual totals reveals that spring (September, October and November – SON) and summer (December, January and February – DJF) account for the majority of the Eastern Cape's annual rainfall on average except in the far west where autumn is also important (**Fig 4.3**). Spring and summer each contribute about 30% total for the coastal zone, whereas summer dominates in the northern interior (40–45%). Autumn (March, April and May – MAM) accounts for about 20–25% of the province's rainfall, with a small region in the far west reaching 30%, whereas winter rainfall accounts for only 15% total on average in the far south.

Due to the obvious strong influence of the summer half of the year over the province, rainfall variability is examined for the spring (SON) and summer (DJF) seasons. Following this introduction, the chapter is divided into five sections: **Section 4.2** highlights the seasonal rainfall climatology, **Section 4.3** investigates interannual variability, **Section 4.4** compares anomalies to the interannual frequency of wet and dry days, **Section 4.5** trends in seasonal rainfall and rainfall characteristics, with **Section 4.6** providing a summary of the findings.

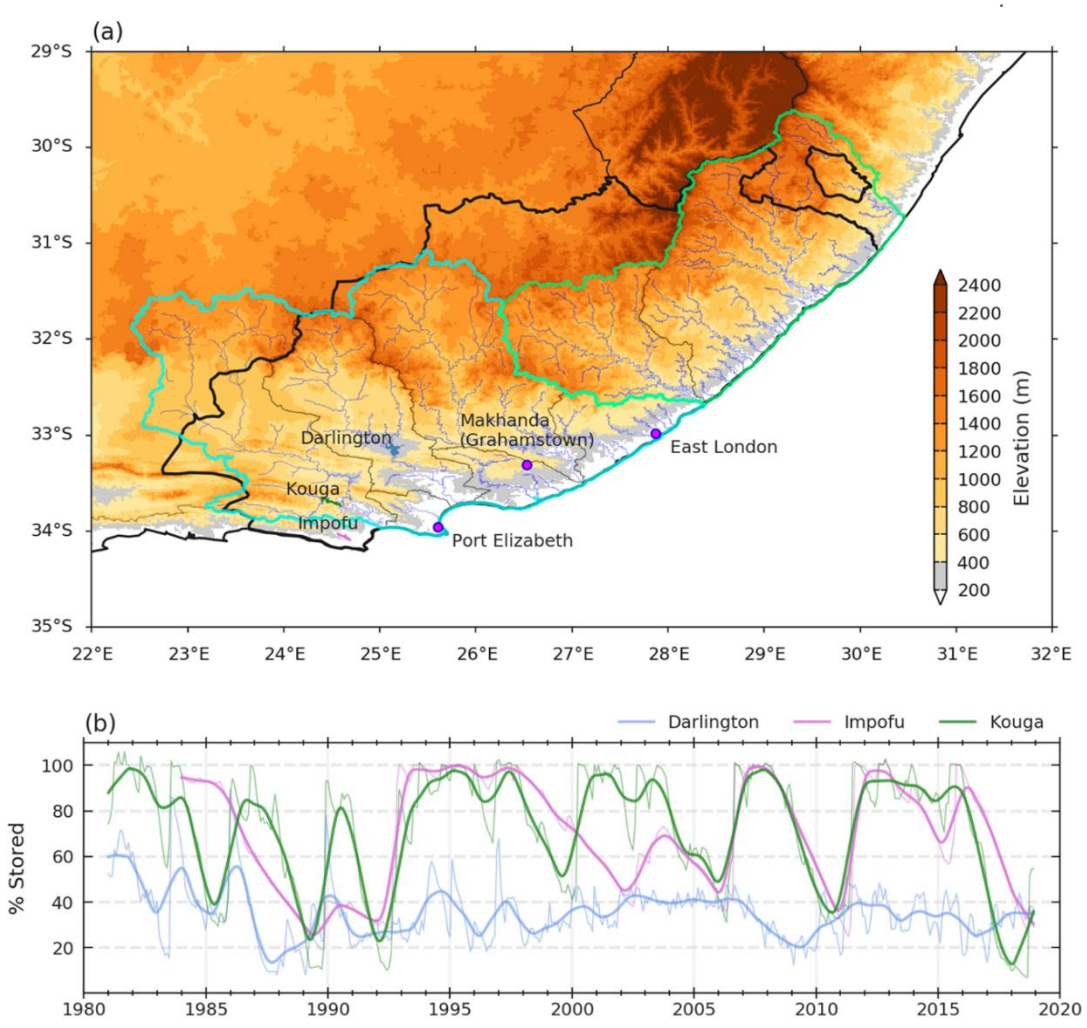

Figure 4.1: **(a)** Illustrates the topography (shaded; m) of the domain along with the various rivers and river basins. The river basins have been merged into a "west" and "east" basin to highlight some of the regional rainfall differences. Also shown are the locations of the main dams of the region that have seen large water level drops as well as locations of the main towns/cities. Panel **(b)** shows the smoothed monthly dam levels (given in % stored) from around 1981 until 2018.

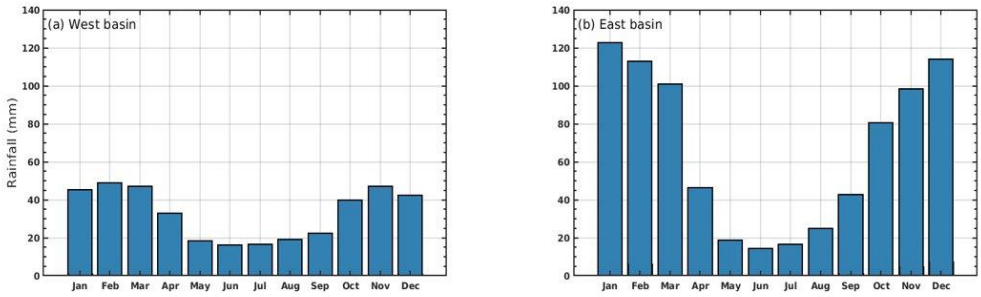

Figure 4.2: Mean (1981–2018) annual cycle of southeast South African rainfall averaged over the **(a)** "west" **(b)** "east" rainfall basins using CHIRPS data.

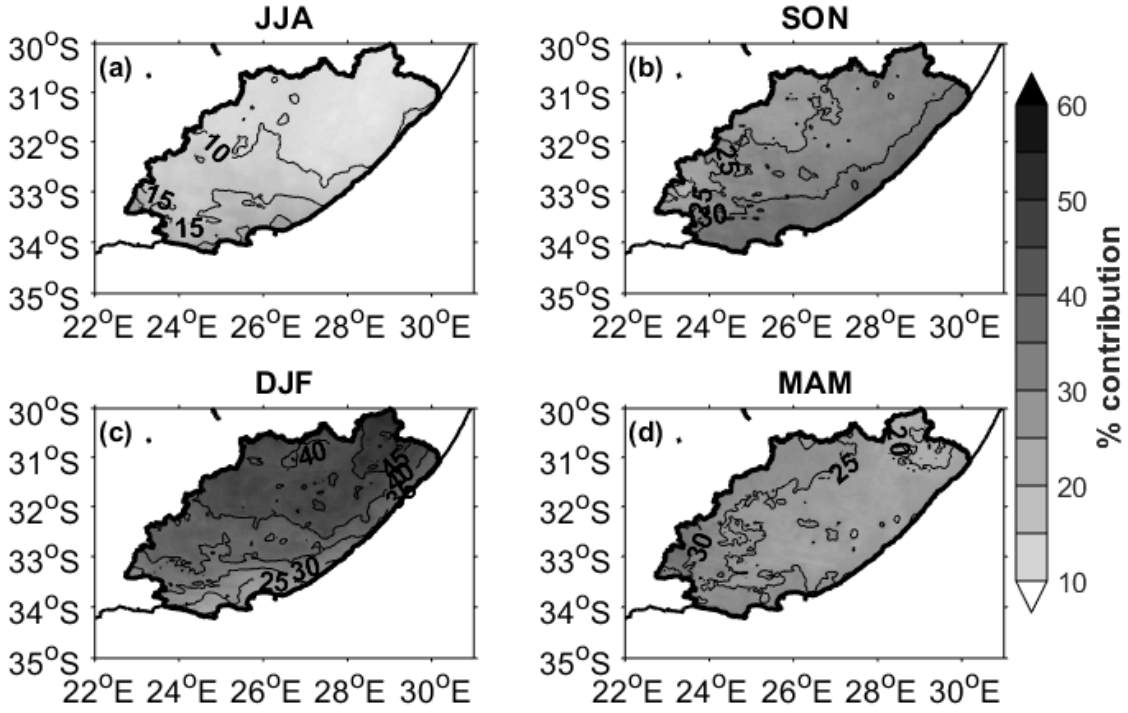

Figure 4.3: The mean seasonal rainfall contribution (shaded with contours; in percentage) to the annual rainfall total for (a) winter—JJA, **(b)** spring-SON, **(c)** summer—DJF, and **(d)** autumn—MAM.

4.2 Seasonal rainfall climatology

4.2.1 The early summer

The spatial distribution of spring mean rainfall averaged over the period 1981–2018 is displayed in **Figure 4.4**. The CHIRPS dataset shows that mean rainfall is low (below 100 mm) over most of the inland part of the west basin. In the early summer, the small region on the south coast receives slightly more rainfall (200 mm), which is brought by midlatitude systems such as frontal systems and ridging anticyclones (Engelbrecht et al., 2015a). Rainfall increases from west to east, with the greatest amounts recorded along the northeast coast at Cwebe Nature Reserve and Port St Johns (over 300 mm). During the early summer, the area around Grahamstown and East London receives 250 mm of rain on average. The observed spatial differences in seasonal totals indicate that the west basin is generally drier than the east basin during the spring. The station dataset (**Fig. 4.4**) shows similar rainfall patterns; correspondence between CHIRPS and station datasets suggests that CHIRPS accurately captures local seasonal rainfall.

Figure 4.5 shows the corresponding climatology of dry days (1 mm/day), light (2 – 9 mm/day), moderate (10 – 30 mm/day), and heavy (> 30 mm/day) rainfall days across the domain. The findings are consistent with the observed seasonal totals, with the drier southwest recording the most dry days (more than 80 days) and the northeast tip of the domain recording the fewest (between 60 – 70 days). Out of 91 days in a spring season, central stations recorded between 60 and 80 dry days (**Fig. 4.5a**). The region receives between 2 – 4 light wet days along the south coast and 4 – 6 days inland of the west basin (**Fig. 4.5b**). The northern tip of the Eastern

Cape receives the most light wet days (between 12 – 14 days), while the larger northeast coast receives 10 – 12 light wet days. There are some disparities between CHIRPS and SAWS stations for light wet days i.e., Philadelphia, Joubertina, and Dohne-AGR. **Figure 4.5c** depicts a sharp gradient in moderate wet days, with the northeast coast receiving the most (between 8 and 10 days) and the western interior receiving less than two moderate wet days (daily rain between 9 – 30 mm) per spring. In addition, **Figure 4.5c** shows that the SAWS dataset records fewer moderate wet days over the northeast than CHIRPS. The south and northeast coasts have the most heavy rainfall days per season (between 2.5 and 3 days). During early summer, the generally high number of dry days in comparison to wet days across the domain suggests that large rainfall events may have a significant influence on seasonal rainfall totals in some years.

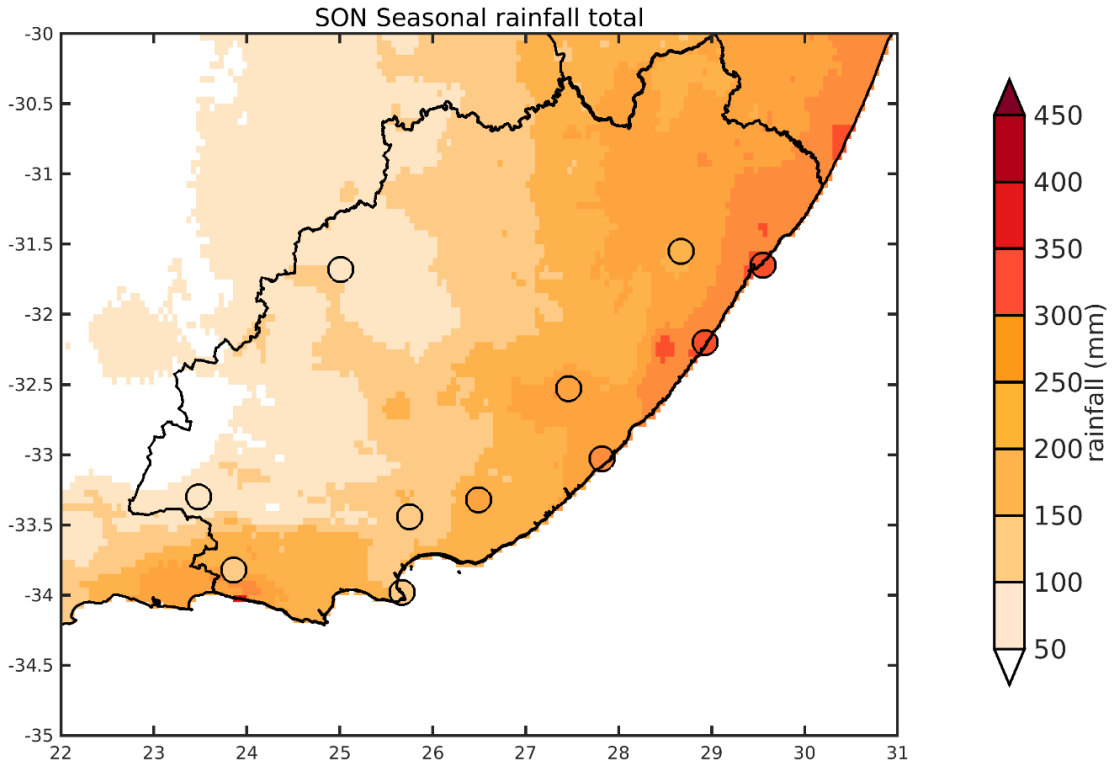

Figure 4.4: The mean spring (September - November) rainfall over Eastern Cape based on CHIRPS (shaded; mm) and SAWS stations (circles; mm) data from1981– 2018.

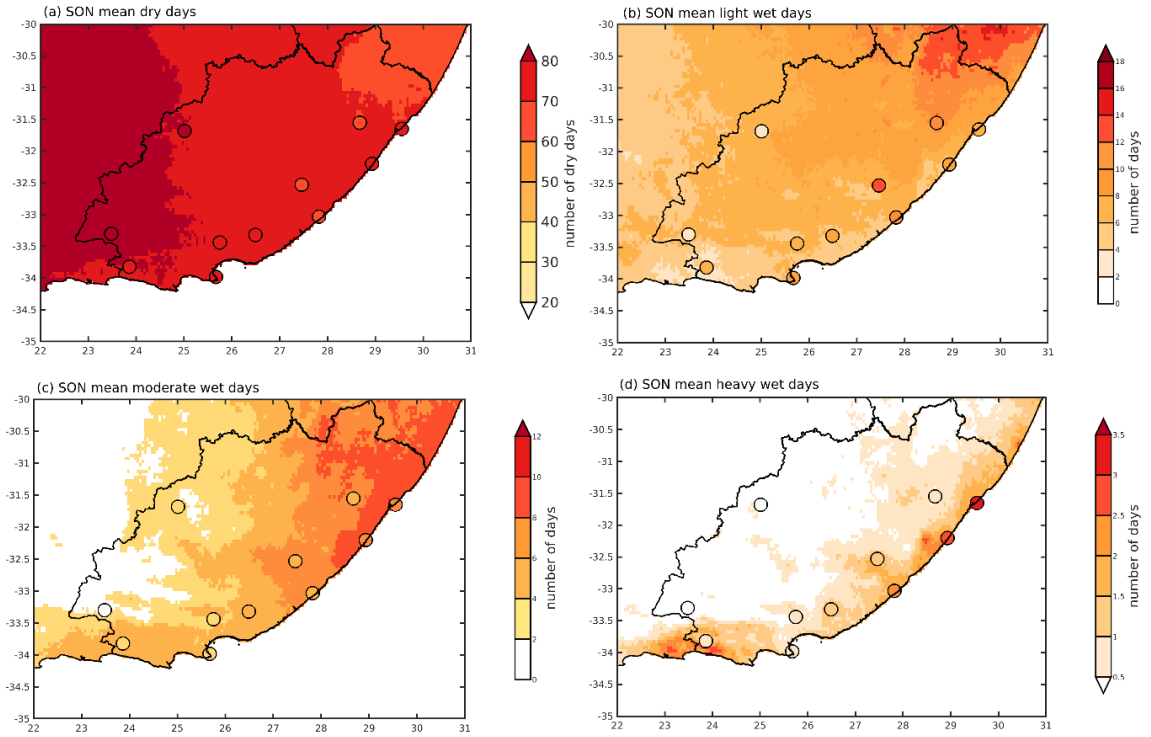

Figure 4.5: The climatological number of austral spring **(a)** dry (daily rain < 1 mm), **(b)** light wet (daily rain 2–9 mm), **(c)** moderate wet (daily rain 10–30 mm), and **(d)** heavy wet (daily rain > 30 mm) days for CHIPRS (shading; mm) and SAWS stations (circles; mm) in Eastern Cape.

4.2.2 The core summer

Figure 4.6 illustrates the spatial distribution of the wet season mean rainfall averaged over the period 1981–2018 for both SAWS and CHIRPS data. Rainfall varies spatially, with a strong rainfall gradient increasing from the southwest to the northeast of the region. During this season, the southwest inland receives about 100 mm of rain, while the northeastern coast receives more than 350 mm. Jury et al. (1993) attributed the large increase in average rainfall along the South African east coast (north of Port Elizabeth, around 23 – 33°S) to the Agulhas Current's proximity to the coast. The south coast, which receives significant rainfall throughout the year, is found to be wetter than the majority of the west basin. However, the summer rainfall totals here are a bit less on average than those in spring due to the southward displacement of

frontal systems in summer. During the core summer months, rainfall is brought by ridging high pressure systems, which contribute primarily to rainfall along the coast (Weldon and Reason, 2014, Engelbrecht et al., 2015) as well as by cloud bands (Hart et al., 2013) and less frequently, cut-off lows. There is overall agreement between stations and CHIRPS on rainfall means, which increases our confidence in CHIRPS ability to capture seasonal rainfall.

In contrast to seasonal totals, the mean number of dry days decreases from west to northeast coast, with inland of southwest, the interior, and northeast recording about 80, 70, and 60 out of 90 dry days, respectively (**Fig. 4.7a**). During the summer, SAWS and CHIRPS stations show similar dry day frequency, with some differences at the Dohne-AGR and Umthatha stations. In comparison to CHIRPS, these stations have fewer dry days (between 50 and 60 days). Light rainfall days do not show any clear gradients, but there are subtle differences between the west and east basins, with the south coast having the fewest (2 – 4 days) light wet days per season. On average, the southeast coast receives between 8 and 12 light wet days per year, with a small region in the north receiving 14 days per year. The area around East London, Dohne-AGR, and Umthatha displays some differences in SAWS and CHIRPS light wet days. **Figure 4.7b** shows that at these stations SAWS data records more light wet (14 – 16 wet days) days than CHIRPS data. The region receives the most moderate wet rain days in the northeast (12 days out of 90 days) and the least in the southwest (2 – 4 days). Moderate wet days show some spatial differences across the west basin, with the south coast recording more moderate days (between 4 – 6 days) than the rest of the basin. Overall, CHIRPS shows more moderate days than SAWS stations; this can be attributed to some of the limitations of satellite-based rainfall estimates, such as measurement uncertainty (Funk et al., 2015). This is primarily because satellite sensors detect certain rainfall systems better than others (for example, convective rainfall is better detected in CHIRPS) and rainfall estimates calculations are based on relationships with gauged

rainfall (Toté et al., 2015, Funk et al., 2015, du Plessis and Kibii, 2021). As a result, the rainfall product may be more sensitive to moderate rainfall and less sensitive to light rainfall. Only the south coast and northeast of the region tend to experience heavy rainfall (2 – 2.5 days per season on average), as shown in **Figure. 4.7d**. During this season, the northeastern stations Cwebe Nature Reserve and Port St Johns have the highest number of heavy wet days (3 days). Increased heavy rain activity over the north may result from more unstable airmasses and greater surface heating being present in summer. Areas further north, such as KZN, and the northern interior of the country also experience more tropical influences in summer (Blamey et al., 2017, Dyson et al., 2015) and sometimes this tropical air may penetrate further south to directly influence the Eastern Cape.

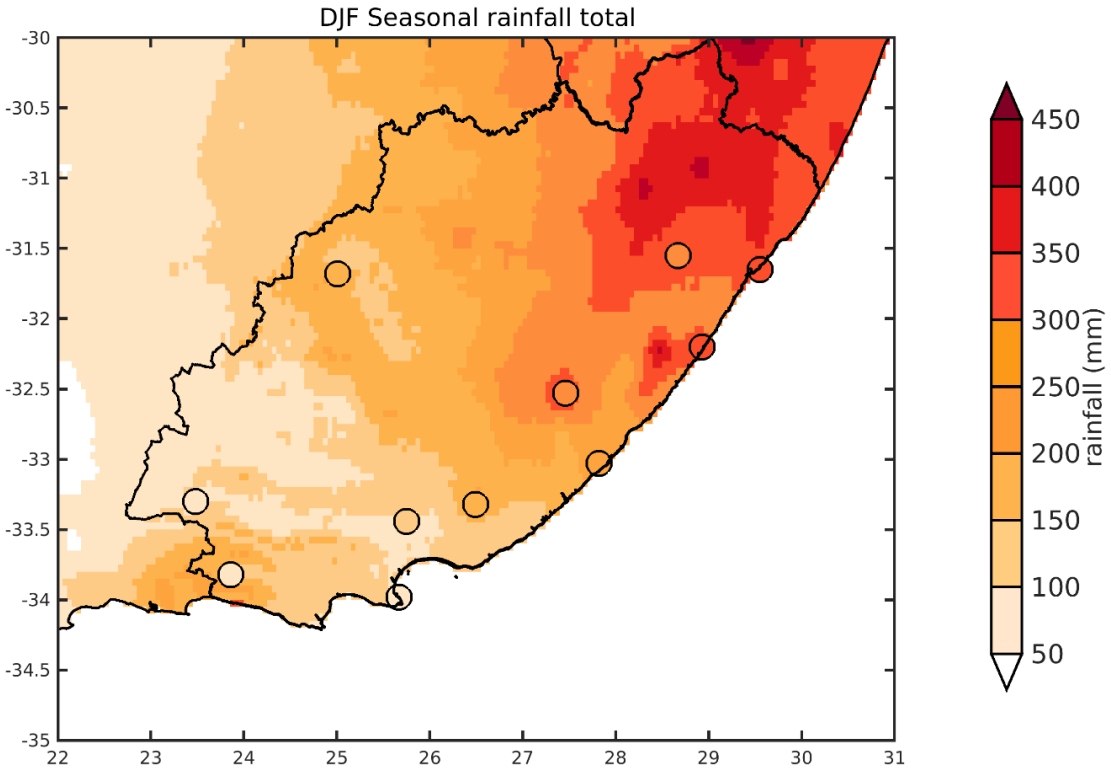

Figure 4.6: The mean summer (December - February) rainfall in Eastern Cape based on CHIRPS (shaded; mm) and SAWS stations (circles; mm) data from1981-2018.

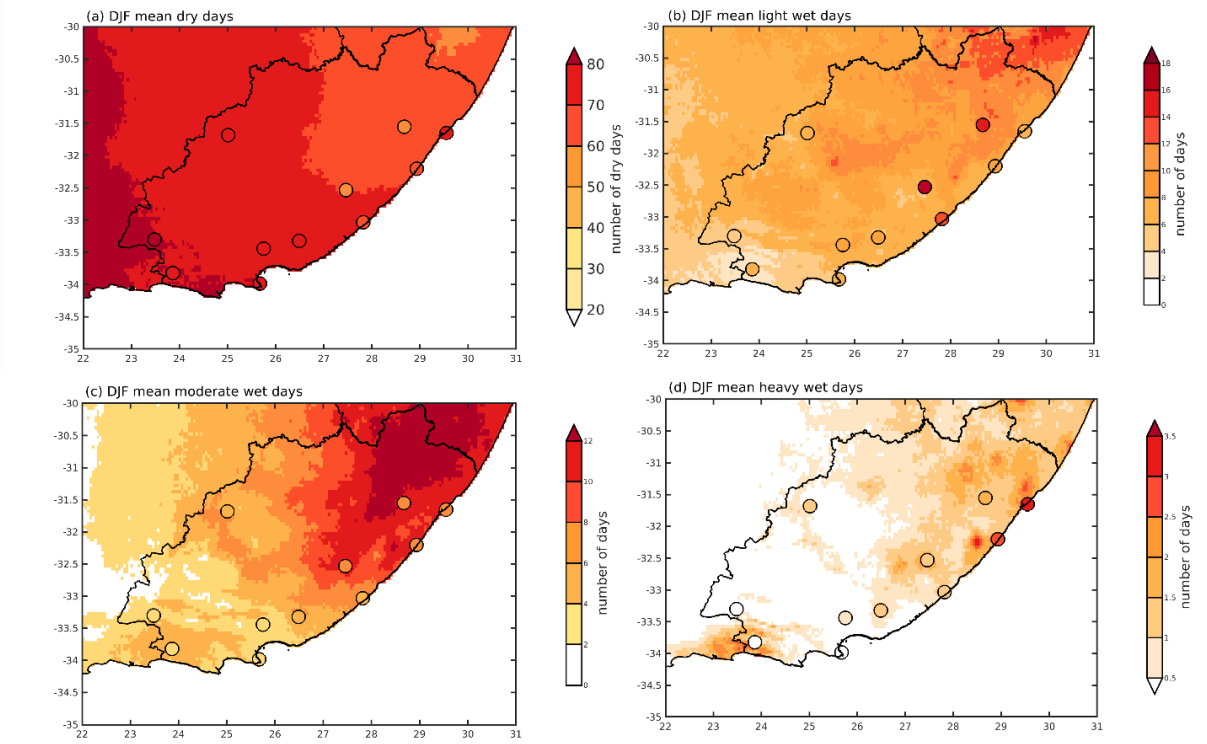

Figure 4.7: The climatological number of austral summer **(a)** dry (daily rain < 1 mm), **(b)** light wet (daily rain 2–9 mm), **(c)** moderate wet (daily rain 10–30 mm), and **(d)** heavy wet (daily rain > 30 mm) days for CHIPRS (shading; mm) and SAWS stations (circles; mm) in Eastern Cape.

4.3 Variability in local climate

4.3.1 The early summer- SON

Figure 4.8 shows the time series for SON rainfall anomalies at the eleven stations across the domain for both SAWS and CHIRPS data. A correlation analysis is performed between the two-time series to further determine whether CHIRPS accurately represents local rainfall. The time series are correlated at 95% significance at each station with r values ranging from 0.61 to 0.90. Although the sign of the anomalies is almost always the same for each station, there are some springs when there are sizeable differences in magnitude at some stations (i.e., Willowmore, Humewood, and Grahamstown). Note that it is possible that topographic effects or other local forcings may lead to the differences between the time series. However, the

correspondence between the two-time series during the almost 40-year period at both coastal and inland stations provides sufficient confidence in the ability of the CHIRPS data to adequately represent rainfall variability and change across the province. Of the eleven stations, Joubertina and Addo Elephant park show the most similarities between wet and dry springs (**Fig. 4.8b, d,** respectively). Prolonged dry and wet periods are also common across stations. Multi-year events were recorded in Cwebe Nature Reserve, Port St Johns, and Umtata between 1985 and 1989; and between 2000 and 2015 for Willowmore, Joubertina, and Humewood. While increased rainfall was received by southwest stations in 2015, northern and inland stations started to receive below-average rainfall during this time period (**Fig. 4.8h-k**). Another difference is that 1996 is recorded as the wettest year over southwest stations, while the wettest season over southeastern stations was 1985. This highlights regional rainfall differences between southwest and northern stations.

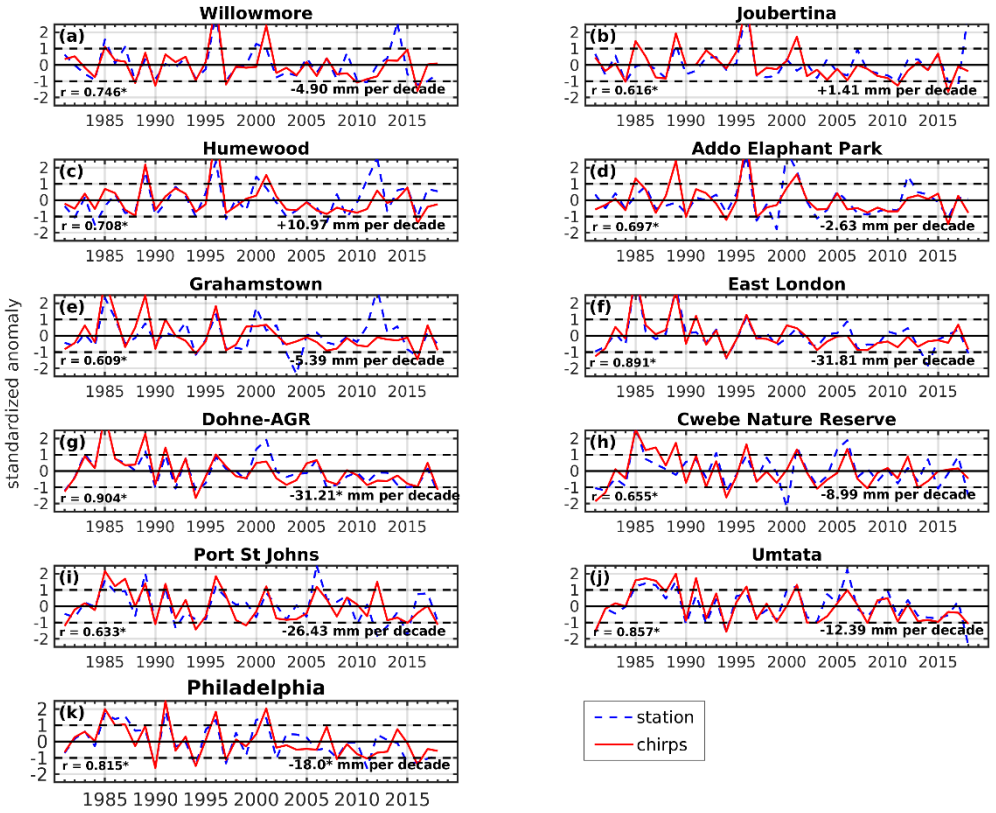

Figure 4.8: Spring (SON) standardized anomalies for the eleven stations (blue-dashed line) across Eastern Cape and the corresponding CHIRPS (red-solid line) anomalies. The station names are indicated at the top of each panel. The correlation between the two datasets is given at the bottom left of each panel. The trend in SON rainfall for each station (trend calculated from station data) is given in the bottom right-hand corner of the panel (in mm per decade). For both the correlation and the trend analyses, the asterisk denotes significance at the 95% level using a Student t-test.

4.3.2 The core summer- DJF

The DJF time series comparison (**Fig. 4.9**) demonstrates similar strong correlations to that of SON between stations and CHIRPS, with r values greater than 0.6 at most stations and around 0.8 – 0.9 at a few. However, Port St Johns has the lowest correlation between the two datasets (r-value of 0.49); anomalies computed from SAWS station data show higher magnitudes compared to CHIRPS between 2003 and 2011, which could account for the low correlation. There is an agreement in wet and dry years with similar magnitudes for stations in proximity i.e., Cwebe Nature Reserve, Port St Johns, and Umtata. Similarly, extremely wet conditions were recorded at Humewood and Addo Elephant Park (**Fig. 4.9 c** and **d**) in 1994 and 2005, however, while the same conditions are recorded over Grahamstown, East London, and Dohne-AGR; the 2005 event was not as severe. The summer of 1985 and 1996 were the wettest in Cwebe Nature Reserve, Port St Johns, and Umtata. The time series also highlights the region is prone to multi-year events during the summer season, observed at all stations between 1982 – 1984, 1990 –1992, and 2015 – 2017, the 1982 – 1984 period being the driest at most stations. Six of the eleven stations have recorded normal to below-average rainfall since 2005 (**Fig. 4.9 c**, **d**, **e**, **h**, **i** and **j**), though the severity of these conditions varies between CHIRPS and SAWS station data. During the 2005 – 2018 period, CHIRPS data show more severe dry conditions, whereas SAWS data show some seasons with above-average rainfall, such as **(d)** Addo Elephant Park, **(e)** Grahamstown, **(i)** Port St Johns, and **(j)** Umthatha. The widespread prolonged dry periods during the core summer, which accounts for the largest proportion of seasonal rainfall would have major implications on water storage.

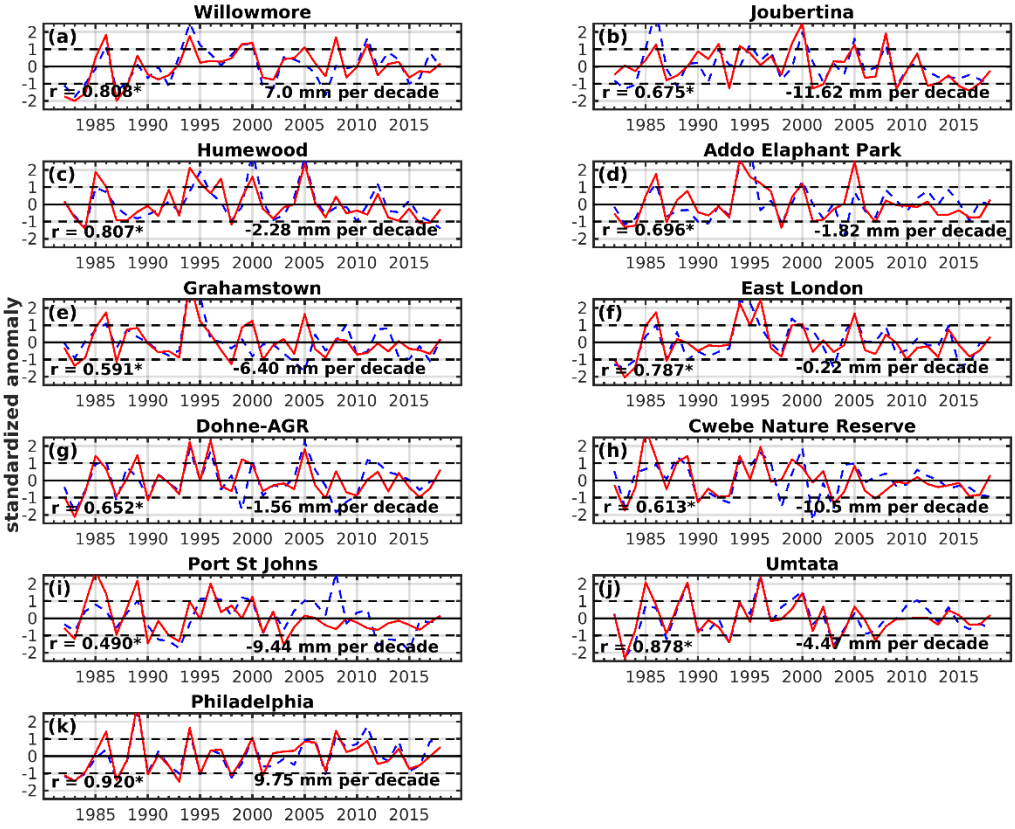

Figure 4.9: Same as **Fig. 4.8**, but for the DJF summer months.

4.4 Analysis of seasonal dry, light, moderate, and heavy wet days at stations

4.4.1 The spring – SON

Interannual variability in the number of dry days (1 mm/day), light (2 – 9 mm/day), moderate (10 – 30 mm/day), and heavy (> 30 mm/day) wet days are investigated along with the influence of the ENSO phenomenon to understand what contributes to a season being overall wet or dry (**Figs 4.10 - 4.15**). Seasonal spring anomalies show that stations have received less than average rainfall since 2015, with some stations such as Humewood, Cwebe, and Port St Johns

experiencing better rainfall in 2016/2017 and 2018. During the 2015 – 2020 period, inland stations like Willowmore and Philadelphia recorded prolonged dry conditions. These stations have also been found to record the most dry days (greater than 80) on average for the spring (**Fig. 4.10b** and **4.15b**). During the protracted dry 2015 – 2020 period they experienced above-average number of dry days and no moderate or heavy rainfall. Seasons recording extremely wet conditions as in 1996 (at Addo Elephant Park, Humewood, Joubertina, and Willowmore and Dohne-AGR) and 2006 (at Cwebe Nature Reserve, Port St Johns, and Umthatha) reveal that these extremely wet springs can result from increased numbers in all of the light, moderate, and heavy wet day categories, or more obviously in some cases from increased moderate and heavy wet days such as at Joubertina in 1996. East London, and Umthatha record the least dry days (65, 67, and 67 days, respectively). Stations with the most dry days (Willowmore and Philadelphia) also record the least number of light wet days (3 and 3.5 days, respectively), moderate (1.5 and 2.6), and heavy (0.3 and 0.4) wet days. Dohne-AGR receives the most light wet days (14 days), while Cwebe and Port St Johns on the northeastern coast have the most heavy wet days. On the other hand, not all very dry seasons show a marked increase in the numbers of dry days. For example at Willowmore, SON 1994 experienced well below average rainfall and considerably less dry days than average (**Figs. 4.10ab**). In general, there is not a close correspondence between dry day variability and rainfall anomalies reinforcing to the need to also consider the rainfall intensity categories used here.

A correlation analysis was used to further analyze the relationship between dry (wet) days and seasonal totals (**Table 4.1**). At all stations, the correlation values of light wet day variability with that of seasonal totals are much less than those with either moderate or heavy wet days with some stations showing virtually no correlation between totals and light wet days. Dry days have a strong correlation with seasonal rainfall. This is most pronounced for inland stations

Willowmore and Philadelphia. In general, the strongest correlations (r - values > 0.7) for wet days are between seasonal anomalies and heavy rainfall days, except at Addo Elephant Park, Umathatha, and Philadelphia, where moderate wet days are slightly higher correlated with totals. Thus, the two heavier rainfall categories play an important role in determining whether the seasonal total as a whole is wet or dry, pointing to the need for seasonal forecasters to consider the possibility of providing more detailed information than just whether the total is likely to be near, well below or well above average. Furthermore, these differences in the relationships between seasonal totals and wet day categories across stations imply that the impacts of large rainfall-producing systems on the various stations may differ. Relatively small differences in the locations of cloud bands (e.g. Hart et al., 2013) across South Africa or the tracks of cut-off lows can have substantial impacts on the spatial distributions of rainfall received. Also, as temperatures increase towards the later spring and air masses become more unstable, the chances of random air mass thunderstorms over particularly the eastern basin of the region starts to increase. Such storms can cause heavy falls and damage at particular stations on occasion such as the tornado occurrence in Umthatha in December 1998 (Rouault et al., 2002).

Since ENSO has been previously found to impact dry spells and wet day occurrences over many parts of South Africa (Reason et al., 2005, Thoithi et al., 2021), the Niño 3.4 index is plotted in each station rainfall figure (**Figs. 4.10-15e)** as well as its correlation with the rain day categories listed in **Table 4.2**. Note however, that in general ENSO typically has a stronger influence on summer than spring rainfall totals over South Africa (Lindesay, 1988, Reason et al., 2002). Thirteen of the forty springs between 1981 and 2020 were El Niño years (1982, 1986, 1987, 1991, 1994, 1997, 2002, 2004, 2006, 2009, 2014, 2015, 2018). Consistent with earlier work suggesting that ENSO typically impacts South African rainfall from December to

March, the correlations between spring rainfall, wet days and ENSO are generally weak. Only Willowmore shows a statistically significant ($r = 0.33$) positive relationship (light wet days). Furthermore, the sign of the relationship varies between stations **Table 4.2** suggests that there is no clear relationship with ENSO rainfall during spring, which may be attributed to the seasonal nature of the mode of variability in which the Indian Ocean SST and atmospheric circulation anomalies over southern Africa are still relatively weak compared to later in the summer (Reason et al., 2000).

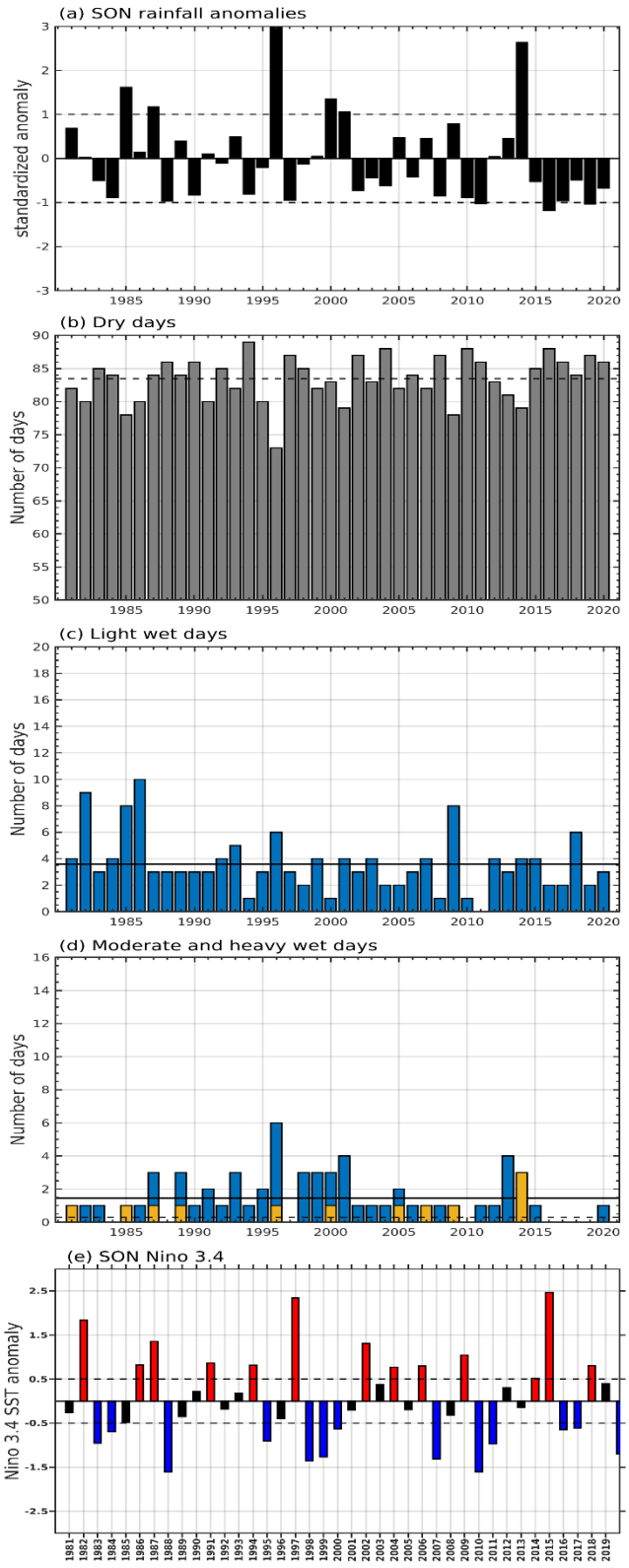

Figure 4.10: Spring (SON) **(a)** standardized anomalies for the Willowmore station (bars), **(b)** dry (σ=3.43) **(c)** light (σ=2.17), **(d)** moderate (blue bars; σ=1.36) and heavy (yellow bars; σ=0.61) wet day totals, solid and dotted lines indicate the seasonal mean for moderate and heavy wet days, respectively. **(d)** Illustrates the corresponding Niño 3.4 SST anomalies. Years indicate the last month of the season i.e., 1982 denotes the 1981/82 season.

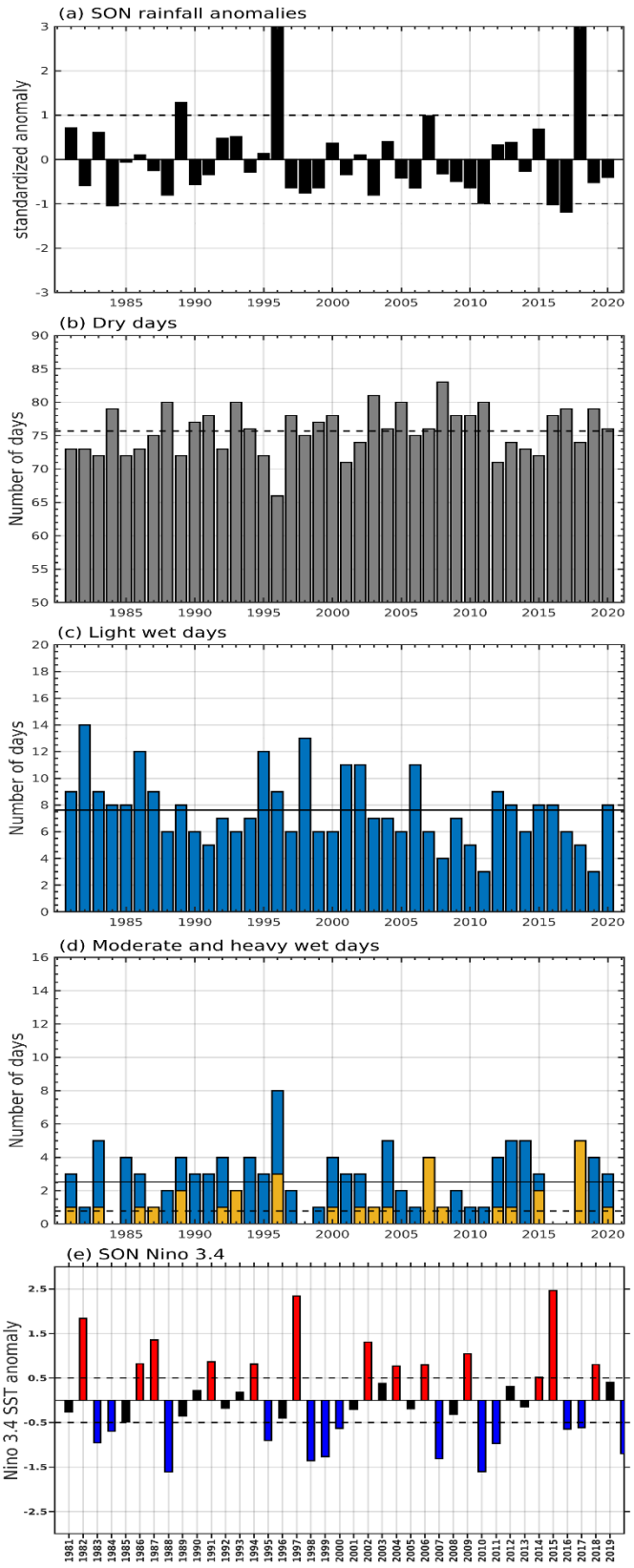

Figure 4.11: Same as **Fig. 4.10**, but for Joubertina station**. (b)** dry (σ=3.50) **(c)** light (σ=2.57), **(d)** moderate (blue bars; σ=1.84) and heavy (yellow bars; σ=1.14) wet day totals, solid and dotted lines indicate the seasonal mean for moderate and heavy wet days, respectively.

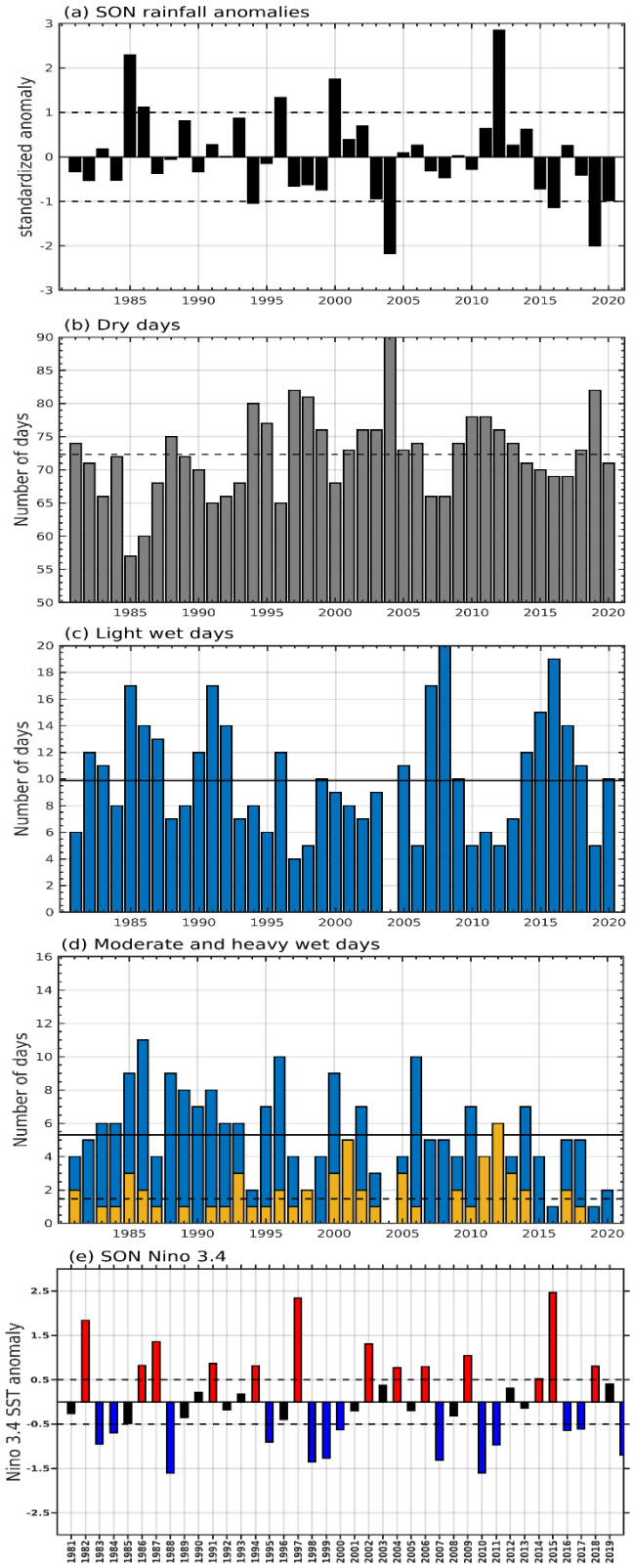

Figure 4.12: Same as **Fig. 4.10**, but for Grahamstown station. **(b)** dry (σ=6.36) **(c)** light (σ=4.51), **(d)** moderate (blue bars; σ=2.65) and heavy (yellow bars; σ=1.43) wet day totals, solid and dotted lines indicate the seasonal mean for moderate and heavy wet days, respectively.

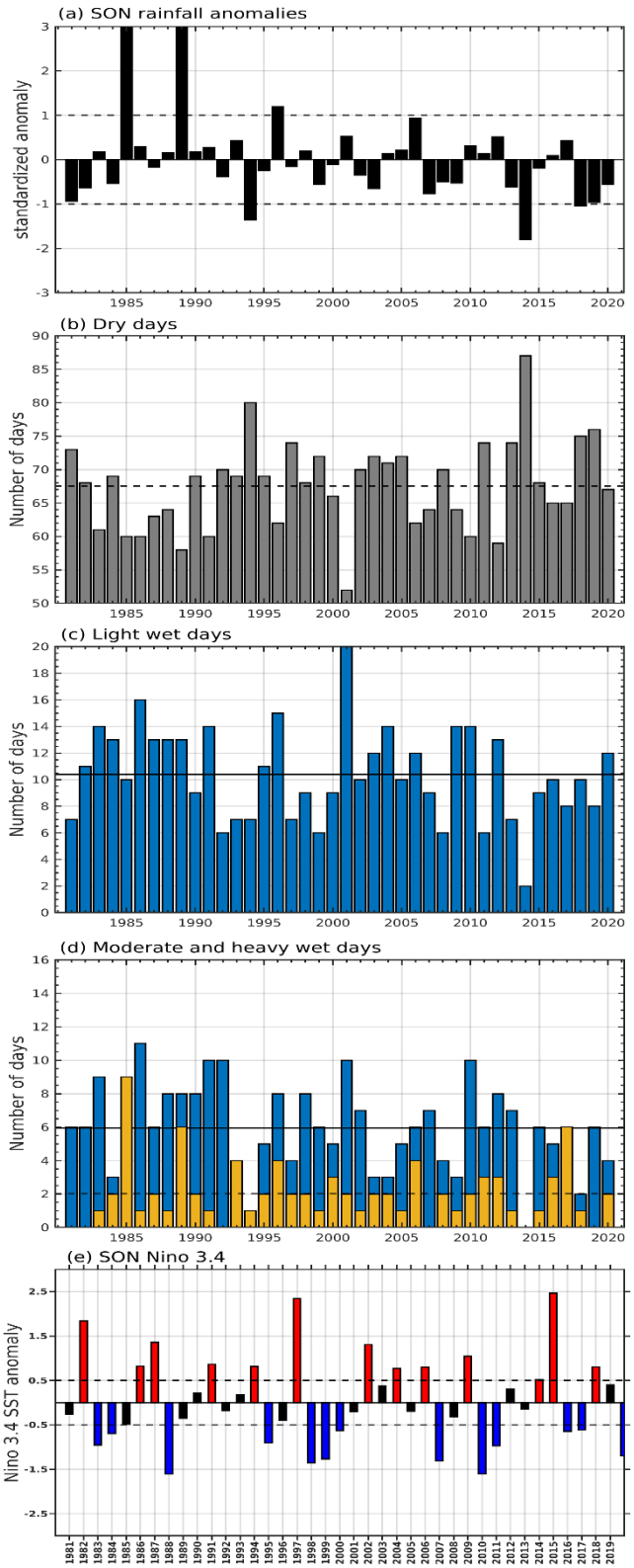

Figure 4.13: Same as **Fig. 4.10**, but for East London station. **(b)** dry (σ=6.65) **(c)** light (σ=3.51), **(d)** moderate (blue bars; σ=2.65) and heavy (yellow bars; σ=1.85) wet day totals, solid and dotted lines indicate the seasonal mean for moderate and heavy wet days, respectively.

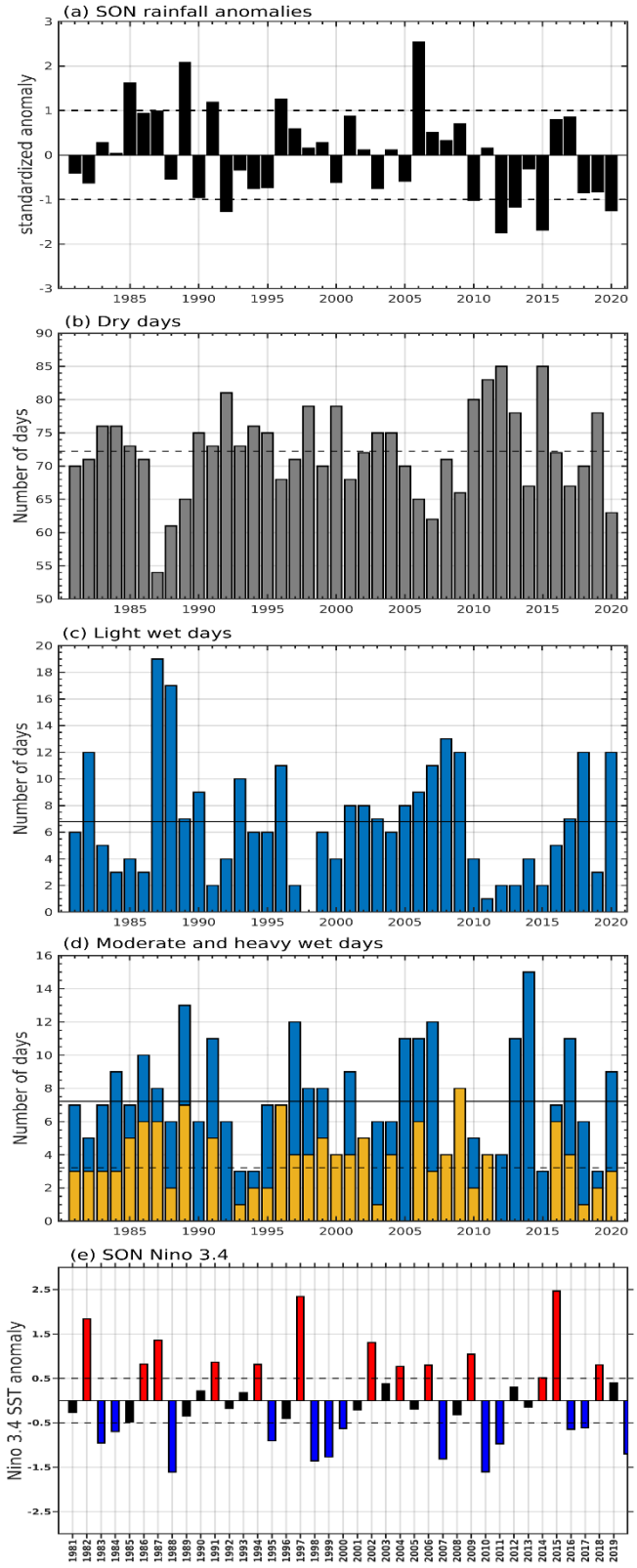

Figure 4.14: Same as **Fig. 4.10**, but for Port St Johns station. **(b)** dry (σ=6.64) **(c)** light (σ=4.37), **(d)** moderate (blue bars; σ=3.21) and heavy (yellow bars; σ=2.24) wet day totals, solid and dotted lines indicate the seasonal mean for moderate and heavy wet days, respectively.

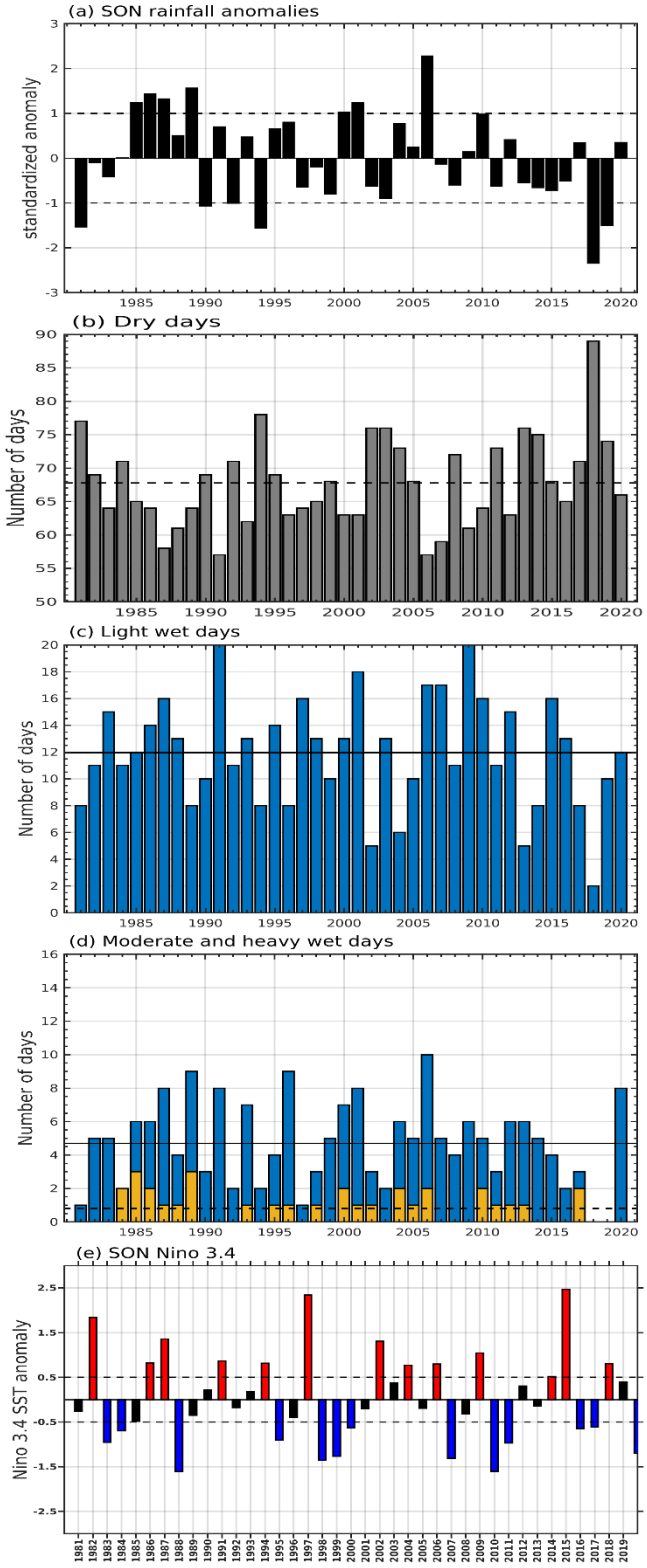

Figure 4.15: Same as **Fig. 4.10**, but for Umthatha station. **(b)** dry (σ=6.72) **(c)** light (σ=4.17), **(d)** moderate (blue bars; σ=2.55) and heavy (yellow bars; σ=0.91) wet day totals, solid and dotted lines indicate the seasonal mean for moderate and heavy wet days, respectively.

Table 4. 1 Correlation values indicate the relationship between dry days, light, moderate, heavy wet days, and spring (SON) seasonal rainfall totals. Highlighted (bold) values indicate significance at the 95% level.

Stations	Dry days	Light wet	Moderate Wet	Heavy wet
Willowmore	**-0.83**	**0.41**	**0.71**	**0.76**
Joubertina	**-0.60**	0.04	**0.58**	**0.85**
Humewood Golf Club	**-0.66**	**0.38**	**0.42**	**0.80**
Addo Elephant Park	**-0.70**	0.27	**0.79**	**0.75**
Grahamstown	**-0.53**	0.13	**0.65**	**0.73**
East London	**-0.66**	**0.38**	**0.45**	**0.84**
Dohne-AGR	**-0.71**	**0.42**	**0.70**	**0.76**
Cwebe Nature Reserve	**-0.55**	**0.31**	**0.45**	**0.82**
Port St Johns	**-0.52**	0.14	**0.44**	**0.83**
Umthatha	**-0.75**	**0.45**	**0.83**	**0.72**
Philadelphia	**-0.83**	**0.46**	**0.83**	**0.53**

Table 4.2 Correlation values at stations between spring seasonal rainfall, light, moderate, heavy wet days, and the Niño 3.4 index. Values that are highlighted (bold) are significant at the 95 percent level.

Stations	Seasonal rainfall	Dry days	Light wet	Moderate wet	Heavy wet
Willowmore	0.02	-0.03	**0.33**	-0.08	0.00
Joubertina	0.08	-0.14	0.15	0.09	0.06
Humewood Golf Club	-0.12	0.28	-0.17	0.09	-0.07
Addo Elephant Park	-0.08	-0.05	0.07	-0.11	-0.08
Grahamstown	-0.10	0.09	0.01	-0.07	-0.06
East London	-0.17	0.19	-0.01	-0.23	-0.19
Dohne-AGR	-0.09	0.15	-0.04	-0.26	0.05
Cwebe Nature Reserve	-0.14	0.07	-0.02	0.04	-0.08
Port St Johns	0.00	0.02	0.02	-0.06	0.00
Umthatha	-0.12	0.12	0.04	-0.05	-0.22
Philadelphia	-0.09	-0.02	-0.11	-0.03	-0.07

4.4.2 The core summer – DJF

Figures 4.16 – 4.21 show time series of summer rainfall anomalies, dry / wet days at each station and the Niño 3.4 index. Summer standardized anomalies show that over the last decade, many stations have received below average totals, particularly since 2015. Multi-year events are not uncommon during summer i.e 1990 – 1993 (Grahamstown, East London, Cwebe Nature Reserve, and Port St Johns) and 1995 – 1997 (Willowmore, Joubertina, Cwebe Nature Reserve and Port St Johns).

As for SON, there is not a one to one correspondence between variability in rainfall totals and the number of dry days. In several cases, the former can be well below average while dry days are close to average or even below average such as for some seasons during 2015 – 2020 at Willowmore and Joubertina (**Figs. 4.16-17ab**). In some cases, very wet summers such as in 1994/95 at Grahamstown (**Fig. 4.18**) can be matched up with obvious decreases in dry days and increases in heavy rain days but in general there are varying contributions from the rainfall categories to the totals received. However, summers in which stations recorded no moderate to heavy rainfall days i.e 1982/83 and 2006/07 at Willowmore; 2017/18 at Willowmore 2014/15 at Port St Johns; 2000/01 at Umthatha (**Fig. 4.16d**, **Fig. 4.20d**, and **Fig. 4.21d**), do correspond to those with below-average seasonal rainfall totals. Given that heavy rain days can cause agricultural or other damage, and that too many dry days are bad for crops even if the seasonal total is favorable, these findings highlight the need for long-term forecasting to consider the possibility of providing more detailed information than is currently provided.

The correlation analysis of summer rainfall totals and wet days (**Table 4.3**) reveals that nine of the eleven stations show stronger relationships between totals and heavy wet days than between the former and moderate wet days although, in all cases, the coefficients are relatively large and statistically significant. Unlike SON, where light rain days were less significantly correlated with totals compared to moderate and heavy rain days, DJF has seven stations with relatively strong coefficients (around 0.5 or larger) for three stations. Thus, **Tables 4.1** and **4.3** imply that all categories of rain intensity are relatively important to anomalies in summer totals whereas in spring, variability in the number of light rain days has little relationship with the seasonal totals. This difference may at least partially result from ridging anticyclones (which in general would be expected to result in lower rain intensities than more organised convective systems like cloud bands) being less likely to produce much rainfall in spring compared to summer when SSTs in the neighbouring ocean beneath the anticyclones are warmer and the overlying air masses more unstable.

As described earlier, ENSO has been shown to have a strong influence on rainfall totals for the summer (DJF) season over South Africa as well as on dry spell frequencies and moderate wet day counts (Usman and Reason, 2004, Reason et al., 2005, Thoithi et al., 2021) with generally reduced rainfall and increased dry spell frequencies during El Niño and the reverse for La Niña summers. **Figures 4.16-4.21** show several exceptions to this expectation, such as average or even below average seasonal rainfall during the 1998/99 La Niña summer at many stations with three exceptions, while the following 1999/2000 summer (also a La Niña summer) was typically wet everywhere. **Table 4.4** further highlights the nonlinear nature in the relationship between rainfall of different intensity and Niño 3.4**.** Moderate rainfall shows the most significant relationship with Niño 3.4 in DJF whereas in SON there were essentially no relationships at all. Seasonal totals at stations exhibit the most coherent signal with the Niño

3.4 index, with summer rainfall being found to be negatively correlated with summer rainfall. This is discovered to be more pronounced and statistically significant at eastern stations (Cwebe Nature Reserve, Port St Johns, Umthatha and Philadelphia).

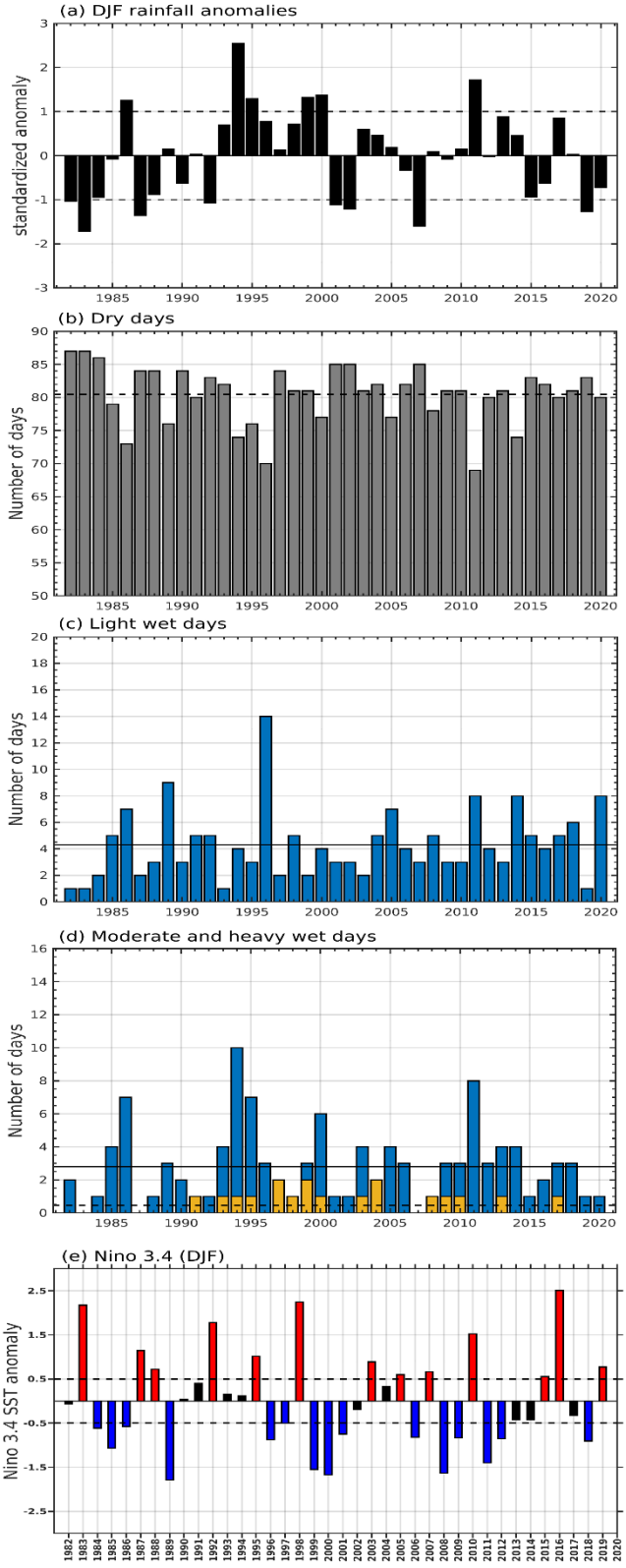

Figure 4.16: Summer (DJF) (a) standardized anomalies for the Willowmore station (bars), **(b)** dry (σ=4.33) **(c)** light (σ=2.64), **(d)** moderate (blue bars; σ=2.28) and heavy (yellow bars; σ=0.64) wet day totals, solid and dotted lines indicate the seasonal mean for moderate and heavy wet days, respectively. **(d)** Illustrates the corresponding Niño 3.4 SST anomalies. Years indicate the last month of the season i.e., 1982 denotes the 1981/82 season.

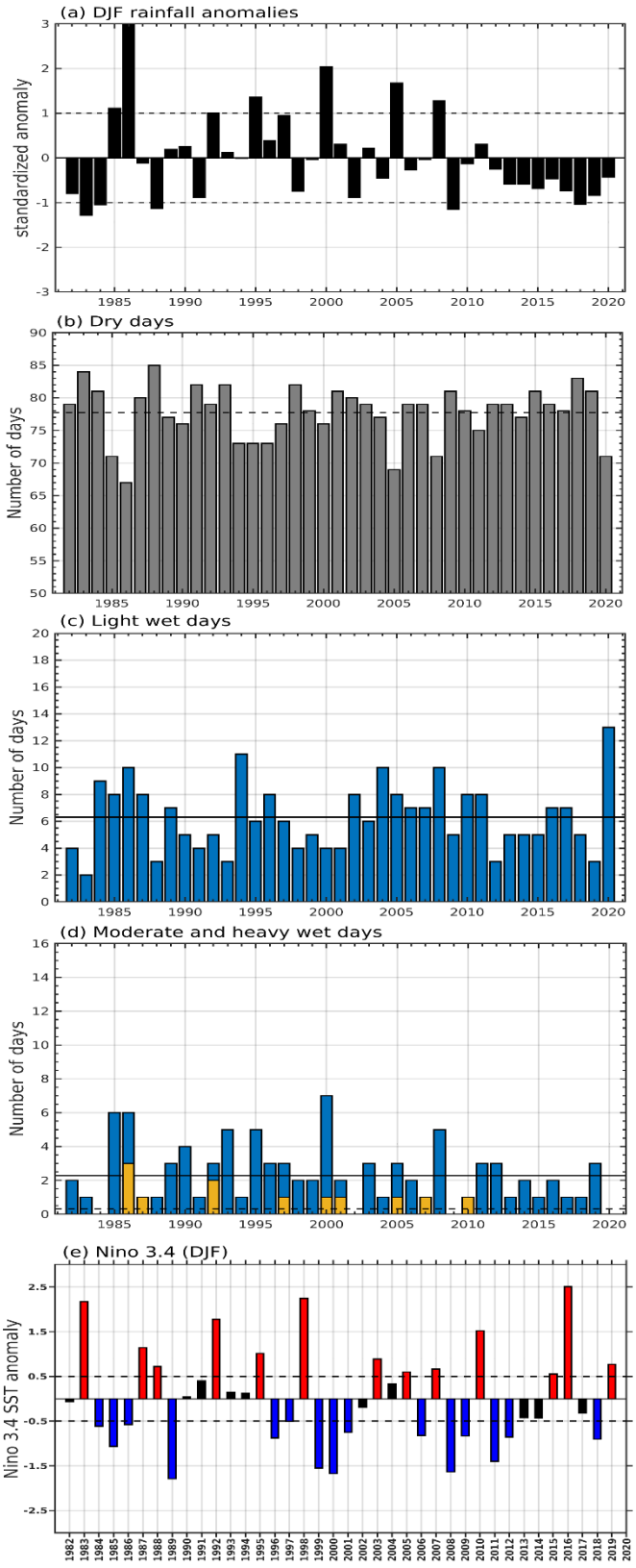

Figure 4.17: Same as **Fig. 4.16** but, for Joubertina station. **(b)** dry (σ=4.18) **(c)** light (σ=2.51), **(d)** moderate (blue bars; σ=1.83) and heavy (yellow bars; σ=0.66) wet day totals, solid and dotted lines indicate the seasonal mean for moderate and heavy wet days, respectively.

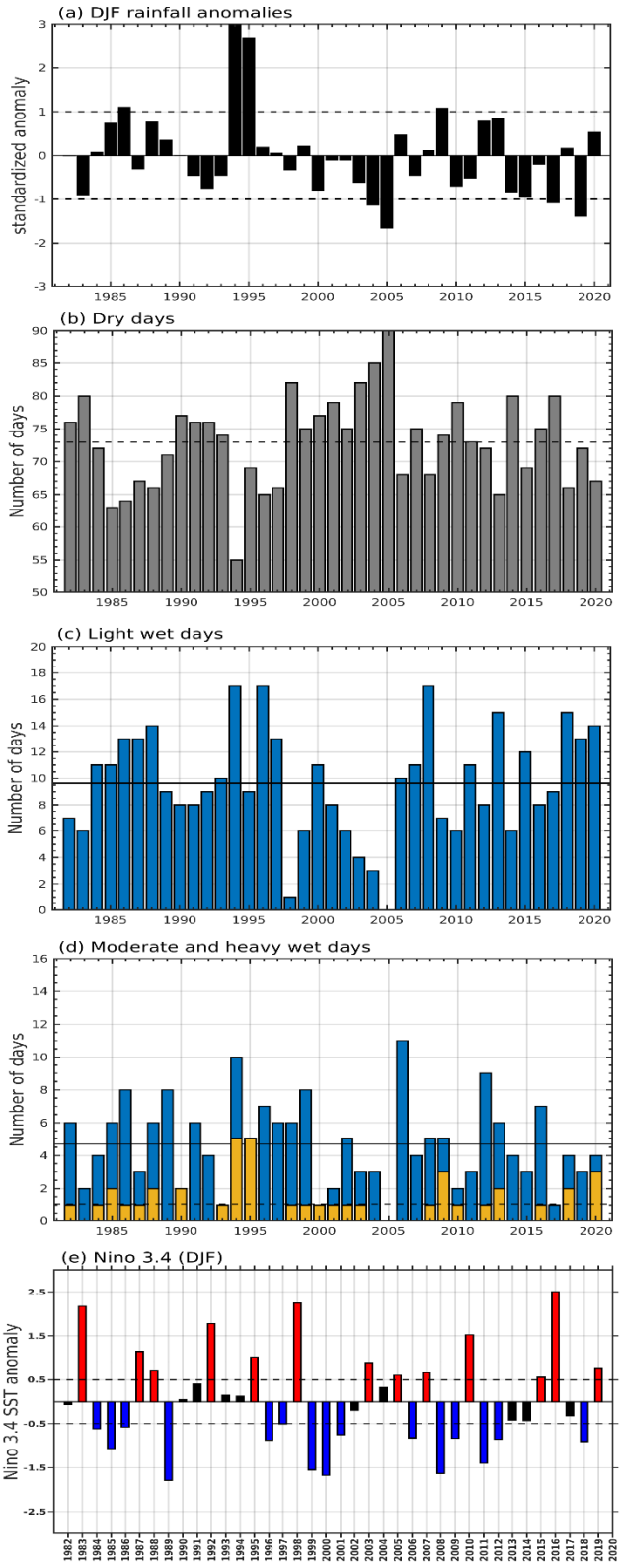

Figure 4.18: Same as **Fig. 4.16** but, for Grahamstown station. **(b)** dry (σ=6.94) **(c)** light (σ=4.16), **(d)** moderate (blue bars; σ=2.59) and heavy (yellow bars; σ=1.26) wet day totals, solid and dotted lines indicate the seasonal mean for moderate and heavy wet days, respectively.

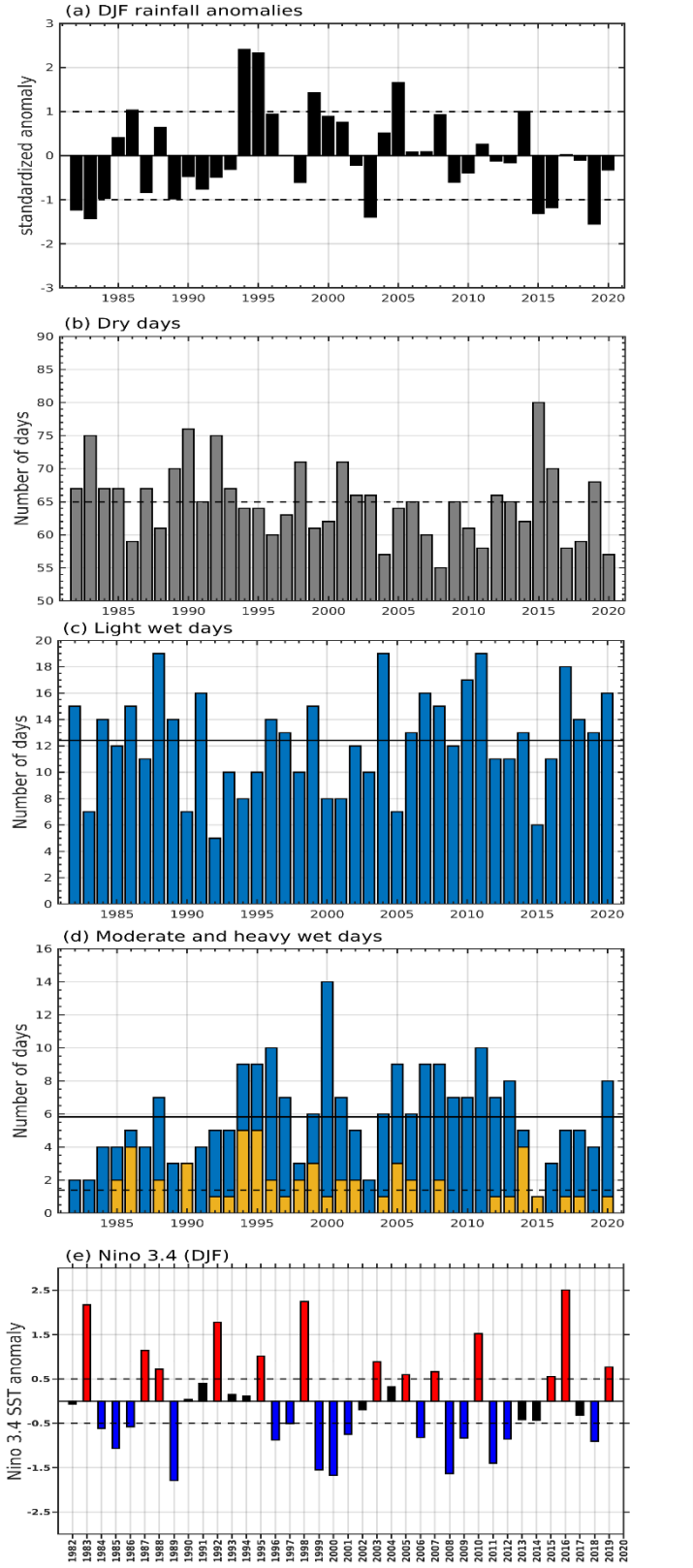

Figure 4.19: Same as **Fig. 4.16** but, for East London station. **(b)** dry (σ=5.67) **(c)** light (σ=3.75), **(d)** moderate (blue bars; σ=2.84) and heavy (yellow bars; σ=1.43) wet day totals, solid and dotted lines indicate the seasonal mean for moderate and heavy wet days, respectively.

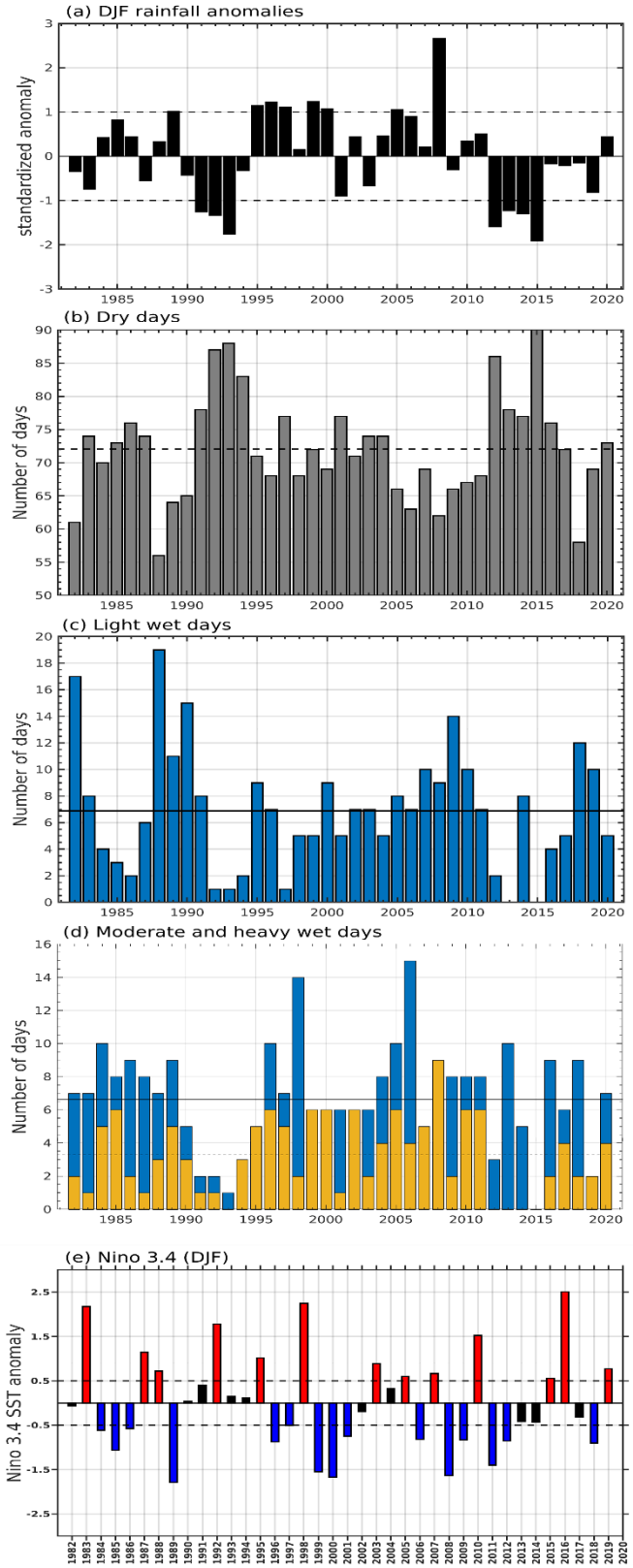

Figure 4.20: Same as **Fig. 4.16** but, for Port St Johns station. **(b)** dry (σ=7.89) **(c)** light (σ=4.53), **(d)** moderate (blue bars; σ=3.35) and heavy (yellow bars; σ=2.31) wet day totals, solid and dotted lines indicate the seasonal mean for moderate and heavy wet days, respectively.

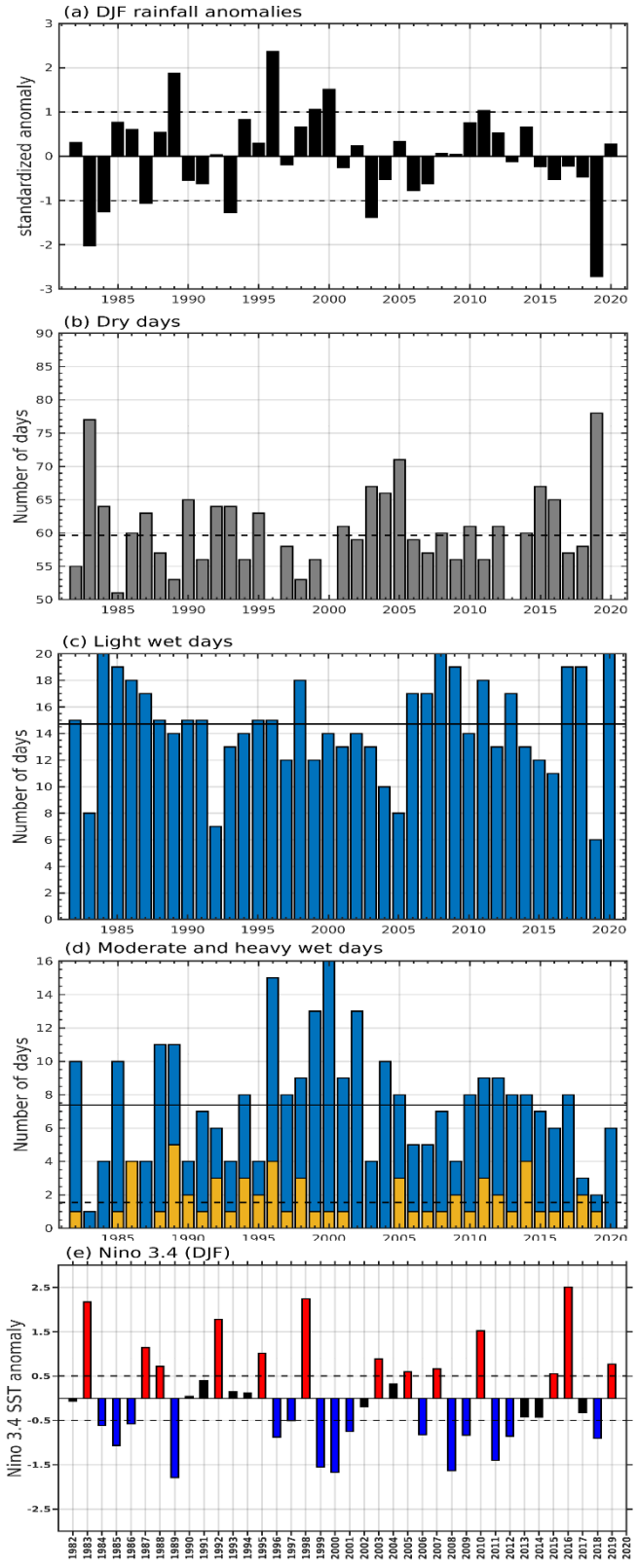

Figure 4.21: Same as **Fig. 4.16** but, for Umthatha station. **(b)** dry (σ=7.02) **(c)** light (σ=3.94), **(d)** moderate (blue bars; σ=3.45) and heavy (yellow bars; σ=1.29) wet day totals, solid and dotted lines indicate the seasonal mean for moderate and heavy wet days, respectively.

Table 4.3 Correlation values indicating the relationship between dry days, light, moderate, and heavy wet days, and summer (DJF) seasonal rainfall totals. Highlighted values indicate significance at the 95% level.

Stations	Dry days	Light wet	Moderate wet	Heavy wet
Willowmore	**-0.76**	**0.32**	**0.85**	**0.53**
Joubertina	**-0.77**	0.30	**0.79**	**0.68**
Humewood Golf Club	**-0.65**	**0.36**	**0.51**	**0.78**
Addo Elephant Park	**-0.66**	**0.47**	**0.57**	**0.70**
Grahamstown	**-0.72**	**0.43**	**0.65**	**0.83**
East London	**-0.50**	0.05	**0.68**	**0.82**
Dohne-AGR	**-0.80**	**0.53**	**0.72**	**0.76**
Cwebe Nature Reserve	**-0.62**	**0.42**	**0.53**	**0.84**
Port St Johns	**-0.62**	0.24	**0.50**	**0.91**
Umthatha	**-0.74**	0.24	**0.78**	**0.61**
Philadelphia	**-0.87**	**0.62**	**0.73**	**0.82**

Table 4.4 Correlation values at stations between summer seasonal rainfall, light, moderate, heavy wet days, and Niño 3.4 index. Values that are highlighted (bold) are significant at the 95 percent level.

Stations	Seasonal rainfall	Dry days	Light wet	Moderate wet	Heavy wet
Willowmore	**-0.32**	**0.38**	-0.29	**-0.32**	-0.09
Joubertina	-0.23	**0.36**	-0.14	**-0.31**	0.09
Humewood Golf Club	-0.21	0.08	-0.04	0.07	-0.21
Addo Elephant Park	**-0.31**	**0.40**	-0.22	-0.26	-0.16
Grahamstown	-0.22	**0.33**	**-0.34**	-0.23	0.02
East London	**-0.32**	**0.45**	-0.27	**-0.38**	-0.14
Dohne-AGR	-0.20	0.20	-0.06	-0.30	-0.03
Cwebe Nature Reserve	**-0.42**	0.25	-0.13	-0.16	**-0.45**
Port St Johns	**-0.38**	0.20	-0.04	-0.08	**-0.38**
Umthatha	**-0.44**	**0.54**	**-0.36**	**-0.42**	-0.22
Philadelphia	**-0.56**	**0.48**	-0.18	**-0.46**	**-0.52**

4.5 Rainfall trends

4.5.1 Trends in SON rainfall

Figure 4.22 shows the trend in SON rainfall for CHIRPS data along with that of the available stations over the 1981–2018 period. Most of the region shows a statistically significant decline in spring rainfall, particularly in the east, north, and northeast. The weak decrease near Port Elizabeth is not significant but part of the catchment areas in the "west" basin to the north and northwest of this city are. Given that the decrease is much stronger in the wetter eastern half of the province, the results imply that the rainfall gradient across the province (**Fig. 4.4**) is weakening, at least in spring. The stronger decrease in the east is concerning given the larger rural population here and its greater importance for agriculture to the provincial economy (particularly dairy, pineapples and tea). Maps of the trends in the number of dry days (< 1 mm per day), light rain days (2–9 mm per day), moderate rain days (10–30 mm per day), and heavy rain days (> 30 mm per day) across the Eastern Cape are plotted in **Fig. 4.23** using CHIRPS and station data. Both stations and CHIRPS show an increase in the number of dry days which is found to be strongest over the north and northeast (**Fig. 4.23a**). This is consistent with the decreasing trends in seasonal rainfall (**Fig. 4.22**). Although similar patterns are observed for light and moderate wet days, light rain days show the strongest decline over the north, northeast and inland (greater than 1 day per decade). In the far west, it is notable that the area of significant decrease in moderate rain days represents part of the Kouga and Impofu dam catchment areas in the "west" basin that feed into the Port Elizabeth urban area. Since on average this area is found to record the most dry days, also corresponding to high frequency of dry spells (such as Thoithi et al., 2021), a decrease in rain days implies a threat to the water security for this catchment. Heavy rain days show a significantly decreasing trend over large areas in the east and northeast (**Fig. 4.23d**).

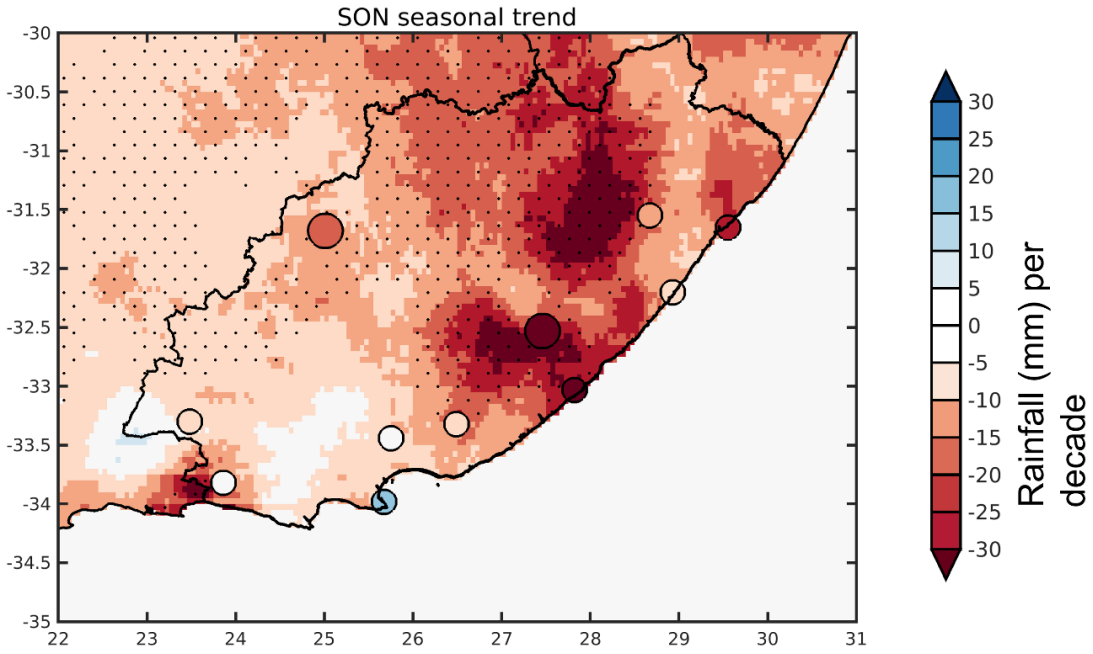

Figure 4.22: Trend in CHIRPS (shaded; mm per decade) and SAWS stations (circles; mm per decade) SON rainfall over the period 1981–2018. Stippling or larger circles denotes values significant at a 95% level using a two-tailed Mann–Kendall test.

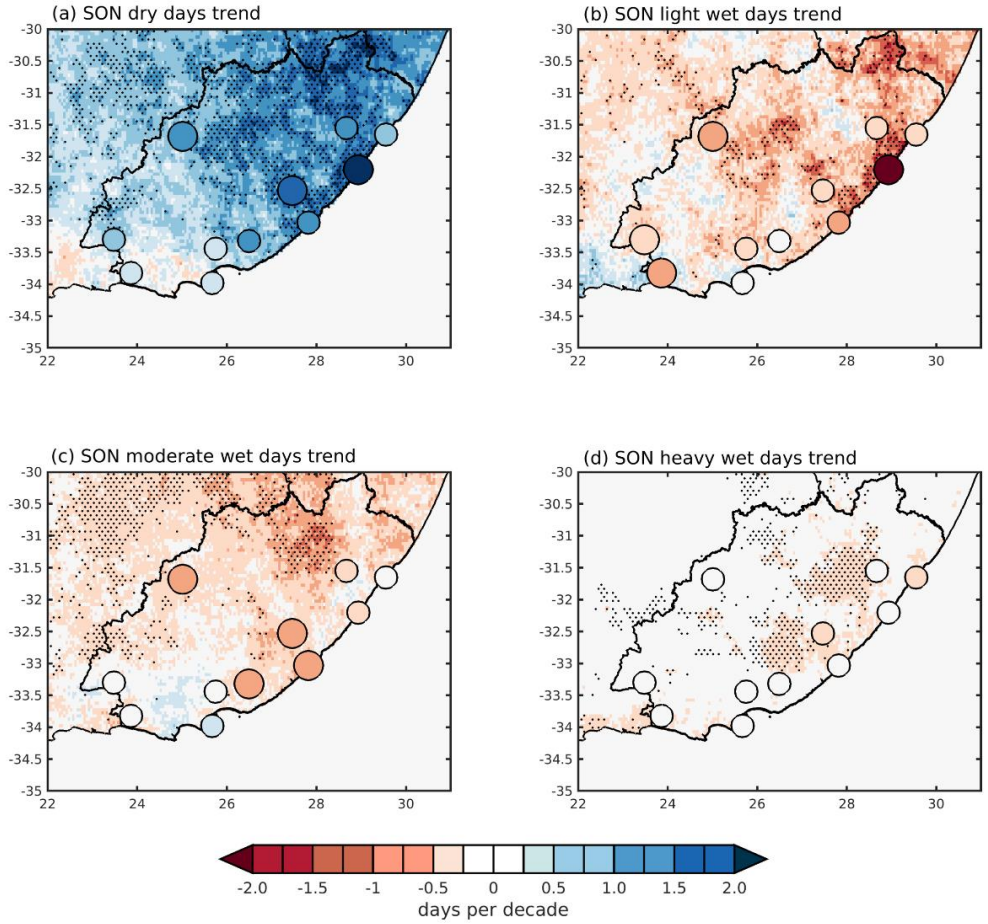

Figure 4.23: Trends in SON CHIRPS (shaded; days per decade) and SAWS stations (circles; days per decade) **(a)** dry, **(b)** light, **(c)** moderate, and **(d)** heavy rainfall days for the 1981–2020 period. Larger circles denote significant trends at the 95% level.

4.5.2 Trends in DJF rainfall

Trend patterns in DJF totals across the region (**Fig. 4.24**) are less robust than for SON which are reflected in the mixed signs of the station circle trends. Two small coastal areas in the far northeast and far southwest have a decreasing trend, but it is not statistically significant. Whereas a relatively large northern inland area indicates significantly increasing rainfall totals in DJF. The latter area also shows a significant decrease in dry day frequencies (also seen at Philadelphia station) consistent with that found by Thoithi et al. (2021) for a band stretching from the Eastern Cape northeast towards Namibia (**Fig 4.25a**). Cwebe Nature Reserve station, together with a small area just north of the Eastern Cape / KwaZulu-Natal provincial border, show significantly increasing trends in dry days somewhat consistent with the rainfall trends here. **Figs. 4.24, 4.25a** suggest that much of the wetting in the northern inland part of the region is due to an increasing trend in moderate wet day counts. Thoithi et al. (2021) found similar trends for the interior southeast South African region, which included the inland Eastern Cape. This region is part of a dry spell frequency gradient that stretches southeast from southern Angola to southern Africa, and it is associated with the preferred westernmost location of cloud band formation. The significant increase in moderate rainfall days observed this season suggests a weakening of the dry spell gradient and more consistent rainfall. **Fig. 4.25d** shows that a few small areas have experienced a statistically significant decrease in heavy wet days but far less than is the case for SON (**Fig. 4.23d**). Some of the DJF areas of significant heavy rain day decrease also show significant light rain day decrease. If these summer trends continue, then there may be significant water implications for the east catchment basin, as this season contributes a significant portion of the annual totals.

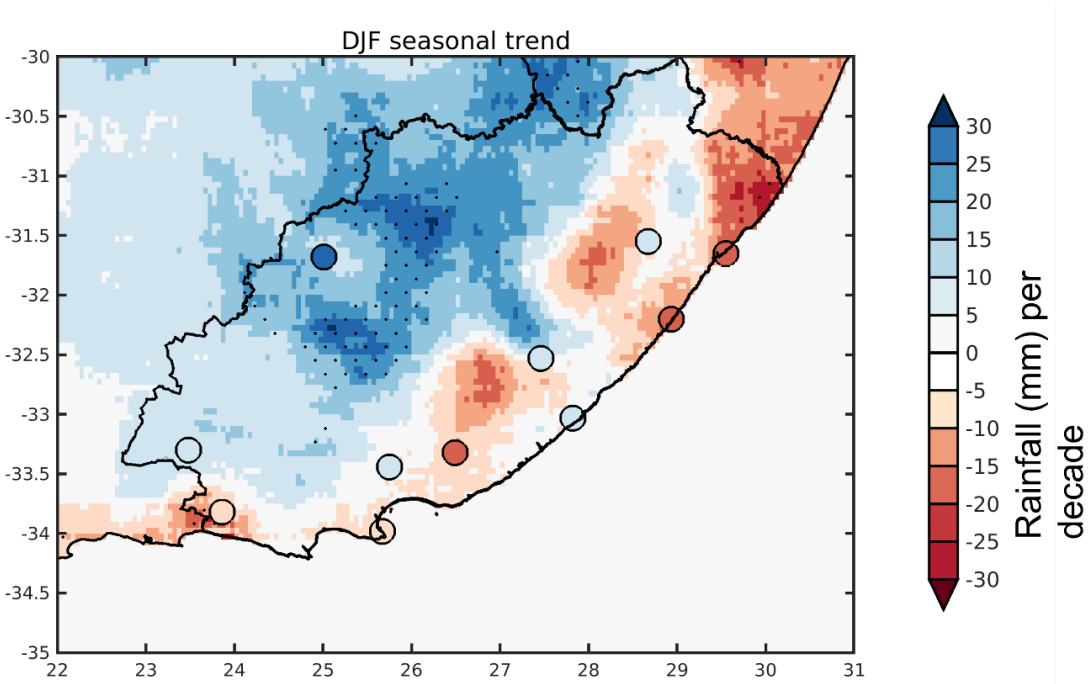

Figure 4.24: Trend in CHIRPS (shaded; mm per decade) and SAWS stations (circles; mm per decade) DJF rainfall over the period 1981–2018. No stations showed significant trends. Stippling denotes values significant at a 95% level using a two-tailed Mann–Kendall test.

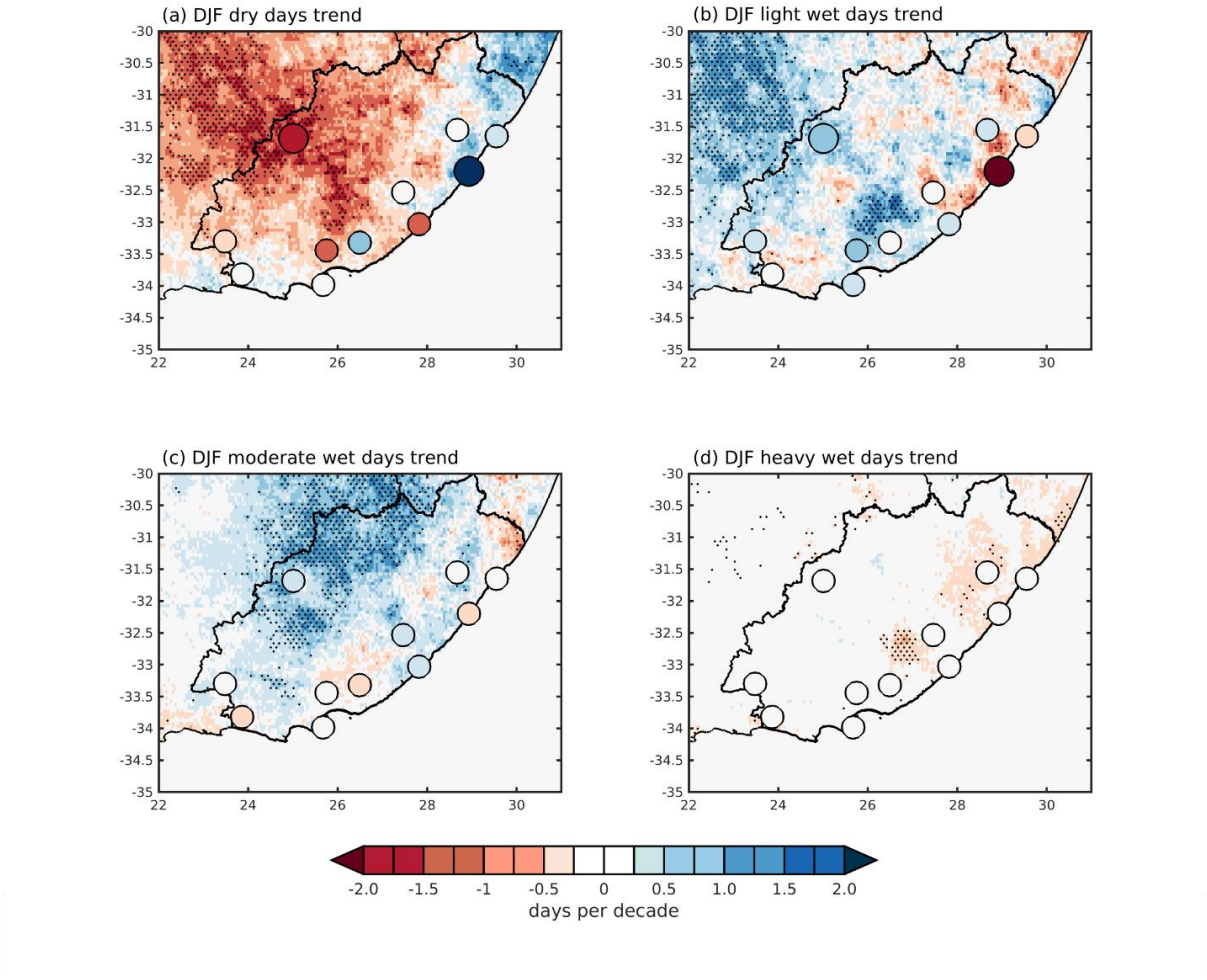

Figure 4.25: Trends in DJF CHIRPS (shaded; days per decade) and SAWS stations (circles; days per decade) **(a)** dry, **(b)** light, **(c)** moderate, and **(d)** heavy rainfall days for the 1981–2020 period. Larger circles denote significant trends at the 95% level.

4.6 Summary

The main purpose of this chapter was to examine spring (SON) and summer (DJF) rainfall characteristics and their variability and trends over the Eastern Cape region. Due to the scarcity of available station data, this chapter used CHIRPS gridded data to be able to consider spatial differences in more detail. Strong correlations between time series of standardized rainfall anomalies for eleven rain gauge stations (SAWS) and the corresponding CHIRPS-derived rainfall for those locations for both spring and summer suggests that CHIRPS can adequately represent rainfall for this part of Africa. Previous studies have found similar good correlations for rainfall anomalies in other parts of South Africa or Botswana (Thoithi et al., 2021, Moses et al., 2022). CHIRPS should however be used with caution as there are some differences in seasonal rainfall at certain locations. Funk et al. (2015), for example, highlight how CHIRPS can sometimes poorly estimate daily rainfall, which is attributed to the processes involved in computing daily CHIRPS-based rainfall data through the disaggregation of a 5-day rainfall product (Funk et al., 2015, du Plessis and Kibii, 2021). Poor daily estimates would then have an impact on derived rainfall characteristics analysis. However, when compared to other remote sensing products, the CHIRPS product has been shown to be the most accurate in Africa (Dinku et al., 2018, Anghileri et al., 2022, Gebrechorkos et al., 2018), providing high spatial and temporal resolution rainfall data for areas with limited station data, such as the Eastern Cape province of South Africa.

Rainfall in the region is found to have a high degree of interannual variability, with frequent occurrences of prolonged dry periods in recent decades, the most recent and common across stations being 2015–2020. Dry conditions during this period are observed for both the spring and summer seasons. To understand the nature of the dry and wet conditions interannual variability in rainfall characteristics was considered. On average, rain days as well as seasonal

rainfall totals typically increase in rainfall from west to east across the province. The west and east basins are used for comparison since they are important for water resource management in the province and to capture regional rainfall differences. The wetter eastern part tends to experience more heavy rainfall days than the west, which is attributed to the warm Agulhas Current being very close to the coast north of about 33°S as well as the increased influence of relatively moist unstable air masses here than further west in the province. Moderate rainfall days appear important for variability in rainfall totals over the inland regions during spring while both this category and heavy rain days are significant over the east basin, particularly in summer. An examination of ENSO's influence on rainfall reveals no obvious relationship for the spring totals or rain days, but a significant relationship with rainfall totals and rain days for many stations during the summer period. ENSO is also found to have a stronger relationship with rainfall over the northeast than the southwest of the province during this season.

Trends in spring and summer rainfall characteristics were also investigated. Most of the province shows a statistically significant decline in spring rainfall totals and increase in dry days, particularly in the east and northeast. This east/northeastern area is in fact part of a larger region of eastern South Africa which shows significant decreasing trends in spring rainfall totals and rain days (**Figs. 4.22-4.23**). Elsewhere, part of the dam catchment areas for the largest city of Port Elizabeth also shows significantly decreasing trends. Overall, the results suggest that the rainfall gradient across the province is weakening, at least in spring. Most of the decreasing rainfall trend seems to result from a reduction in the number of light and moderate wet days. Summer rainfall from CHIRPS shows a significant increase inland (largely due to a significant increase in moderate wet days) and at the single available SAWS station (Philadelphia). This lack of adequate station data inland poses problems for verifying satellite derived rainfall data sets such as CHIRPS and GPM. Two small coastal areas showed a

significant decrease in rainfall totals and in moderate wet days. In general, however, the summer trend patterns are less coherent than those in spring. Summer rainfall trends are consistent with findings of a decrease in dry spell frequency along the western bound of the preferred cloud band location during the season (Thoithi et al., 2021). On the contrary, early summer observes an increase in the frequency of dry spells. This has serious implications for agricultural activity in the region because most farmers rely on rainfed agriculture, so early summer rains are critical for the start of the planting season. In addition, the region's water shortages are exacerbated by a persistent decrease in rainfall in parts of the northeast between spring and summer.

Having considered variability and trends in rainfall totals and rain day frequencies for spring and summer, the following chapter investigates circulation and SST anomalies that may be associated with these characteristics.

Chapter five: Circulation patterns and regional features influencing anomalous spring and summer rainfall

5.1 Introduction

The previous chapter has shown that rainfall across Eastern Cape has a high degree of interannual variability, often with a run of seasons tending to be either very dry or very wet. Recent decades have been found to be more prone to dry conditions, which has serious implications for water availability throughout the region. Rainfall is also found to vary spatially with a strong gradient both along the coast and, particularly in the west, from the coast towards the inland where the southern part of the Great Karoo semidesert is located. To highlight the spatial differences in rainfall patterns, the Eastern Cape is classified into two subdomains, the west and east basins, which represent the province's water management areas. The majority of the province has seen a statistically significant decrease in spring rainfall totals, particularly in the east and northeast (Mahlalela et al., 2020). During this season, trends indicate a weakening of the rainfall gradient between the west and the east of the province. For the summer, the chapter showed that the trends are not as coherent; however, the inland is found to have a significant increase in seasonal rainfall which is associated with an increase in moderate rainfall days, whereas the northeast coast experiences a decrease in rainfall for this season, but it is not statistically significant.

The purpose of this chapter is to investigate the circulation patterns and features associated with the observed interannual variability and trends over the region. A composite analysis is used to examine the circulation anomalies associated with anomalously dry and wet seasons during the study period. **Table 5.1** shows that the springs (SON) of 1981, 1990, 1994, 2008, and 2016 were considered anomalously dry, while the springs of 1985, 1989, 1993, 1996, and 2001 were considered anomalously wet. Summers (DJF) in 1981/82, 1982/83, 1983/84, 1986/87, and 1992/93 are considered anomalously dry, while summers in 1985/86, 1988/89,

1995/96, 1999/00, and 2010/11 are considered anomalously wet. These wettest and driest seasons were selected with the proviso that they were also dry or wet for the entire Eastern Cape. There were similarities between dry and wet years from the two rainfall subdomains, therefore, the entire domain was considered for composites. However, there are also some differences, owing to the severity of the dry or wet conditions across the province. For example, in the springs of 1981 and 2008, the east basin was severely dry, while the west basin was only slightly dry. Similarly, there are some differences in selected summer years; for example, while the summers of 1981/82 and 1983/84 were dry across both subdomains, the region's northeastern tip was relatively wet. These spatial differences are found to be insignificant when comparing dry and wet years from the east and west basins separately.

The impact of large-scale modes of variability is also investigated further to better understand any spatial differences in the nature of the relationship between rainfall and large-scale modes of variability. Among the modes of variability studied here are the El Niño-Southern Oscillation (ENSO) and the Southern Annular Mode (SAM). The ENSO phenomenon is known to have a strong influence on rainfall over South Africa (Reason et al., 2000, Cook, 2000, Lyon and Mason, 2007, Blamey et al., 2018). The influence of the Southern Annular Mode (SAM) is suggested to have a more prominent role in winter rainfall (Reason and Rouault, 2005, Mahlalela et al., 2018). A negative (positive) SAM phase has been associated with positive (negative) rainfall anomalies over western South Africa due to equatorward (poleward) shifts in the jet and storm tracks (Reason and Rouault, 2005, Sousa et al., 2018, Mahlalela et al., 2018).

This chapter is divided into five sections: **Section 5.2** looks at circulation anomalies associated with wet and dry seasons, **Section 5.3** considers large scale modes of variability, **Section 5.4** at trends in key regional features influencing rainfall, and **Section 5.4** provides a summary of the findings.

Table 5.1 Spring and summer seasons used for the composites. For DJF, the year represents the last month of the season.

Season	Dry	Wet
Early summer – SON	1981,1990,1994, 2008,2016	1985,1989,1993, 1996, 2001
Core summer – DJF	1982,1983,1984, 1987,1993	1986,1989,1996, 2000,2011

5.2 Potential mechanisms behind wet and dry periods

5.2.1 Composite Anomalies – SON

Figure 5.1 shows that dry (wet) springs over the Eastern Cape are associated with a cyclonic (anticyclonic) anomaly to the southeast of South Africa which is part of a wavenumber 3 or 4 pattern in the Southern Hemisphere midlatitudes. Further north over Namibia, Botswana, and Angola there are positive (negative) anomalies implying a stronger (weaker) mid-level Botswana High which has been previously associated with drier (wetter) conditions over subtropical southern Africa in late summer (Reason, 2016, Driver and Reason, 2017). Spatial correlations between southern African rainfall and a Botswana High index (**Fig. 5.2a**) show that the Botswana High has a significant (r = -0.4) inverse influence on rainfall during spring. The Botswana High index is calculated using ERA5 reanalysis data at 500 hPa. The index represents geopotential height anomalies extracted at the core of the 5870m contour for each season. The 5870m contour was discovered to be the highest well-defined contour, allowing

for the tracking of the Botswana High in various seasons. There are also spatial variations in the relationship, with the northern parts of the region showing stronger correlations than the southwest. As shown in **Figure 5.2b**, the relationship between rainfall over Eastern Cape and the Botswana High exhibits significant decadal variation. Reason (2019) found that the Botswana High shows considerable decadal variability, which could be linked to observed decadal variability in summer rainfall. **Figure 5.2b** shows that, with the exception of decades between 2011 and 2014, the Botswana High has always had a negative relationship with Eastern Cape rainfall. The dominant negative relationship between the BH and rainfall is consistent with the geopotential height composite analysis findings, which show that a stronger (weaker) mid-level Botswana High is associated with drier (wetter) conditions. The 1996–2005 period has the strongest relationship (r = -0.7), while the 2006–2015 period has the weakest and is not significant.

The cyclonic (anticyclonic) anomaly southeast of South Africa is also evident at lower levels leading to an enhancement (reduction) in offshore dry flow (**Fig. 5.3b, c**) relative to the 850 hPa climatological moisture flux (**Fig. 5.3a**) in the dry (wet) springs. There is anomalous divergence (convergence) of this low-level moisture over the neighbouring Agulhas Current unfavourable for the strengthening (weakening) of rain-producing weather systems in the region such as ridging anticyclones, cold fronts, and cloud bands. Composites of 200hPa zonal winds reveal a strengthening (weakening) in the subtropical jet during dry (wet) springs. During wet springs the weakening in the subtropical jet (STJ) over South Africa is coupled with a strengthening in the polar jet throughout the Southern Hemisphere (**Fig. 5.4b**). Changes in the strength and location of the jets have implications for storm development and tracks into the regions (Archer and Caldeira, 2008). Synoptic scale disturbances tend to form in the regions of maximum jet stream wind speed and propagate downstream along storm tracks that follow

the jet axes (Archer and Caldeira, 2008). Therefore, when the STJ is located further south warm tropical air is advected into higher latitudes making the regions closer to the mean jet latitude drier than usual.

Figure 5.5 plots time series of ridging days along the south coast as well as the number of mid-latitude storms upstream over the South Atlantic in various latitude bands to better understand the influence of ridging on mid-latitude storms. A comparison of the two-time series **(Figs. 5.5a-d)** indicates a significant relationship. Positive correlations between the number of ridging days and storms suggest that storms at certain bands are more associated with ridging along the south coast. This is significant at 30–50° S, 40–50° S, and 40–60° S (r = 0.49, 0.59, and 0.33, respectively).

SST composites (**Fig. 5.6**) indicate cooler (warmer) anomalies in the greater Agulhas Current region which have previously been associated with dry (wet) summers over eastern South Africa (e.g., Walker, 1990, Mason, 1995, Reason and Mulenga, 1999, Reason, 1999). During wet springs, warmer SSTs over the southwest South Atlantic (near southern Argentina) are also visible in the SST composite anomalies (**Fig. 5.6b**). Since this region is critical for cyclogenesis in the South Atlantic basin (Jones and Simmonds, 1993, Hoskins and Hodges, 2005), the observed SST anomalies during wet seasons are suggestive of more cyclones being formed in the South West Atlantic which then track towards the oceans immediately south of South Africa. Furthermore, SST composites over the equatorial Pacific show that wet springs are associated with cooler SSTs, indicating La Niña conditions. However, the dry composites do not show an El Niño-like SST anomaly in the Pacific, and although there are negative anomalies in the Southwest Atlantic, these are very weak implying little change to cyclogenesis upstream of South Africa. **Figure 5.6b** also suggests a weak negative IOD signal associated

with wet springs. Other important modes of variability over the Atlantic and Indian oceans include the Benguela Niño, the Southern Indian Ocean Dipole (SIOD), and the South Atlantic Ocean Dipole (SAOD). However, the influence of these modes is not visible in the spring SST composite. These modes have been identified as seasonal in nature, for example, the Benguela Niño is thought to be strongest in FMA (Rouault et al., 2003, Reason and Smart, 2015) and the Indian Ocean Dipole (IOD) in OND (Saji and Yamagata, 2003, Behera et al., 2006). In summary, the most consistent SST signal in the composites are the cool (warm) anomalies in the greater Agulhas Current region during the dry (wet) springs and the La Niña pattern in the Pacific and tropical Indian Ocean (Reason et al., 2000) for the wet springs.

The omega anomalies (**Fig. 5.7a, b**) support the suggestion of changes in the strength of rain-bearing weather systems over the Eastern Cape with strong relative subsidence (uplift) over most of the Eastern Cape as well as much of South Africa and the ocean to the south of the country in the dry (wet) composite. The northwest-southeast orientation of the omega anomalies across western southern Africa suggests unfavourable (favourable) conditions for cloud band development during the dry (wet) springs. In fact, using the met-bot cloud band tracking methodology (Hart et al., 2012), found that there are 1–2 fewer (more) cloud band days than average during the dry (wet) springs over much of South Africa, including most of the Eastern Cape (N. Hart 2021, pers. comm.). Also evident in **Figure 5.3b, c** is a weakening (strengthening) of the Angola Low and relative offshore (onshore) moisture flow from the tropical Southeast Atlantic. A stronger Angola Low and this moisture inflow have been found to be important for both synoptic and seasonal scale wet spells in summer over South Africa and the reverse during dry conditions (Mulenga et al., 2003, Cook et al., 2004) since it often acts as the source region for cloud bands. **Figure 5.8** shows the corresponding OLR composite anomalies again revealing a northwest–southeast orientation which is consistent with less

(more) cloud bands/other convective systems and hence decreased (increased) rainfall over the Eastern Cape during the dry (wet) spring seasons.

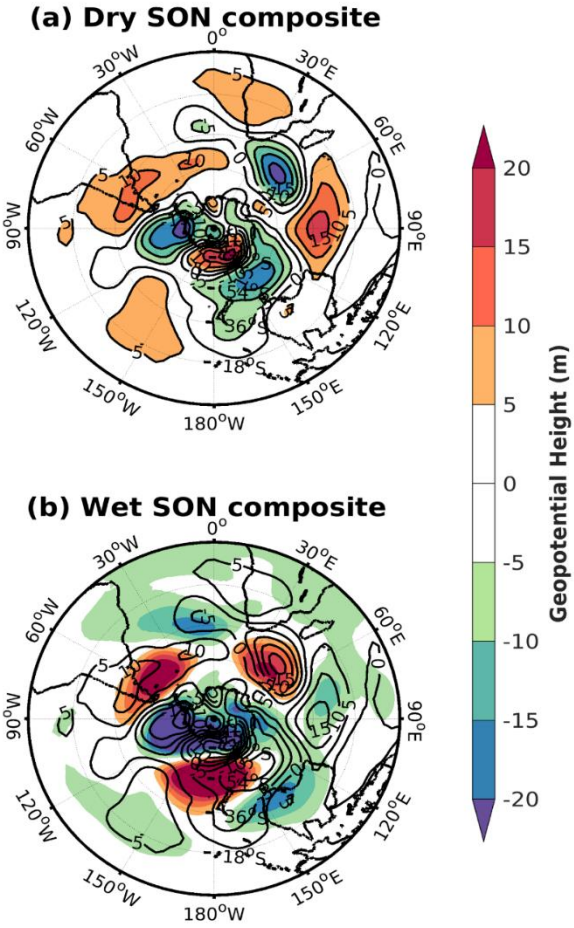

Figure 5. 1: SON geopotential height composite anomaly (shaded with contours; m) at the 500 hPa level for **(a)** dry and (**b)** wet springs**.**

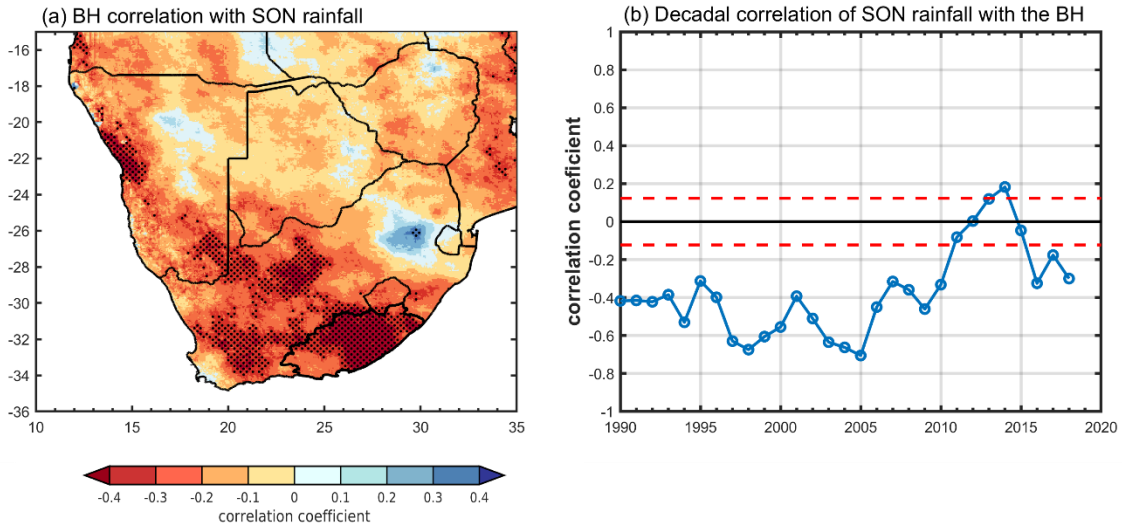

Figure 5.2: **(a)** Spatial correlation between spring BH index derived from NCEP and CHIRPS rainfall for the period 1981–2018. Stippling shows significance at the 95% level. **(b)** 10-yr running correlation of rainfall averaged across the Eastern Cape with the Botswana High, dashed line indicates statistical significance at the 95% level. The years denote the last year of the sliding window (i.e., 1990 represents the 1981–1990 decade).

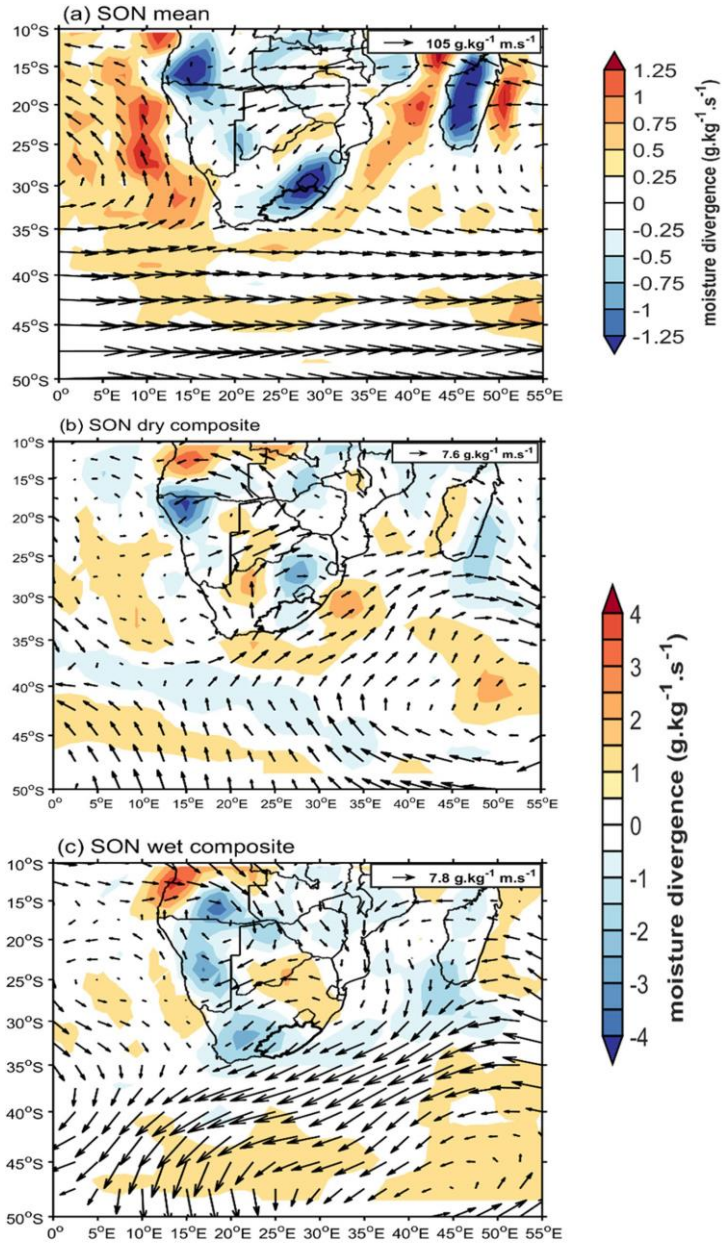

Figure 5.3: **(a)** The mean moisture flux divergence (shaded; $g.kg^{-1}$. $S^{-1} \times 10^{-5}$) and moisture flux (scale vector shown) during SON at the 850 hPa level. Panels (**b)**, (**c)** show the composite anomalies for dry and wet springs respectively (shaded; $g.kg^{-1}$. $S^{-1} \times 10^{6}$).

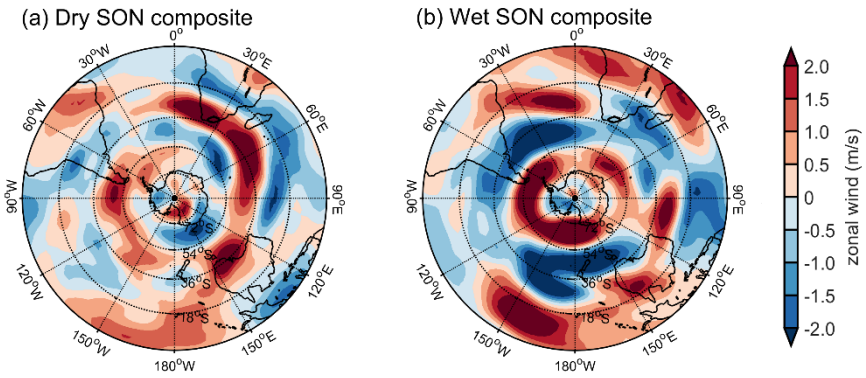

Figure 5.4: The composite anomaly of the 200 hPa zonal wind for **(a)** dry and **(b)** wet springs (shading with contours; units are $m.s^{-1}$).

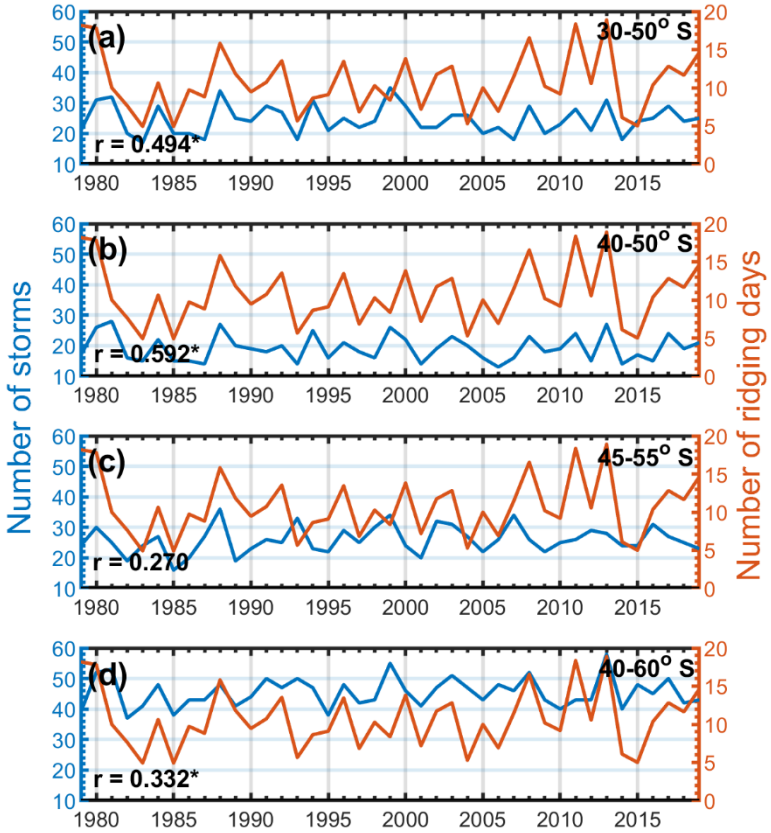

Figure 5.5: Time series comparison of spring storms (blue) as well as the number of days linked with ridging (orange), from 1981 to 2018. At the top of each panel, the storm bands used in each row are displayed. The correlation between the two series is shown at the bottom left of each panel. The asterisk indicates significance at the 95 percent level, as determined by a Student's t-test.

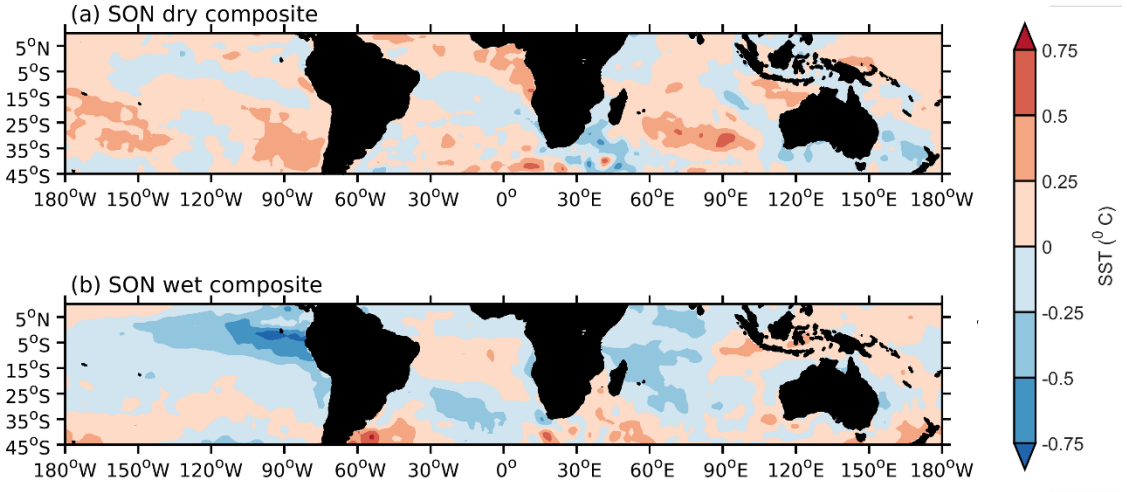

Figure 5.6: NOAA OI SST (shading; ^{o}C) composite anomalies for **(a)** dry and **(b)** wet years during spring.

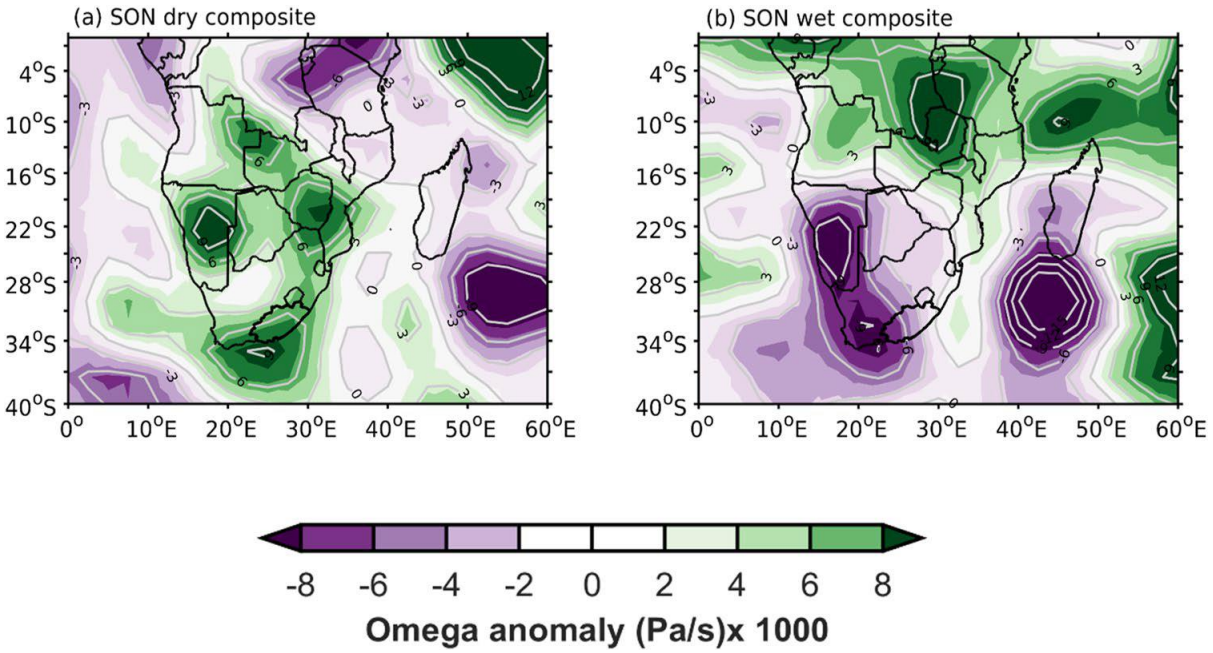

Figure 5.7: SON composite anomaly of omega (shaded with contours; Pa s^{-1}) at the 500 hPa level for (**a)** dry and (**b)** wet springs.

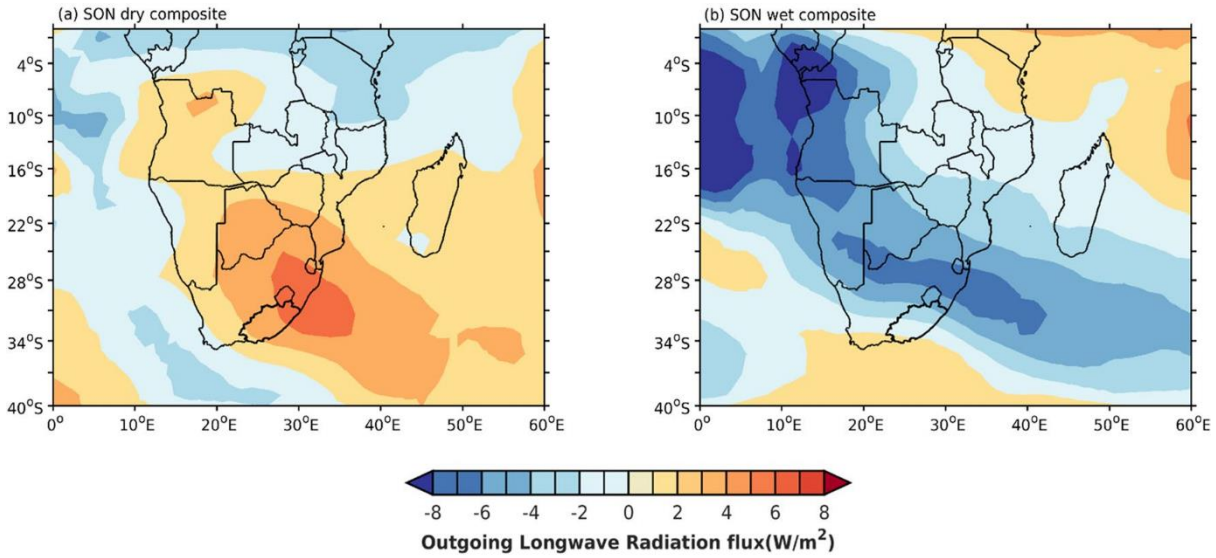

Figure 5.8: Composite anomaly of OLR (shaded; W/m^{-2}) for (**a)** wet and (**b)** dry springs.

5.2.2 Composite Anomalies -DJF

During the summer, **Figure 5.9** illustrates dry (wet) summers are associated with cyclonic (anticyclonic) anomaly at mid-levels south of the country, which forms part of a wavenumber 4 pattern in the mid-latitudes. Over subtropical southern Africa, there are anticyclonic (cyclonic) anomalies, particularly in the west, indicating a stronger (weaker) Botswana High during the dry (wet) summers. This summer pattern over the land is similar to what was found in spring but more pronounced. **Figure 5.10a** depicts a strong negative relationship between rainfall and the Botswana High; this relationship is statistically significant across most of southern Africa, including virtually the entire Eastern Cape province. Reason and Driver (2017) discovered a similar strong Botswana High influence on late summer (JFM) rainfall as well as in the frequency of dry spells. **Figure 5.10b** shows that the relationship has always been negative and stronger than for spring (**Fig. 5.2b**). Except for part of the 2000–2009 decade, the relationship is found to be significant between 1981 and 2018. Rainfall and the Botswana High have the strongest correlations at the beginning and end of the period. Similar decadal variations in the relationship between the Botswana High and summer rainfall across southern

Africa were found by Reason (2019), with relatively wet decades associated with a weaker and more southward positioned Botswana High as well as lower subcontinental surface temperatures and increased cloud cover. On the other hand, a stronger Botswana High leads to more mid-level subsidence, hindering cloud band development and therefore leading to less rainfall over southern Africa (Driver and Reason, 2017, Reason, 2019).

Compared to the mean **Figure 5.11a,** there are westerly moisture flux anomalies at 850 hPa over the South East Atlantic and southern South Africa, including the Eastern Cape (**Fig. 5.11b)**. Such a pattern implies more advection of cool, dry Atlantic air, previously found to be associated with some dry summers over northern South Africa (Mulenga et al., 2003). Further north, the anticyclonic anomalies over western tropical southern Africa imply a weaker Angola Low. Although there are some areas of relative low level moisture convergence over central South Africa / western Botswana, these do not link to increased convergence south of the country implying a limited impact on cloud band development, and there is also relative divergence over the western regions (including part of the Eastern Cape) and adjoining ocean areas. On the other hand, the wet summers (**Figure 5.11c**) show enhanced easterly transport of moist air from the Agulhas Current region towards the Eastern Cape (favourable for rainfall via ridging anticyclones in particular as well as for strengthening the midlatitude component of the cloud bands). Strong anticyclonic anomalies south of South Africa support the suggestion of ridging along the south and east coasts in helping to explain the wetter summers. The western regions show increased moisture flux convergence which link up with relative convergence over the Agulhas Current south of the Eastern Cape favouring cloud band strengthening over at least the western half of the Eastern Cape province. The anomalies in the Angola Low region are less coherent but there is increased onshore flow of tropical South East Atlantic-derived moisture into southern Angola / northern Namibia favourable for the tropical

source of the cloud bands affecting Namibia, the Northern Cape, and parts of the Eastern Cape provinces.

Zonal wind composites indicate that dry (wet) summers are associated with subtropical jet strengthening (weakening) in the South African region (**Figure 5.12**). During dry (wet) seasons, this is found to also correspond with a weaker (stronger) polar jet (**Fig. 5.12**). The observed pattern between the subtropical and polar jets suggests that during dry seasons, the westerly wind belt expands northward towards South Africa (**Fig. 5.12a**) leading to westerly moisture flux anomalies over southern South Africa (**Fig. 5.11b**), whereas during wet seasons, it contracts towards Antarctica leading to increased ridging over the south coast and easterly moisture flux anomalies over the Eastern Cape (**Fig. 5.11c**). Taken together the changes in the jet and mid-level circulation (**Figs. 5.9, 5.12**) imply a negative (positive) SAM pattern during dry (wet) summers (discussed further in the next section).

Ridging over the south coast is found to have an influence on storm activity over the midlatitude in summer. **Figure 5.13** shows a positive correlation between storms in different bands and ridging days, which is significant at 30–50 ° S and 40–50 ° S (r=0.31 and 0.49, respectively). As a result, wet (dry) summers are associated with increased (decreased) storm tracking into the Eastern Cape. This is due to increased ridging during wet summers caused by a poleward shift in the westerly wind belt.

Figure 5.14b shows that dry (wet) summers are associated with a much more obvious El Niño (La Niña) SST pattern in the tropical Pacific than was the case for spring. In general, DJF or JFM is the season of strongest rainfall impacts over subtropical southern Africa with El Niño

(La Niña) typically associated with above (below) average rainfall (Lindesay, 1988, Reason et al., 2000, Blamey et al., 2018) although there are obvious exceptions like the lack of severe drought during the very strong 1997/98 (Reason and Jagadheesha, 2005) and moderately strong 2009/10 El Niño summers (Driver et al., 2019).

Over the South Atlantic, dry (wet) summers are associated with cool (warm) anomalies to the southwest of South Africa which would tend to weaken (strengthen) approaching fronts, and hence the midlatitude inputs into the cloud bands (**Fig. 5.14**). A favourable pattern of warmer SSTs also exists in the wet summers (**Fig. 5.14b**) in the far southwest South Atlantic, off the coast of southern Argentina, which is a key region for cyclogenesis in the South Atlantic basin (Jones and Simmonds, 1993, Hoskins and Hodges, 2005) in the southwest South Atlantic. Furthermore, wet summers are characterised by warmer SSTs immediately south of South Africa which creates conducive conditions for moisture transport by ridging high pressures during the summer months (Engelbrecht et al, 2015, Ndarana et al., 2020) and roughly the reverse during dry summers (**Fig. 5.14a**). The SST composites also shows warmer (cooler) SSTs off the coast of Namibia and Angola during wet (dry) summers (**Fig. 5.14**) seasons which may combine with the low-level moisture flux anomalies (**Fig. 5.11**) to lead to more (less) transport of moist tropical South East Atlantic air into the Angolan region and hence stronger (weaker) tropical extratropical cloud bands (Harrison, 1984, Hart et al., 2010, 2013).

Figure 5.15 supports the suggestion of less (more) favourable cloud band conditions during the dry (wet) summers since there is a diagonal band of relative sinking (uplift) extending from Angola south-eastwards over the land and out over the neighbouring South West Indian Ocean. These patterns suggest less or weaker cloud bands forming over the land during the dry summers (and potentially more over and east of Madagascar) as typically happens during El

Niño when the SICZ is weakened and displaced (Cook, 2001, Fauchereau et al., 2009, Hart et al., 2018). The enhanced subsidence apparent in **Figures 5.9a, 15a** generally suppresses convection and the development of rain-bearing weather systems. More or less the reverse is apparent in the wet summers (**Figs.5 9b, 15b**) as is generally the case for La Niña.

OLR composite anomalies (**Figure 5.16)** are consistent with the omega and geopotential height anomalies showing large areas of reduced (enhanced) convective cloud in the northwest-southeast diagonal band across the region during dry (wet) summers. These patterns further support the suggestion of lesser (greater) cloud band activity thus less (more) rainfall over the Eastern Cape during the dry (wet) summers.

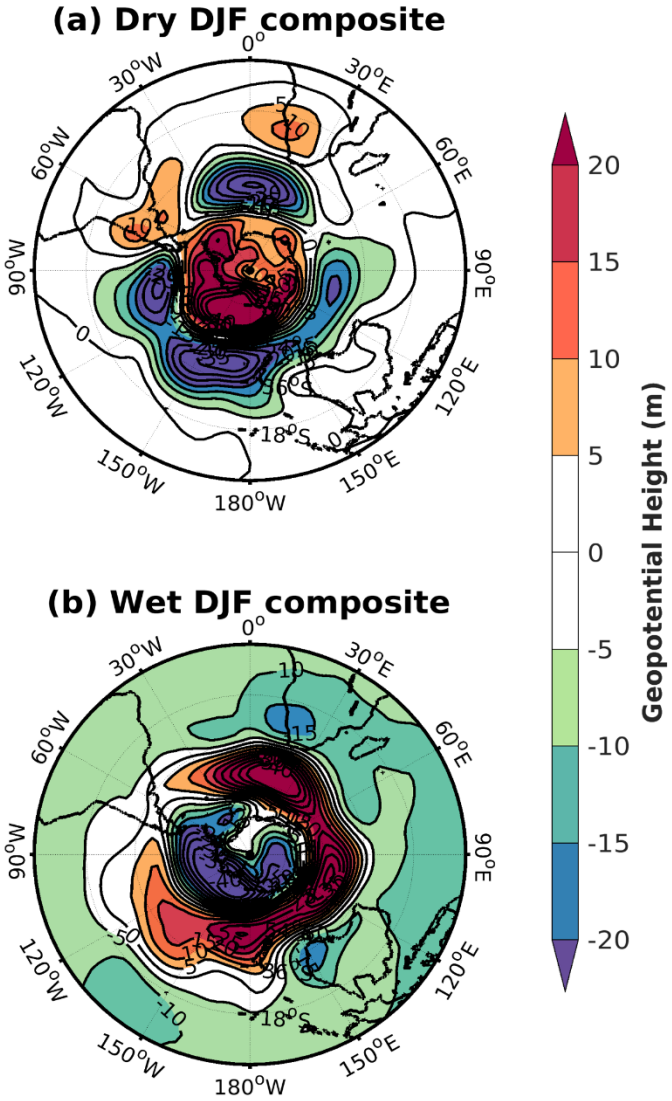

Figure 5.9: DJF geopotential height composite anomaly (shaded with contours; m) at the 500 hPa level for **(a)** dry and **(b)** wet summers.

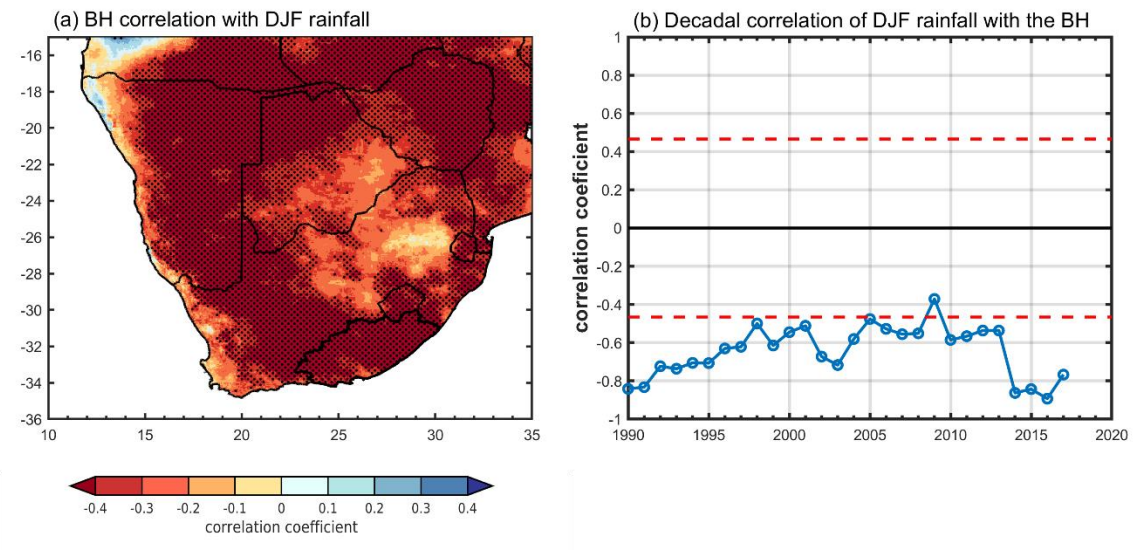

Figure 5.10: **(a)** Spatial correlation between summer BH index derived from NCEP and CHIRPS rainfall for the period 1981–2018. Stippling shows significance at the 95% level. **(b)** 10-yr running correlation of rainfall averaged across the Eastern Cape with the Botswana High, dashed line indicates statistical significance at the 95% level. The years denote the last year of the sliding window (i.e., 1990 represents the 1981–1990 decade).

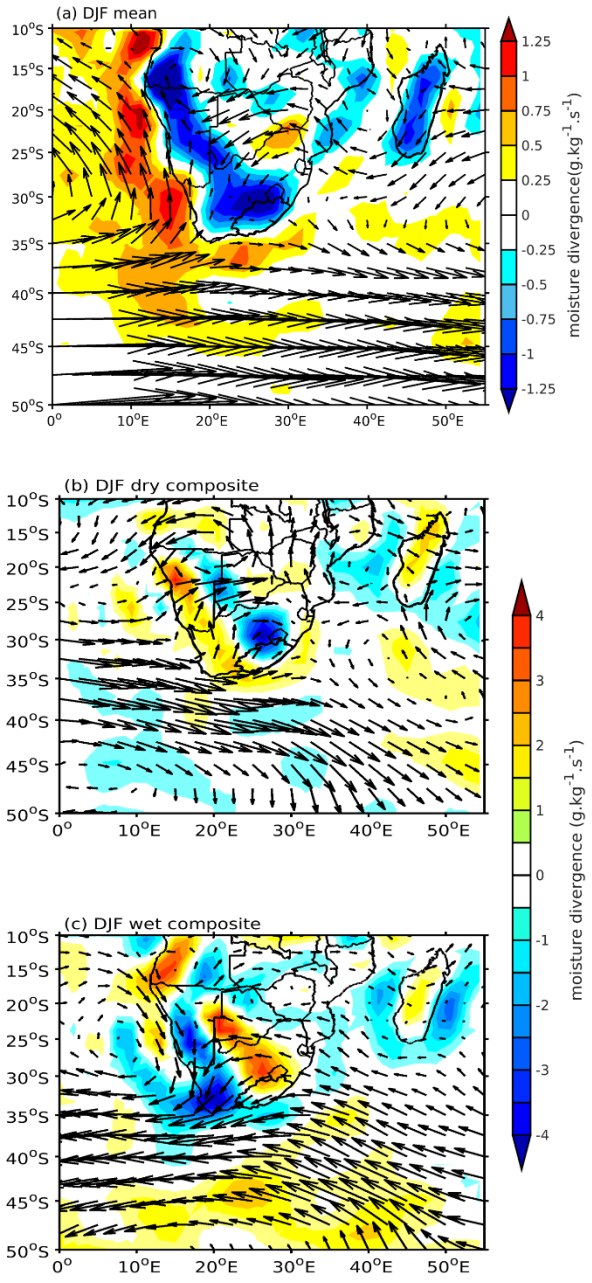

Figure 5.11: **(a)** The mean moisture flux divergence (shaded; g. kg^{-1}. $s^{-1} \times 10^{-5}$) and moisture flux (scale vector shown) during DJF at the 850 hPa level. Panels **(b)**, **(c)** show the composite anomalies for dry and wet summers respectively (shaded; $g.kg^{-1}$. $s^{-1} \times 10^{6}$).

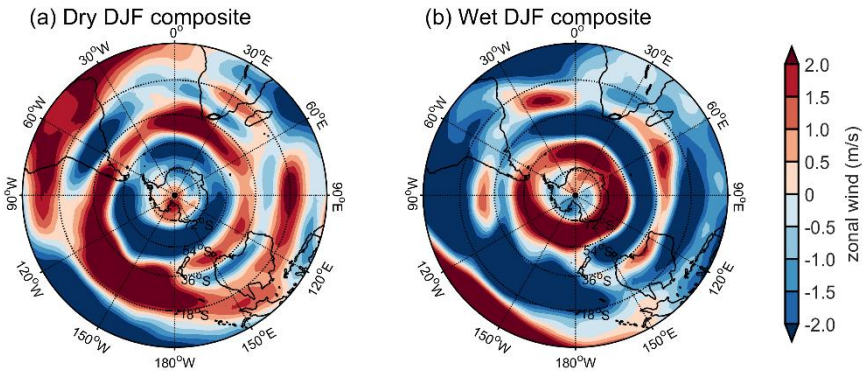

Figure 5.12: The composite anomaly of the 200 hPa zonal wind for **(a)** dry and **(b)** wet summers (shading with contours; units are $m.s^{-1}$).

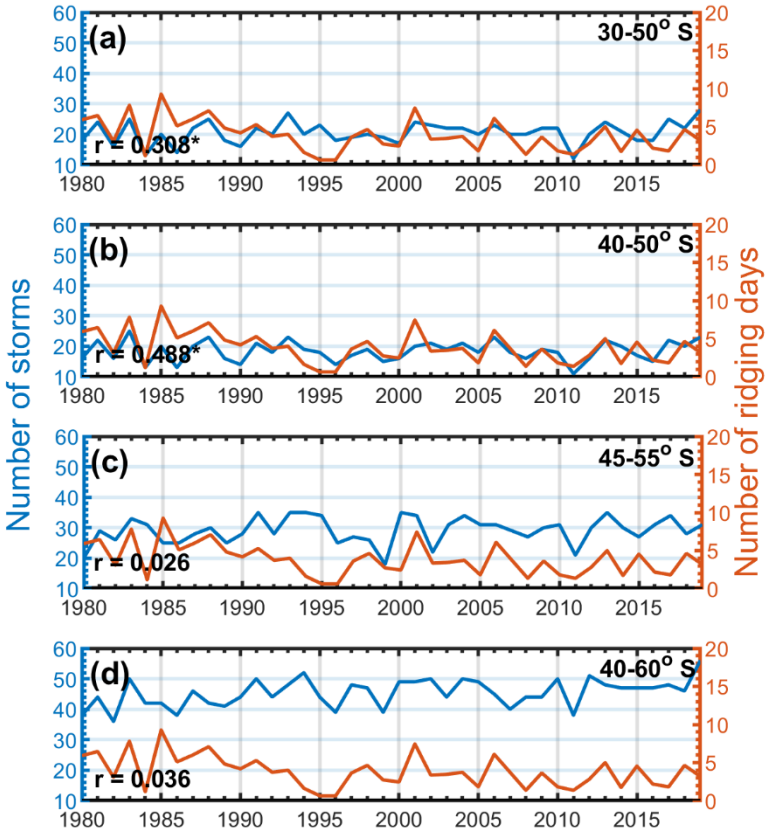

Figure 5.13: Time series comparison of summer storms (blue) as well as the number of days linked with ridging (orange), from 1981 to 2018. At the top of each panel, the storm bands used in each row are displayed. The correlation between the two series is shown at the bottom left of each panel. The asterisk indicates significance at the 95 percent level, as determined by a Student's t-test.

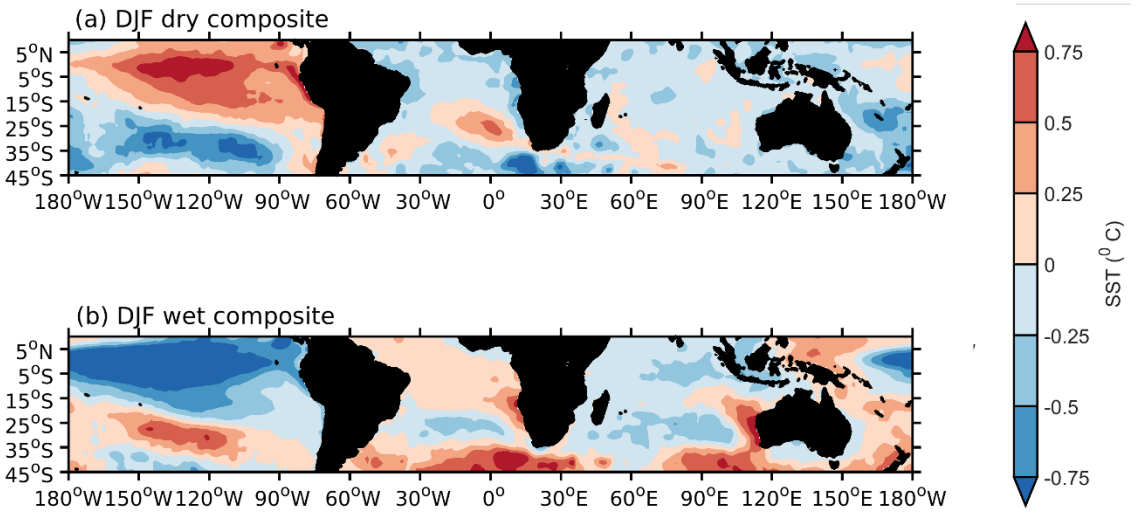

Figure 5.14: NOAA OI SST (shading; ^{o} C) composite anomalies for **(a)** dry and **(b)** wet years during summer.

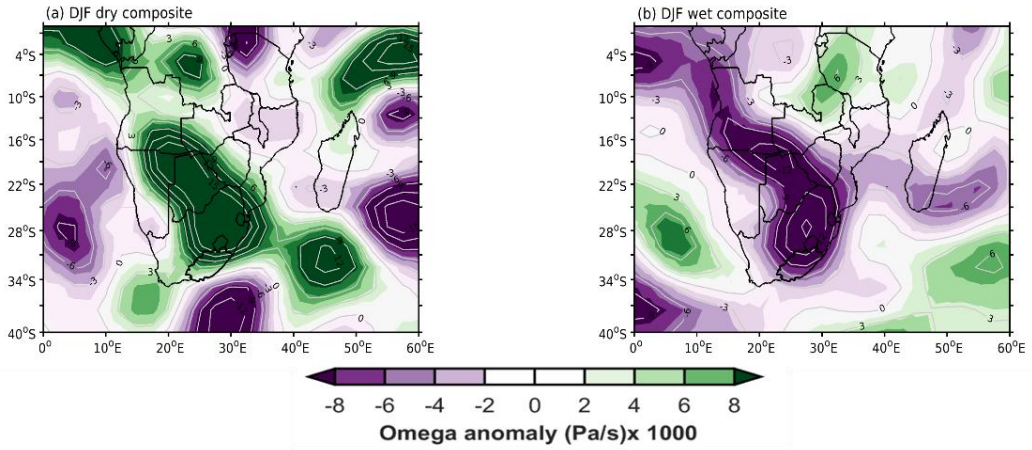

Figure 5.15: DJF composite anomaly of omega (shaded with contours; Pa s^{-1}) at the 500 hPa level for **(a)** dry and **(b)** wet summers.

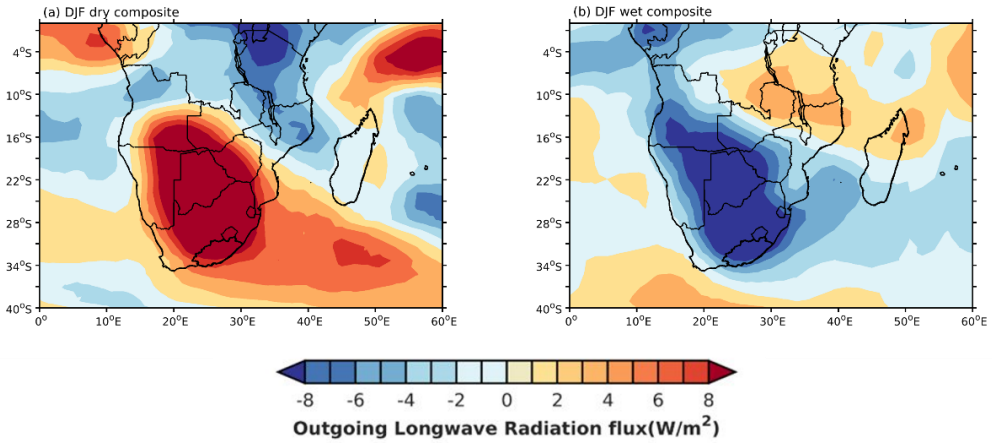

Figure 5.16: Composite anomaly of OLR (shaded; W/m^{-2}) for **(a)** wet and **(b)** dry summers.

5.3 Correlations between rainfall anomalies and indices for climate modes and circulation

The previous section showed composite patterns that resembled ENSO or SAM for DJF but less obviously for SON. To explore connections further, this section determines correlations between the rainfall anomalies and various indices for ENSO, SAM, and other circulation patterns such as the zonal wave number 3 and the spatial extent of the SAHP and the SIHP.

5.3.1 The spring – SON

While **Figure 5.1** showed a Botswana High influence as well as a wavenumber 3 or 4 pattern, the anomalies are not reminiscent of ENSO or the SAM. Indeed **Figure 5.17** shows that there is no significant relationship between either ENSO or SAM over the Eastern Cape region. Although most of subtropical southern Africa shows an inverse relationship between rainfall and the Niño 3.4 index, it is only significant in the Limpopo River Basin region and further north in eastern Zimbabwe. However, it is known from previous work that it is the DJF or JFM season that typically has the strongest ENSO impacts on southern African rainfall (Lindesay,

1988, Reason et al., 2000) so these results are not unexpected. No significant correlations were found with the SIOD either - again this mode typically impacts in JFM and also further north in southern Africa than the Eastern Cape (Behera and Yamagata 2001, Reason 2001, 2002). Although a positive SAM rainfall correlation has been found in summer (Gillett et al. 2006) over much of the region and a negative correlation over western South Africa in winter (Reason and Rouault, 2005), spring correlations using the Marshall (2003) index are mixed over the southern part of South Africa and nowhere significant (**Fig. 5.17b**).

Although there does not appear to be any obvious linkage between these large-scale climate modes and spring rainfall over the Eastern Cape, the wavenumber 3 or 4 patterns in **Figure 5.1** suggest that changes in the South Atlantic or South Indian Ocean semi-permanent anticyclones might be important. On average during spring, the former anticyclone tends to move south eastward towards southwestern South Africa, signalling the end of the winter rainy season there (Reason, 2017, Sousa et al., 2018). The South Indian Ocean High (SIHP) also tends to retreat south-eastwards in spring and the continental high over southern Africa breaks down then, coincident with the end of the dry winter half of the year for southern Africa (except the far southwest). The position of the anticyclones' outer extents is taken into account to determine the impact of their position on rainfall. The anticyclone extents are calculated as the outer boundary of the 1020 hPa contour in the mean sea level pressure field (MSLP). This contour level was selected because it is easily identified as a closed contour level surrounding anticyclones that is not intersected with neighbouring land masses in either the early or late summer periods. The latitude and longitude of the South Indian Ocean High are defined here as the location with the maximum in the MSLP field within the climatological mean area (40°-110° E; 15°- 40° S). For the SIHP, its eastern extent (**Fig. 5.18a**) is strongly negatively correlated with SON rainfall over the west basin of the Eastern Cape as well as most of western South Africa. Although the west basin also shows a negative correlation with the northern

extent of the SIHP, it is too weak to be significant (**Fig. 5.18d**). The only other significant correlation (also negative) is between rainfall over the far east of the province (and neighbouring areas in Lesotho and KZN) with the western extent of the SIHP (**Fig. 5.18c**). These statistical and negative relationships with the eastern or western extent of the SIHP may imply a reduced easterly moisture flow into northern South Africa and a subsequent weaker northerly moisture inflow towards the Eastern Cape, and thus drier conditions when the SIHP extends further in a zonal direction. **Figure 5.19** shows that there are no significant relationships between any of the outer bounds of the SAHP and rainfall over the Eastern Cape region. Only the eastern extent (**Fig. 5.19a**) is found to have a significant negative correlation with rainfall over the southwest tip of South Africa, likely because a SAHP extending less far west towards South Africa than usual in spring allows cold fronts to impact the southwestern parts of the country more easily. However, this relationship does not extend as far east as the Eastern Cape.

Changes in the extent of the SIHP or the SAHP could be related to those in the midlatitude wavenumber 3 pattern. Although **Figure 5.1** indicated shifts in this pattern, it can be seen that only the circulation anomaly in the midlatitude South Indian Ocean is consistent between the dry and wet spring composites since the anomalies in the midlatitude South Pacific and South Atlantic are not exactly in the same place. Nevertheless, using a zonal wavenumber 3 index such as that proposed by Raphael (2004) leads to a fairly strong and statistically significant correlation (**Fig. 5.20a**) with spring rainfall over much of the Eastern Cape as well as part of the northeast of South Africa. If an index for only the South Indian Ocean component of the wavenumber 3 index is used (standardized anomalies in 500 hPa geopotential height spatially averaged over 45–50° S, 45–60° E), then **Figure 5.20b** indicates a statistically significant correlation over the central third of the Eastern Cape (with stronger r values than for the full

index) as well as some other parts of subtropical southern Africa in a NW–SE cloud band type orientation.

In summary, these wavenumber 3 correlations, as well as those seen earlier for the Botswana High, seem to be the strongest relationships that exist for SON rainfall over the Eastern Cape. Neither ENSO nor SAM appears to be important for rainfall in this season.

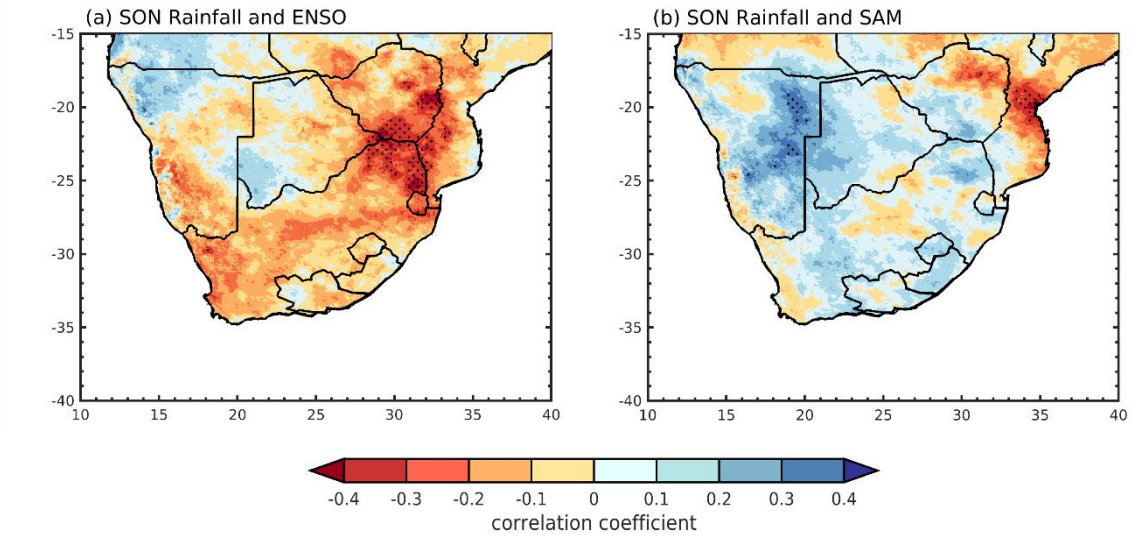

Figure 5.17: Correlations between **(a)** Niño 3.4 index and **(b)** Marshal (2003) SAM index and spring CHIRPS rainfall over southern Africa, for the 1981–2018 period. Stippling indicates significance at the 95% confidence level.

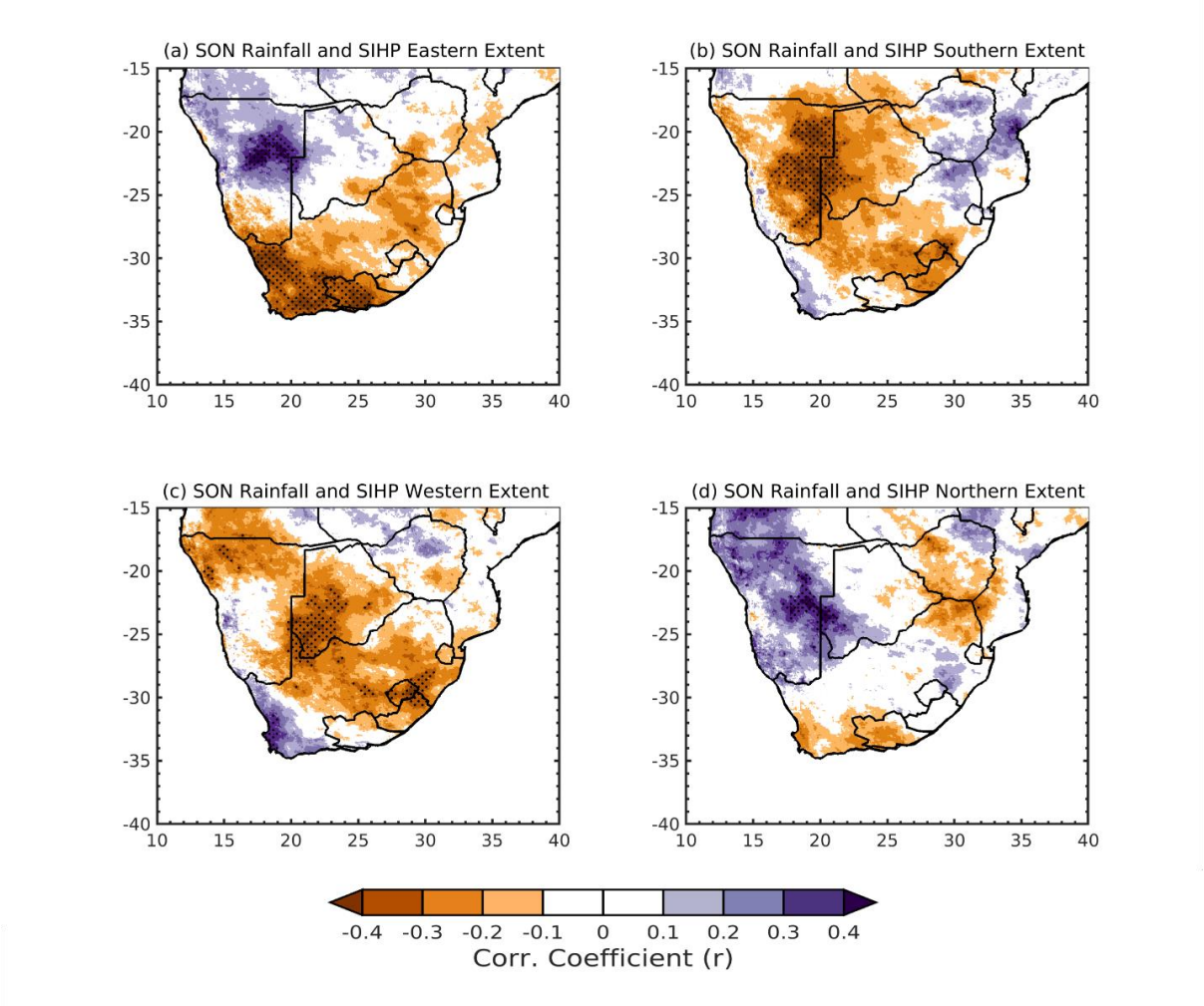

Figure 5.18: The correlation between SON rainfall and **(a)** eastern, **(b)** southern, **(c)** western and **(d)** northern extent of the South Indian Ocean High Pressure (see text for details). Areas that are statistically significant at the 95% level are denoted by stippling. The location of the Eastern Cape River basins is denoted with the black polygon.

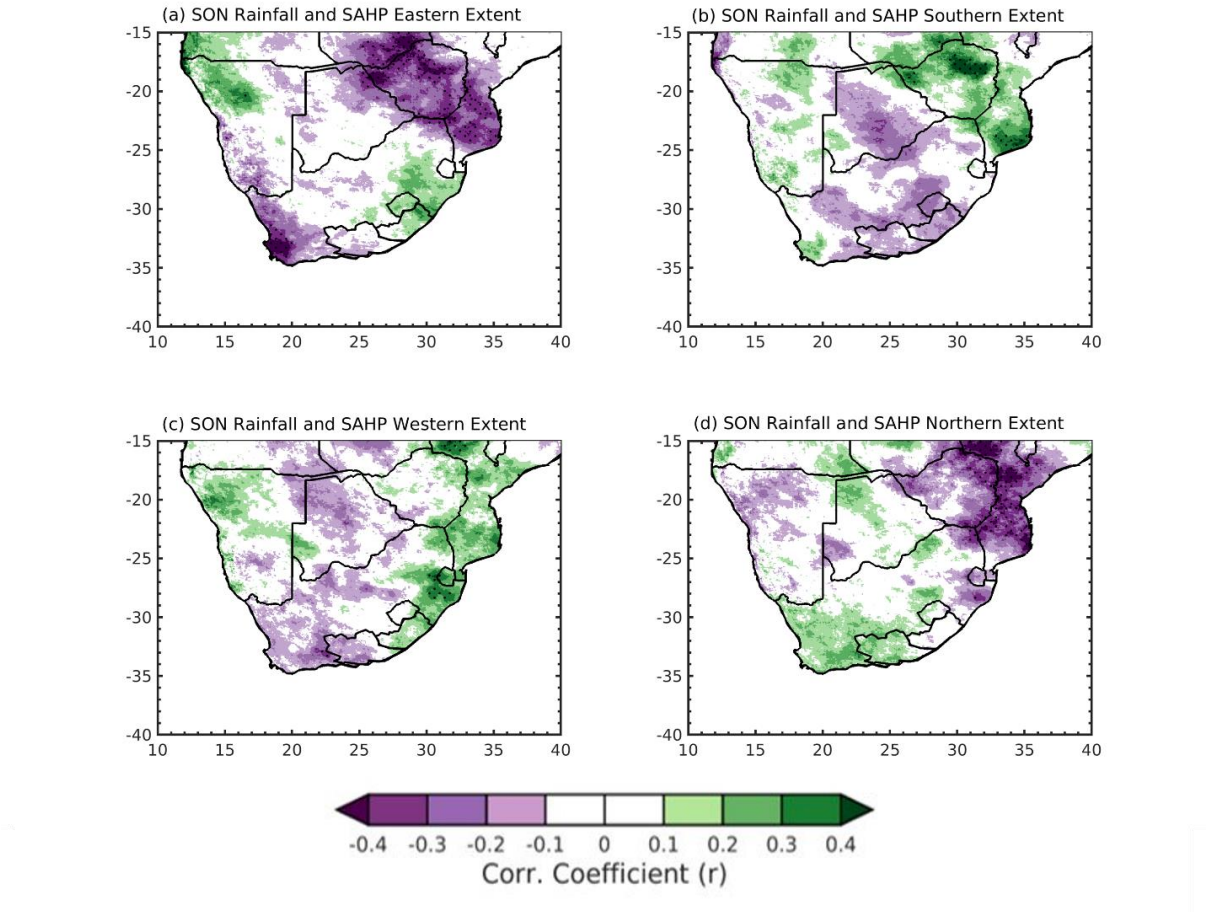

Figure 5.19: The correlation between SON rainfall and **(a)** eastern, **(b)** southern, **(c)** western and **(d)** northern extent of the South Atlantic Ocean High Pressure (see text for details). Areas that are statistically significant at the 95% level are denoted by stippling. The location of the Eastern Cape River basins is denoted with the black polygon.

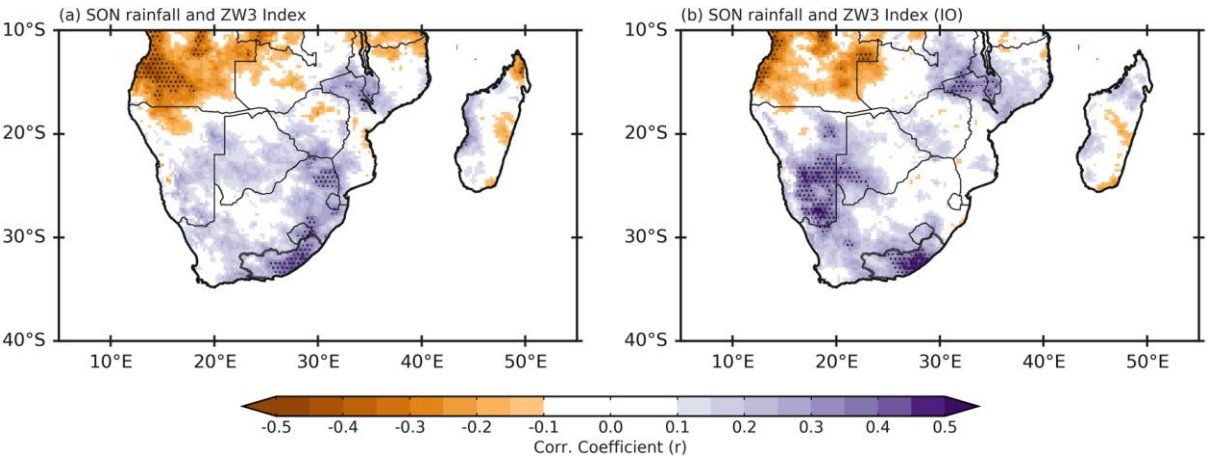

Figure 5.20: The correlation between spring (SON) rainfall and **(a)** the zonal wave number 3 index of Raphael (2004) and **(b)** only the South Indian Ocean High component of that index. Areas that are statistically significant at the 95% level are denoted by stippling. The location of the Eastern Cape River basins is denoted with the black polygon.

5.3.2 The summer- DJF

In summer, the influence of both ENSO and SAM is evident, as highlighted in the composite analysis (**Section 5.2.2**). Circulation and SST anomalies showed clear ENSO, SAM, and Botswana High signals. In particular, three (four) of the dry (wet) years used to compute the composite anomalies correspond to El Niño (La Niña) events. Regional circulation patterns also correspond to typical ENSO conditions i.e., weakening in the Angola Low during dry summers (**Fig. 5.11b**) and a stronger Botswana High (**Fig. 5.9a**). A stronger (weaker) Angola Low and South Indian High pressure has been linked to favourable (unfavourable) rainfall conditions during La Niña (El Niño) (Cook et al., 2004, Reason and Jagadheesha, 2005, Reason et al., 2006, Manhique et al., 2011, Munday and Washington, 2017, Blamey et al., 2018). Indeed, **Fig. 5.21a** shows that the Eastern Cape, and particularly the eastern basin, has one of the strongest areas of negative correlation ($r < -0.4$ significant at 95%) in South Africa between rainfall and the Niño 3.4 index. In general, it is estimated that ENSO-influenced rainfall variability in southern Africa accounts for approximately 30% of rainfall variance in this season (Mulenga et al, 2003, Meque and Abiodun, 2015, Blamey et al., 2018b). The exact mechanisms through which ENSO affects southern African rainfall remain to be fully understood but involve changes in the subtropical jet and cloud band locations (Hart et al., 2018) as well as in the Angola Low or Botswana High (Driver and Reason, 2017) which in turn may be affected by regional SST anomalies driven by those in circulation over the Indian (Chambers et al., 1999, Reason et al., 2000) and Atlantic Oceans (Colberg et al., 2004) as a result of the tropical atmospheric bridge (Klein et al., 1999) or Pacific South America (Mo and Paegle, 2001) teleconnection patterns.

Mid-troposphere geopotential height composite anomalies (**Fig. 5.9**) also highlight positive (negative) pressure anomalies over polar (midlatitude) regions during dry summers, with these circulation conditions associated with negative SAM periods. Contrary wet conditions over the Eastern Cape are associated with positive SAM conditions, the associated rainfall correlation with the Marshall (2003) index shows a significant positive correlation over most of the Eastern Cape region, particularly the eastern basin, as well as in a narrow band over the Northern Cape and far southern Namibia. Positive (negative) SAM conditions have been associated with increased (decreased) ridging along the south coast of South Africa, which is related to the mid-latitude circulation retreating poleward (pushing equatorward), resulting in an increase (decrease) in coastal rainfall along South Africa's southeast (Malherbe et al., 2014, Ndarana et al., 2020). Due to the onshore flow of moisture these anticyclones bring from the warm Agulhas Current region onto the landmass, such synoptic features can cause rainfall along the southeast coast (Weldon and Reason 2013, Engelbrecht et al, 2015, Engelbrecht and Landman 2016, Ndarana et al., 2020).

At the interannual scale, SAM and ENSO have been shown to interact, with El Niño (La Niña) events sometimes corresponding to negative (positive) SAM phases. This interaction is thought to be due to how ENSO forces SAM variability, with 25% of SAM variance linearly related to the ENSO state (L'Heureux and Thompson, 2006, Pohl et al., 2010). This suggestion is supported by the observed circulation and SST patterns (**Figs. 5.9, 5.14**), and by several of the dry summers in **Table 5.1** showing El Niño / negative SAM values and the reverse for the wet summers.

Motivated by the mid- and low-level circulation anomalies (**Figs. 5.9, 5.11**), correlations were performed between rainfall and the spatial extent of the SIHP and the SAHP. **Figure 5.22** shows that there are no significant correlations between any of the boundaries of the SIHP and Eastern Cape rainfall with only the northern extent showing any significant influence elsewhere in South Africa (positive relationship with rainfall in northern KZN and in western South Africa which is of little interest since this western region receives very little rain in summer). **Figure 5.23** suggests a stronger influence between some aspects of the SAHP and summer rainfall. The western and southern extents of the SAHP (**Fig. 5.23b, c**) are found to be significantly negatively correlated with rainfall over parts of the west basin and the interior of South Africa. This suggests that rainfall over these regions may be favoured by the SAHP extending less far into the midlatitudes and less close to the Cape Town region than is typical in summer. Such a situation would then be more favourable for cold fronts to provide more midlatitude input into cloud bands affecting the western basin and western interior. A positive SAM, as has often occurred in recent decades, would weaken cold fronts, and shift the SAHP further south leading to less rainfall over the southern part of the country (Sousa et al., 2018, Mahlalela et al., 2019) potentially also reducing the onshore flow of moisture from the adjacent ocean (d'Abreton and Lindesay, 1993, D'Abreton and Tyson, 1996, Rapolaki et al., 2020).

Using a zonal wavenumber 3 index results in a statistically significant correlation (**Fig. 5.24a**) with summer rainfall over relatively small parts of both the western and eastern basins in the province. Unlike the case for SON, only the South Indian Ocean component of the wavenumber 3 index (**Figure 5.24b)** shows essentially no correlation at all over the Eastern Cape, although there is a small area of significant correlation just west of eSwatini.

In summary, ENSO and SAM are important for summer rainfall over the Eastern Cape, whereas they were not found to be as influential in SON. The latter season also showed a significant negative correlation with the Botswana High which becomes even stronger for DJF. While the wavenumber 3 pattern is somewhat important for DJF, it is even more important in SON.

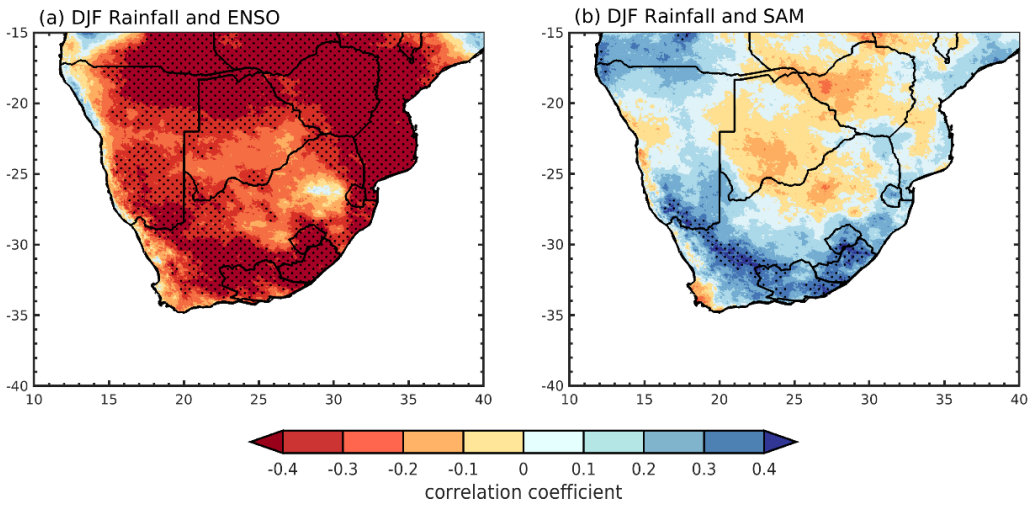

Figure 5.21: Correlations between **(a)** Niño 3.4 index and **(b)** Marshal (2003) SAM index and summer CHIRPS rainfall over southern Africa, for the 1981–2018 period. Stippling indicates significance at the 95% confidence level.

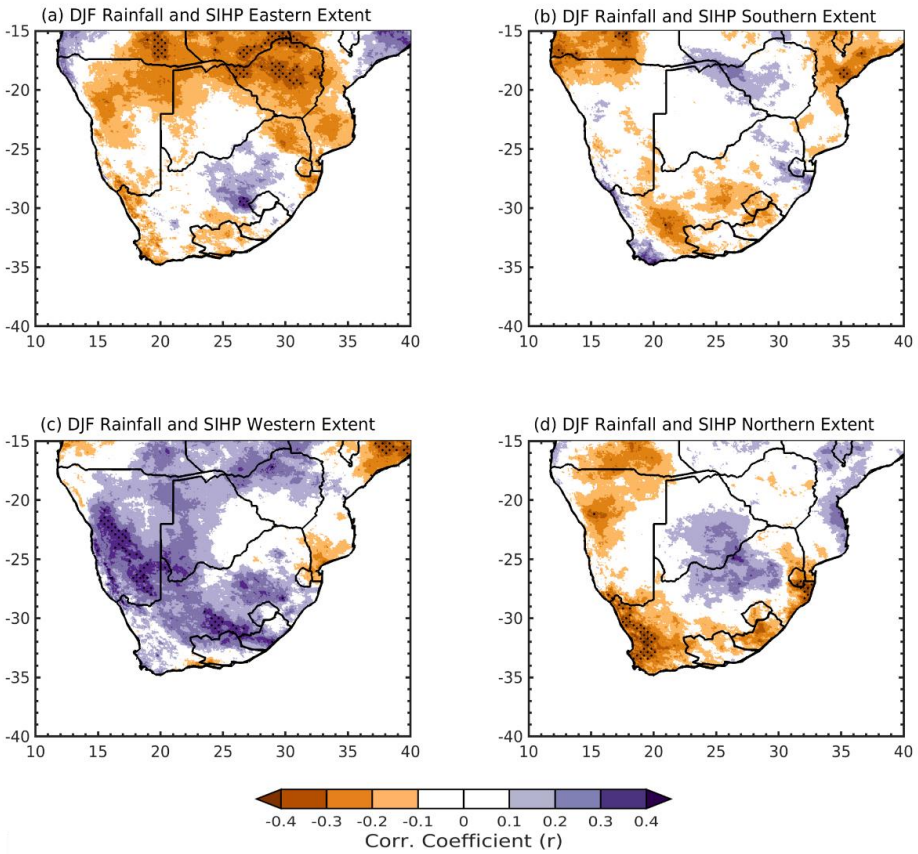

Figure 5.22: The correlation between DJF rainfall and **(a)** eastern, **(b)** southern, **(c)** western and **(d)** northern extent of the South Indian Ocean High Pressure (see text for details). Areas that are statistically significant at the 95% level are denoted by stippling. The location of the Eastern Cape River basins is denoted with the black polygon.

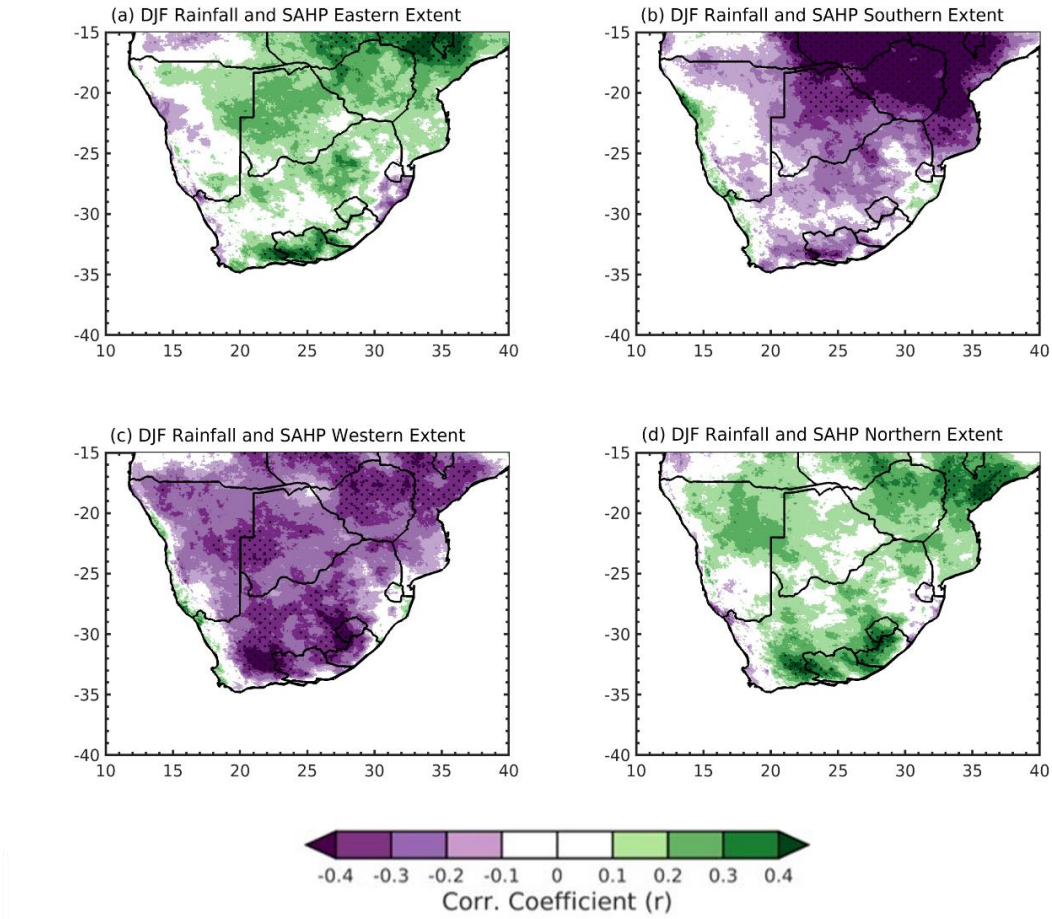

Figure 5.23: The correlation between DJF rainfall and **(a)** eastern, **(b)** southern, **(c)** western and **(d)** northern extent of the South Atlantic Ocean High Pressure (see text for details). Areas that are statistically significant at the 95% level are denoted by stippling. The location of the Eastern Cape River basins is denoted with the black polygon.

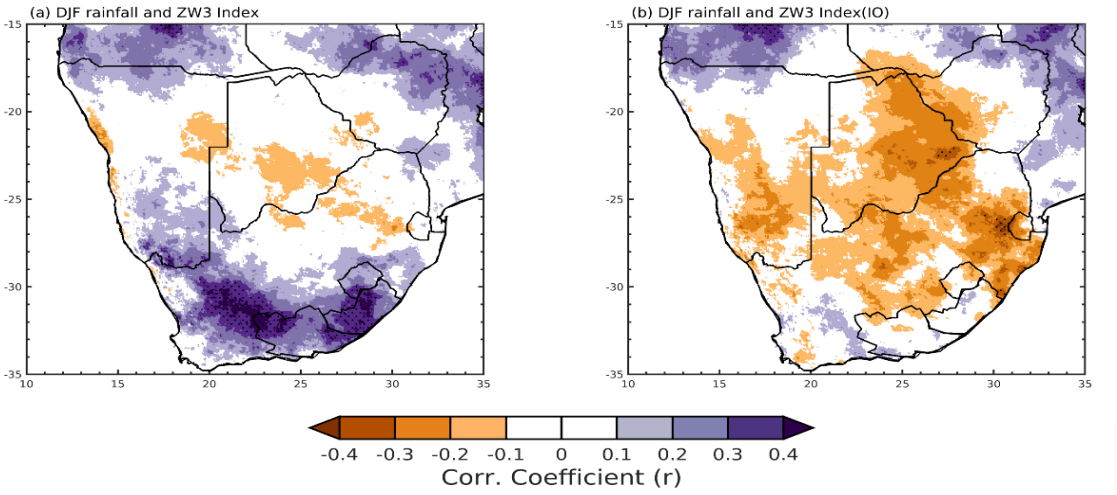

Figure 5.24: The correlation between summer (DJF) rainfall and **(a)** the zonal wavenumber 3 index of Raphael (2004) and **(b)** only the South Indian Ocean High component of that index. Areas that are statistically significant at the 95% level are denoted by stippling. The location of the Eastern Cape water management areas is denoted by the black polygon.

5.4 Trends in regional features

The composite analysis has highlighted regional features influencing rainfall i.e., ridging over the south coast and jet streams. SAM has also tended to be more often in positive phase in recent decades which affects the jet streams. This section aims to examine trends in these features in order to better understand observed seasonal rainfall trends shown in **Chapter 4**.

For spring, trends in the 850hPa geopotential height show areas of significant decreasing trends over the South West Indian Ocean as well as over the land where the Kalahari heat low forms in spring due to surface heating (Howard and Washington, 2019) and extending down across the Karoo to the Eastern Cape (**Fig. 5.25a**). On the other hand, there are positive trends near Antarctica due south of South Africa as well as in the Pacific sector. The weakening geopotential height trends in spring imply less anticyclonic conditions and hence reduced easterly moisture transport from the warm South West Indian Ocean towards the eastern parts of South Africa. Many previous studies have invoked this mechanism to help explain dry

seasons over this part of the country (e.g., Walker, 1990, Mason, 1995, Reason and Mulenga, 1999). On the other hand, a stronger SIHP and deeper Angola Low form a steep north-south pressure gradient, allowing easterly moisture to move further inland over South Africa (Rapolaki et al., 2020, Xulu et al., 2020).

For DJF, **Fig. 5.25b** also shows an area of significant weakening trend in the South West Indian Ocean but over a much smaller area than in SON. The SAM tendency towards positive phase in recent years (e.g., Fogt et al., 2009, Abram et al., 2014) is now clear with most of the Antarctic region showing significant weakening trends and large areas of the South Pacific and South Atlantic midlatitudes showing strengthening trends. The associated increased geopotential height near the south coast during the summer months suggests increased anticyclonic ridging over this region (**Fig. 5.25b**). Ridging has been identified as a contributor to summer rainfall, it encourages onshore flow, which improves moisture transport and rain-bearing weather in summer (Engelbrecht et al, 2015, Ndarana et al., 2021). Overall, the trends in **Fig. 5.25** correspond with seasonal rainfall findings, which revealed a significant decrease in seasonal spring rainfall over much of the Eastern Cape and smaller areas of increasing trend in summer rainfall.

Rainfall from the east and west basins is found to have a negative relationship with subtropical jet winds at 200 hPa over the southeast Atlantic and south Indian oceans (**Fig. 5.4** and **Fig. 5.11**) for both spring and summer. This inverse relationship indicates that a weakening (intensification) of the subtropical jet is associated with wetter (drier) conditions over the Eastern Cape region calculated over 1979–2016, **Figure 5.26** depicts the seasonal trend in 200hPa zonal winds. The STJ shows no discernible trend during the spring months (**Fig. 5.26a**)

in the South African region although the jet appears to have weakened over much of the South Pacific and over a small area just east of southern Brazil. Further south, the polar jet has been decreasing in the Indian Ocean sector of the high latitude Southern Ocean (south and southeast of South Africa) as well as in the Australian sector. In contrast, the subtropical jet has weakened over almost the entire eastern Atlantic / South Indian Ocean sector from 20°W east to about 140°E in summer (see **Figure 5.26b**), while the polar jet has strengthened over much of the Southern Ocean. Again, this pattern reflects the tendency towards positive SAM phase in recent decades. Such a pattern implies more ridging along the south coast (Mahlalela et al., 2019, Ndarana et al., 2020), which could help explain parts of the province showing a significant wetting trend in summer.

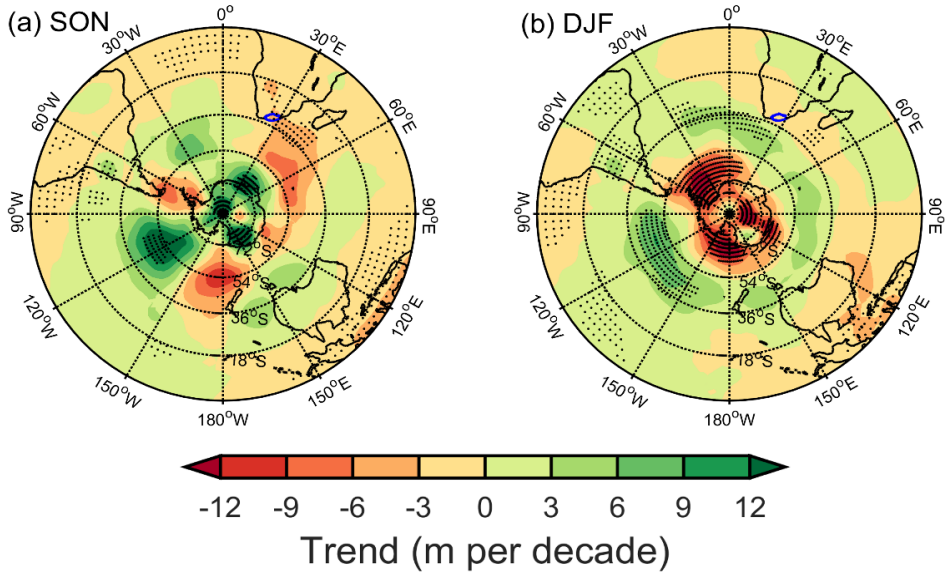

Figure 5.25: Global geopotential height trends at 850hPa (shading m/decade) during the **(a)** spring, and **(b)** summer months for the period 1979–2016. Stippling denotes significance at 95% level.

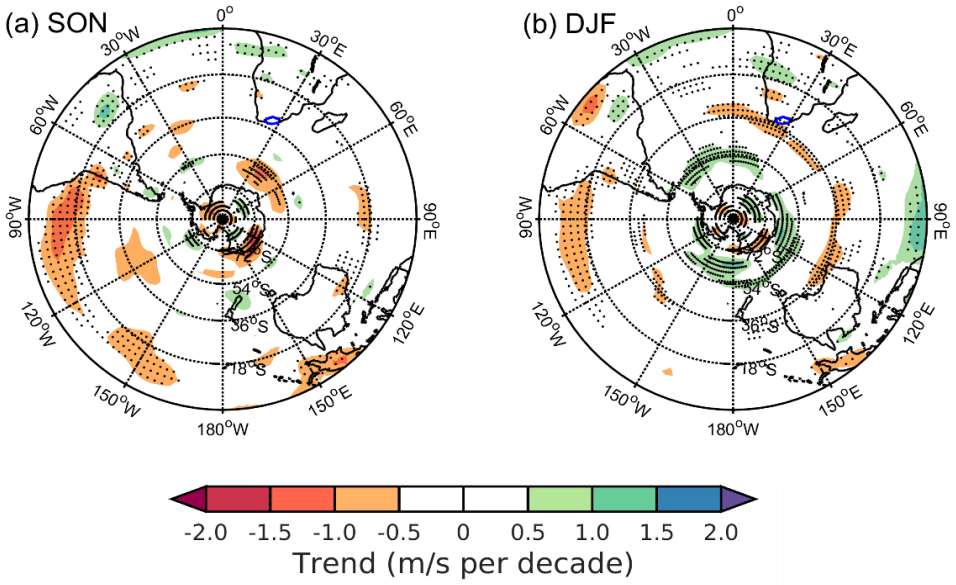

Figure 5.26: Trends in the U200 winds (shading m/s per decade) during the **(a)** spring (Sep – Nov) and **(b)** summer (Dec – Feb) months for the period 1979–2016. Stippling denotes significance at 95% level.

5.5 Summary

This chapter has analysed the circulation anomalies associated with wet and dry seasons over the Eastern Cape region as well as trends in circulation. A composite analysis of the five driest (wettest) spring and summers since 1981 chosen on the basis of widespread anomalously dry (wet) conditions in the spring or summer was used. The composites show that dry (wet) seasons were related to large cyclonic (anticyclonic) mid-tropospheric anomalies located to the south and southeast of South Africa, which appears to be linked to changes in the zonal wavenumber 3 pattern. Over southern Africa, the composites suggest that dry (wet) springs are associated with a weaker (stronger) near-surface Angola Low and stronger (weaker) mid-level Botswana High with enhanced (reduced) subsidence which lead to less (more) favourable conditions for cloud bands to develop. Although there is a weakening in the Angola Low during dry summers,

it is unclear whether there is a strengthening during wet summers. However, dry (wet) summers are clearly linked with a stronger (weaker) Botswana High.

Circulation anomalies suggest that there is no obvious relationship between the large-scale climate modes known to affect subtropical southern Africa. Focus was placed on the two dominant modes of variability, ENSO, and SAM, thought to have the most impact on South African rainfall (Lindesay, 1988, Reason et al., 2000, Cook, 2001, Reason & Rouault, 2005, Gillett et al., 2006). Consistent with previous studies (Lindesay 1988, Mason 1995, Reason et al., 2000), ENSO was found to have a strong influence on summer rainfall over the Eastern Cape region but not on SON rainfall. Similarly, SAM was also found to influence summer rainfall (consistent with Gillett et al. 2006) but not spring rainfall. These relationships were established here on the basis of circulation and SST anomalies as well as through correlations with the Niño 3.4 index and the Marshall (2003) index.

Although El Niño (La Niña) is generally associated with dry (wet) summers there are spatial differences since the relationship is much stronger over the eastern basin than the western basin of the province, and in fact weakens below significance level over a small central area of the western basin. During El Niño, circulation changes occur over southern Africa leading to less low-level moisture convergence, uplift and instability which influences cloud band development and rainfall over the subcontinent (Cook, 2000, Mulenga et al., 2003, Hart et al., 2018). Some of these circulation anomalies are evident in the composite analysis for dry (wet) summers, such as a stronger Botswana High (Reason, 2016, Driver and Reason, 2017) and a weaker Angola Low (Cook et al., 2004, Reason and Jagadheesha, 2005, Reason et al., 2006, Blamey et al., 2018b) during El Niño seasons. Of the driest and wettest summers, three (four) of the dry (wet) years used to compute the composite anomalies correspond to El Niño (La

Niña) events. It should however be noted that the ENSO rainfall relationship is nonlinear and there are very strong events (e.g., 1997/98 and 2015/16) whose rainfall anomalies over the Eastern Cape were insufficiently large to be included in the composite.

The SAM is also found to have a significant positive influence on summer rainfall over the southwest and north-eastern parts of Eastern Cape. This suggests that positive (negative) SAM conditions are associated with increased (reduced) rainfall over this region. Similar findings were made by Gillett et al. (2006), the increased rainfall during positive SAM is found to be associated with increased ridging over the south coast, which favours rainy weather over coastal areas (Weldon and Reason, 2013, Engelbrecht et al, 2015, Engelbrecht and Landman 2016, Ndarana et al., 2020). A comparison of ridging days and storm counts in the South Atlantic suggests that ridging along the south coast is significantly related to storms upstream in certain latitude bands. Relationships between the extents of the SAHP or the SIHP and Eastern Cape rainfall were patchy in both seasons. However, stronger relationships were found with the zonal wavenumber 3 pattern over the province, particularly in spring.

Chapter 4 showed evidence of a drying trend over much of the Eastern Cape in spring and to lesser extent a wetting trend in summer. In terms of circulation, there was a cyclonic trend in spring in the South West Indian Ocean but a strong anticyclonic trend in the South Atlantic and south of South Africa in summer as well as a weaker subtropical jet. The latter is consistent with the increasing tendency for positive SAM in recent decades (e.g., Fogt et al., 2009, Abram et al., 2014). These patterns suggest a potential for more (less) anticyclonic ridging over the south coast in summer (spring). Increased ridging here then provides for greater transport of moisture across the warm Agulhas Current towards the Eastern Cape.

In addition, there was a significant weakening in 850 hPa geopotential height over the interior in spring near the Kalahari heat low and stretching towards the Eastern Cape. In summer, there is a weakening trend extending from the Angola Low towards the South West Indian Ocean but it is not significant. Lower pressure over the interior leads to a steep north-south pressure gradient, allowing easterly moisture to feed into southern Africa and enhance cloud band development (Hart et al., 2018, Rapolaki et al., 2020, Xulu et al., 2020).

In summary, while the interannual variability in spring and summer rainfall can be understood to some extent via changes in the regional circulation, the trends present more of a challenge. Insight into trends may follow from climate model projections which are considered in the next chapter.

Chapter six: Future rainfall and circulation patterns projections

6.1 Introduction

The previous chapters discussed the drivers behind observed interannual variability and trends in rainfall over Eastern Cape. Understanding rainfall trends has become increasingly important not only for proper planning and water resource management, but also for determining how regional climate may be impacted through a warming world. More research would provide a clearer picture of what changes have already occurred to the global climate, as it was anticipated in the second Assessment Report of the Intergovernmental Panel on Climate Change (IPCC, 1995) that one of the effects of global warming would be an increase in weather and climate extremes (Fauchereau et al., 2003, James and Washington, 2013, Pohl et al., 2017). Observational studies of recent climate trends can also be used to validate climate model results, giving us more confidence in future climate projections (MacKellar et al., 2014, Kruger, 2006). A comparison of observed trends in rainfall and temperatures around South Africa with statistically downscaled global climate model (GCM) simulations was provided by MacKellar et al. (2014). The analysis revealed that observed rainfall trends were poorly represented by model simulations, but there was better correspondence with temperature trends (MacKellar et al., 2014). Hoerling et al. (2006) and Engelbrecht et al. (2015b) both note similar inconsistencies between observed rainfall trends and climate models. The discrepancies are thought to be due to either the parameterisations of sub-grid scale physics (e.g., cloud physics, convection) in these models or the methods used to downscale model results to particular regions (Hoerling et al., 2006, MacKellar et al., 2014, Lazenby et al., 2016, Engelbrecht et al., 2015b, Dieppois et al., 2019).

Similar inconsistencies between model simulations and observations in Africa occurred when using regional climate models such as in the Co-ordinated Regional Downscaling Experiment (CORDEX; Endris et al., 2013, Meque and Abodiun, 2015, Mounkaila et al., 2014, Abiodun et al., 2015, Manzanas et al., 2020, Dosio et al., 2022). Endris et al. (2013), for example, found

that individual models have significant biases in different regions; however, the multi-model ensemble mean adequately represented eastern African rainfall and can thus be used to assess future climate projections. Abiodun et al. (2016), found that over southern Africa, two of the CORDEX models performed worse than reanalysis in representing extreme rainfall events. The same study discovered that for the Western Cape region of South Africa, the models underestimated the extreme rainfall events (Abiodun et al., 2016). The uncertainty in rainfall projections has been attributed to a poor simulation of deep convection (Engelbrecht et al., 2015b, Abiodun et al., 2016, Tamoffo et al., 2022, MacKellar et al., 2014).

Most parts of Africa are vulnerable to the effects of anthropogenic climate change (Boko et al., 2007, Niang et al., 2014), partly due to the relatively strong projected climate change signals for Africa, and partly due to the relatively low adaptive capacity of many communities (Engelbrecht et al., 2015b). Another difficulty is that there are numerous uncertainties surrounding future rainfall patterns in Africa. This poses a threat to the large proportion of Africa's population that depends on subsistence farming, which relies on rainfed agriculture in a climate system with a high degree of natural variability.

In this Chapter, future rainfall projections in the region are considered using 36 models from the Coupled Model Intercomparison Project Phase 5 (CMIP5) ensemble, with the goal of determining some insight into future rainfall scenarios, a topic of great interest to both the public and the government. Although CMIP6 model projections have recently become available, computational limits meant that only CMIP5 data (which had previously been downloaded onto local servers) could be used. To better understand future rainfall scenarios, the chapter also presents projected changes in regional circulation. The observed trends for the

Eastern Cape region indicate a drying trend in spring months, which marks the start of the rainy season and the first opportunity for surface and groundwater resources to start replenishing, particularly if the previous summer has been drier than average (Roffe et al., 2020, Roffe et al., 2021). The majority of the interior and northeastern South Africa typically shows the rainfall season starting in late spring whereas the south coast receives rainfall throughout the year (Weldon and Reason, 2014, Engelbrecht et al., 2015a). As seen in Chapter 4, on average, most of the Eastern Cape is relatively dry in winter with spring and particularly summer making the largest contributions to the annual total. However, if current trends of spring, and to lesser extent, summer drying continue, it could have substantially negative impacts on the local communities as well as agricultural production, particularly citrus fruit, and dairy farming, which are common in the Eastern Cape province. As a result, further research into seasonal rainfall projections across the region is required.

Figure 6.1a plots the annual cycle of rainfall over the Eastern Cape for 36 CMIP5 models and for two observed gridded rainfall products that have similar resolution to the models (GPCP and CMAP). The latter show a weak bimodal cycle with November and February as the wettest months; however, the bimodal aspects in the dry season are not obvious since May, June and July are all very similar and then the average rainfall starts increasing from August. This bimodal cycle is a weaker version of that evident in Southern Hemisphere regions (and related to the semi-annual oscillation) which are located more in the mid-latitudes such as southern Victoria, Australia which extends to 38°S as compared to the Eastern Cape which lies north of 33–34°S. Almost all the models show a much wetter summer half of the year than winter but only some show February or November as the wettest months. In general, most of the models are too wet so that the multi-model mean (black dashed line), although showing February as the wettest month (but no secondary peak in November), indicates up to 2 mm per day more

rainfall than CMAP or GPCP on average. However, during spring, the wet bias is smaller (1 mm per day) with November being the wettest month as observed. **Figure 6.1b, c** plots the mid-century (2040–2060) projections in the annual cycle under the RCP8.5 scenario for each model and the multi-model mean together with the difference from the current climate. These figures indicate that the models are projecting a slight flattening of the annual cycle with the winter becoming wetter and the summer drier. The observed trend corresponds to trends in rainfall seasonality identified by Roffe et al. (2021) suggesting a shorter rain season for south parts of South Africa. For the spring and summer months, the multi-model projections indicate a drying, but this is found to be less pronounced in spring than in summer.

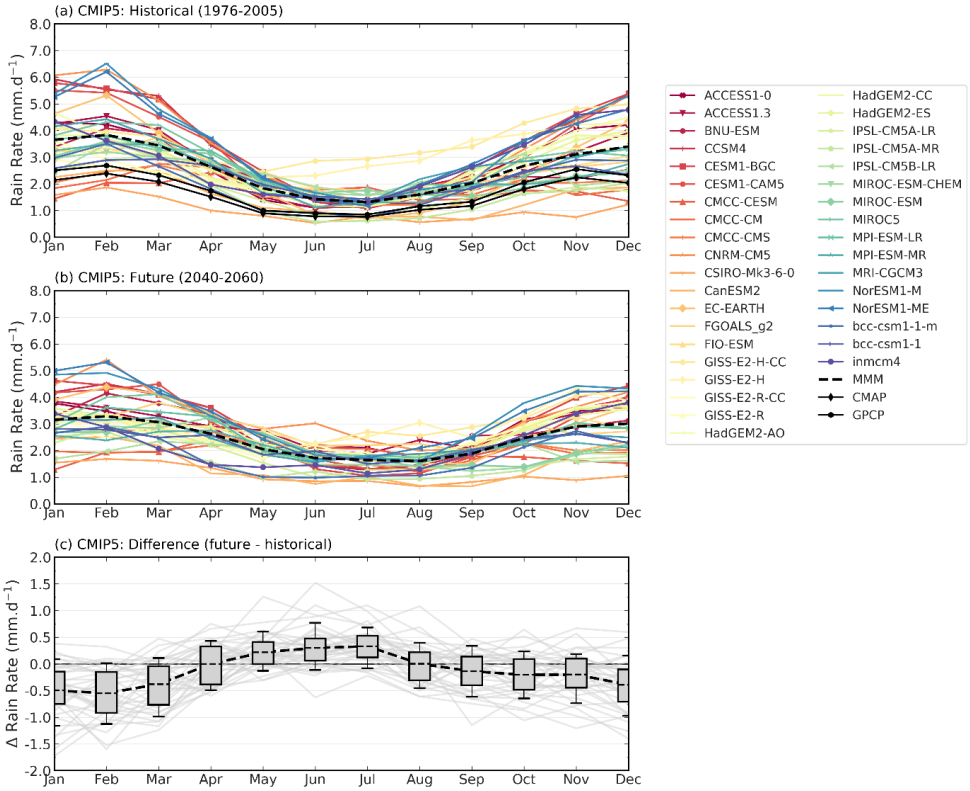

Figure 6.1: The annual cycle of rainfall (rain rate; mm/day) averaged across the river basin polygon for the Eastern Cape in 36 CMIP5 models for **(a)** the historical runs for the 1979–2005, **(b)** the mid twenty first century projections (2040–2060) and (**c)** the difference between the mid-twenty-first century projections and the historical runs under the RCP8.5 scenario. For comparison, two observation products (CMAP and GPCP) are included in **(a)** (black solid lines). The multi-model mean (MMM) is represented by a black dashed line in all three panels. Box plots in **(c)** cover the 10th–90th percentile range of a change in rain rate.

6.2 Mid-twenty-first century summer rainfall projections

Figure 6.2 shows that the majority of the 36 CMIP5 models project drying in spring, but because 8 models (ACCESS1-3, BNU-ESM, CMCC-CM, FIO-ESM, HadGEM2-ES, IPSL-CM5A-MR, and NorESM1-M) project wetter conditions, the multi-model mean indicates only very slight drying in this season when averaged across the province's river basin. The MIROC-ESM-CHEM model records the driest spring conditions for the mid-twentieth century. **Figure 6.3** shows similar weak correspondence across models for the summer, with 3 (ACCESS 1-0, HadGEM2-CC, and HadGEM2-ES) of the 36 models projecting wetter conditions for summer rainfall over the Eastern Cape. The multi-model mean also indicates that the region will experience some drying during the summer. Given the complex topography and meteorology of this province, as well as the highly varying soil and vegetation conditions (e.g., 6 of the 7 biomes found in South Africa also occur in the Eastern Cape), and the presence of the highly variable and intense Agulhas Current to its south, it is not surprising that the models show a spread in projections and have difficulty accurately representing its climate. Some CMIP5 models have been found to show an excessive precipitation bias over southern Africa and the Indian Ocean (Lazenby et al., 2016). This has been attributed to the excessively high low-level moisture flux discovered in the models around the Angola Low due to model circulation biases (Lazenby et al., 2016).

Various climate model experiments have indicated a shift toward more extreme rainfall events in southern Africa under global warming (Fauchereau et al., 2002, Pohl et al., 2017). Pohl et al., (2017) found that the number of rainy days decreased in summer over the region while extreme rainfall events increased, using data from the IPCC's fifth assessment report for the twenty-first century. Furthermore, over the midlatitudes, an intensification in the westerlies caused by the observed positive trend in Southern Annular Mode, resulting in a poleward shift

in storm tracks, has been identified as one of the primary mechanisms by which the subtropical belt (30°–40°N/°S) will become drier under the highest emission scenario (Bengtsson et al. 2006, Pohl et al., 2017). These conditions are unclear in the model projections for spring rainfall. They are, however, consistent with observed summer trends associated with poleward (equatorward) jet shifts associated with positive (negative) Southern Annular Mode conditions creating favourable (unfavourable) conditions over the Eastern Cape and thus more (less) moisture transport into the Eastern Cape during summer.

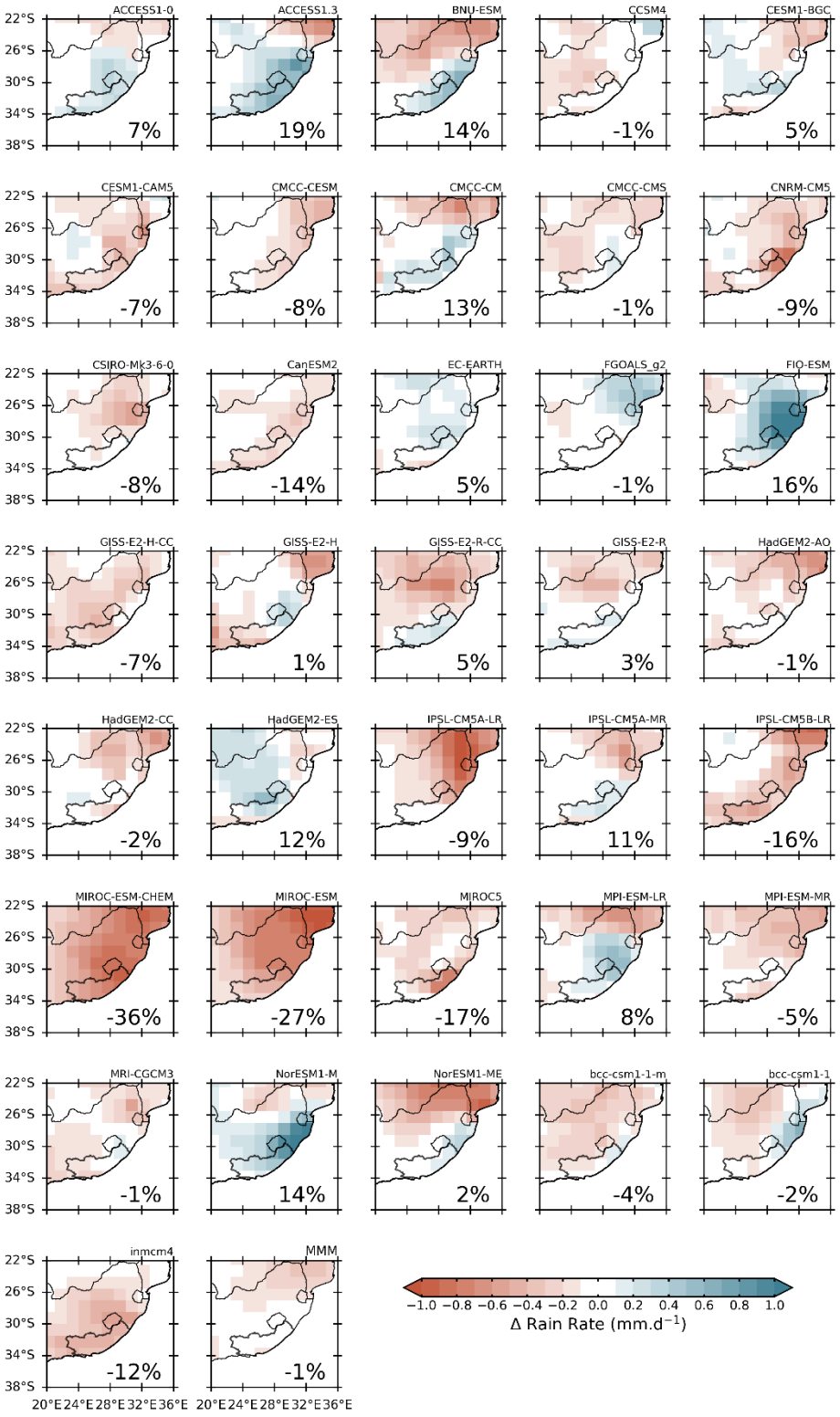

Figure 6.2: Mid-twenty-first century (2040–2060) projected changes in austral spring (SON) rainfall (shaded; in mm per day) in comparison to the historical period of 1976–2005 for the eastern half of South Africa in 36 CMIP5 models under the RCP8.5 scenario. The percentage change (%) given in the right-hand corner of each panel denotes the change averaged across the polygon (charcoal line) across the Eastern Cape River basins. The multi-model mean (MMM) in given in the last panel.

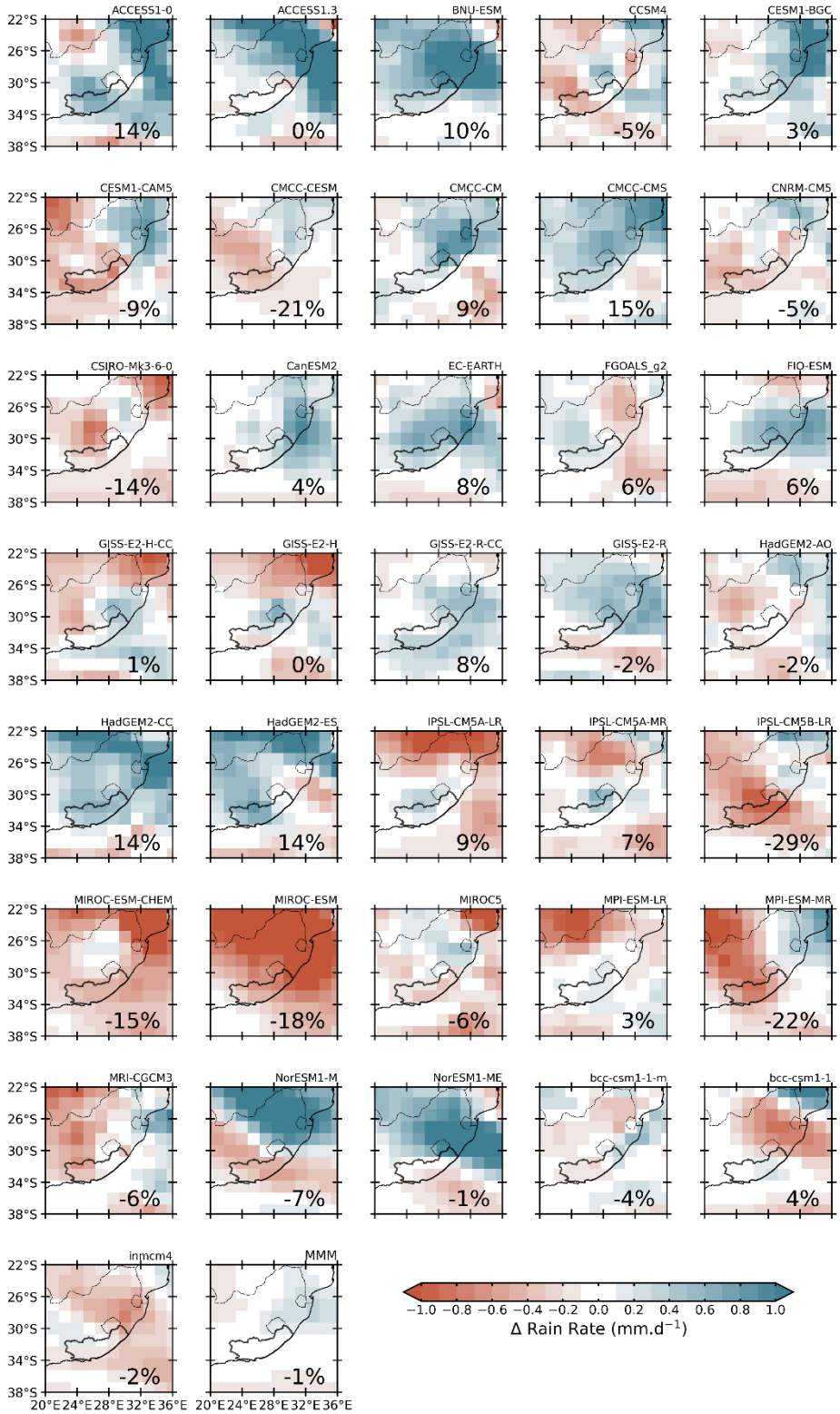

Figure 6.3: Mid-twenty-first century (2040–2060) projected changes in austral summer (DJF) rainfall (shaded; in mm per day) in comparison to the historical period of 1976–2005 for the south of South Africa in 36 CMIP5 models under the RCP8.5 scenario. The percentage change (%) given in the right-hand corner of each panel denotes the change averaged across the

polygon (charcoal line) across the Eastern Cape River basins. The multi-model mean (MMM) in given in the last panel.

6.3 Projected changes in regional circulation

Previous studies (e.g., Pohl et al., 2017, Sousa et al., 2019, Burls et al., 2020) have highlighted poleward shifts in the midlatitude westerly storm tracks as important for drying trends in the southern parts of South Africa. In this section, circulation projections from CMIP5 models are considered to see whether there are projected shifts in the subtropical high-pressure systems over the neighbouring South Atlantic and Indian Oceans. **Figure 6.4** plots the difference in mean sea level pressure for the mid-twentieth century (2040–2060) minus the historic run (1976–2005) from the CMIP5 model mean to highlight patterns that may be behind the projected rainfall changes. **Figure 6.4a** shows that in the spring future climate, models are projecting higher surface pressure over the midlatitudes and lower pressure over Antarctica, or a positive SAM tendency. This result corresponds to the observed tendency of a positive SAM in recent decades (Fogt et al., 2009, Abram et al., 2014, Sousa et al., 2018, Mahlalela et al., 2019). As highlighted in the previous section, a positive SAM phase has been identified as a primary mechanism by which the subtropical belt becomes drier under a warming climate due to an intensification in the westerlies resulting in a poleward shift in storm tracks and cold fronts (Bengtsson et al., 2006, Pohl et al., 2017, Fogt and Marshall, 2020). Furthermore, increased pressure south of South Africa, particularly over the South East Atlantic, indicates increased anticyclonic activity to the south and southwest of the country as well as poleward shifts in westerly moisture fluxes in the mid-21st Century relative to the historic period. These conditions are unfavourable for fronts and midlatitude storms approaching South Africa from the South Atlantic, as they will most likely be weakened and pushed to the south of the country as well as supplying less moisture to the midlatitude component of the cloud bands, resulting

in less rainfall over southern South Africa in the spring. Typically, cloud bands can produce significant rainfall over the Eastern Cape from about October (Hart et al., 2013). Although the increased anticyclonic conditions southeast of South Africa might be favourable for Eastern Cape rainfall via anticyclonic ridging, if the westerly moisture fluxes are further south than in the current climate, such a process may lead to less onshore moisture reaching the Eastern Cape than previously. **Fig. 6.4** differs slightly from the observed trends in low-level geopotential height (**Fig. 5.25,** Chapter 5) which had a negative trend over the South West Indian Ocean and therefore not an obvious positive SAM pattern. Nevertheless, both **Figs. 6.4** and **5.25** show an increasing trend over most of the subtropical – midlatitude South Atlantic in spring, indicating less favourable conditions for rainfall over southern South Africa in the mid-21st Century relative to the historic period.

Also evident is a decrease in pressure in the mid-21st Century relative to the historic period over the southwestern interior of subtropical southern Africa extending south across Namibia to the Northern Cape region of South Africa (**Fig. 6.4a**). This region is associated with the development of the Kalahari heat low in spring, so the observed pattern in the model mean difference suggests a strengthening of this heat low. Previous research predicted that early summer drying in southern Africa would be associated with an increase in the Kalahari and Angola heat lows (Cook and Vizy, 2013, Dunning et al., 2018, Howard and Washington, 2019). This is due to the way the heat low has been linked to the dynamics involved in the formation of drylines during the early summer (Howard and Washington, 2019).

Figure 6.4b shows similar patterns, with increased (decreased) surface pressure over the midlatitude (polar) regions in the projected mid-21st Century relative to the historical period, i.e., a clear positive SAM difference pattern. The summer and autumn seasons have been

highlighted to show significant positive trends in SAM since the 1950s (Barrucand et al., 2018, Schneider and Fogt, 2018, Gulev et al., 2021), and the CMIP5 models (**Fig. 6.5**) are projecting these trends to continue during the 21st Century. As for spring, increased anticyclonic conditions over the midlatitude South Atlantic are unfavourable for westerly disturbances tracking towards the ocean areas south of South Africa and hence the midlatitude input into the cloud bands. Although there are also increased anticyclonic conditions in the South West Indian Ocean, these differences are only significant south of 40°S so it is unclear whether this implies more ridging along the south coast, which in the current climate, has been identified to contribute to rain bearing weather over the south and east coasts of the country (Weldon and Reason, 2014, Engelbrecht et al., 2015). Ridging near the south coast encourages onshore flow, which improves moisture transport and rain-bearing weather in summer (Engelbrecht et al, 2015, Ndarana et al., 2020). However, the difference pattern in **Fig. 6.5b** suggests a more easterly, rather than directly onshore, flow near the Eastern Cape which is not necessarily favourable for increased rainfall. Note that compared to spring, the anticyclonic increase over the South West Indian Ocean in the mid- 21st Century relative to the historic period is much further south in summer. Further north and to the east of Madagascar, the projected relative increase in the tropical South Indian Ocean implies less favourable conditions for tropical storms tracking towards that island. Closer to the mainland, there are no significant differences in the Mozambique Channel whose characteristics (upper ocean temperature, tropical cyclone heat potential, Mozambique Channel Trough) have been shown to be important for the climate of southeastern Africa (Barimalala et al., 2018, 2020, Mawren et al., 2022).

While the surface pressure differences give a somewhat mixed indication of potential rainfall changes, those at mid-levels (**Fig. 6.5**) clearly show large differences in height over the entire southern African region and neighbouring oceans which are unfavourable for wetter

conditions. In spring (**Fig. 6.5a**), the strongest increases in height in the mid-21st Century relative to the historic period are centred just north of the Eastern Cape implying strong relative increases in subsidence over eastern South Africa in particular. Similar conditions are evident in the sixth IPCC report's CMIP6 models, with mid-tropospheric subsidence around 20-30°S implying a stronger Botswana High (Arias et al., 2021). Such conditions are not conducive for convective weather development including cloud bands (Hart et al., 2013, Driver and Reason, 2017, Reason, 2019) although they may not necessarily hinder light rain days over the south and east coastal regions via anticyclonic ridging. Further north over southern Angola and northern Namibia, the large increases in height imply a stronger Botswana High, which from **Fig. 5.2** (Chapter 5) was found to significantly correlate with spring rainfall in the current climate over almost all over the Eastern Cape except the far west. The observed spring strengthening of the Botswana High is consistent with the observed recent trend of a decrease in cloud bands (N. Hart 2021, pers. comm).

In summer (**Fig. 6.5b**), there are again projected large increases in height over the entire region, particularly near the core Botswana High which is centred over southern Namibia / western Botswana in summer (Reason, 2016, Driver and Reason, 2017) as well as in the 40–50°S band across the South Atlantic. Both these regions of large projected increases are very unfavourable for cloud band development as they imply stronger subsidence in the future climate as well as weaker midlatitude disturbances tracking south of South Africa. Note that Chapter 5 (**Fig. 5.10**) showed an even stronger relationship between summer rainfall over the Eastern Cape and the Botswana High than spring. The projected large increases in height over subtropical southern Africa in (**Fig. 6.5b**) also suggest less favourable conditions on average for other forms of convective rainfall. However, it is entirely possible that the region may see fewer but more intense rainfall events since (**Fig. 6.5**) are seasonal results; thus, on a seasonal basis, convection

might be less favourable in the projected future climate but, if individual events are able to break through the mid-level "convective lid", then particular weather systems could intensify more in a warmer climate and produce more intense rainfall (Fauchereau et al., 2003, Pohl et al., 2017, Pepler et al., 2021, Adelekan et al., 2022). Note also that the midlatitude increases in projected heights in **Fig. 6.5** are very much larger than those projected over the Antarctic region, so these patterns are not inconsistent with the increasing positive SAM pattern projected by the surface plots (**Fig. 6.4**).

While the CMIP5 model projections seem relatively clear and coherent in terms of both surface and mid-level circulation in both spring and summer, the projections for rainfall are not (**Figs. 6.2, 6.3**). It has been argued above that the projections for cloud bands, and convective weather more generally, are unfavourable on a seasonal basis (MacKellar et al., 2014, Engelbrecht et al., 2015, Lazenby et al., 2014, Abiodun et al., 2015, Dieppois et al., 2019). However, there may be increases in light rain days via more anticyclonic ridging along the south coast. Rainfall events themselves could be fewer in frequency, due to the increased anticyclonicity over subtropical southern Africa, but more intense when they do occur leading to mixed signals in terms of seasonal rainfall totals. It is also possible that existing climate models are not ideal for capturing the rainfall characteristics of the Eastern Cape region with its strong gradients in topography, vegetation, and sea surface temperatures (between the Agulhas Current and ambient waters). In the current climate, spring shows a clear decreasing trend in rainfall during 1981–2018 over most of the Eastern Cape (**Fig. 4.32**) whereas the summer trends are mixed (**Fig. 4.34**). Near the coast, and immediately inland, there are decreasing trends (but not significant) while much further inland in the central parts, there are significant increasing trends in summer. Chapter 5 argued that the decreasing observed trend in spring rainfall was related to decreased ridging along the coast and less onshore transport of moist, unstable marine air

towards the Eastern Cape. However, the future projections (**Fig. 6.4a**) imply increased ridging in spring. In summer, the observed trends showed increased anticyclonicity near the south coast and a more positive SAM phase, both favourable for increased Eastern Cape rainfall. In the future projections (**Fig. 6.4b**), the positive SAM pattern is clear but the increased anticyclonicity is further south and thus the rainfall mechanisms are less obvious. Based on this, the very slight drying projected for both seasons in the multi-model mean (-1% but not significant) in (**Figs. 6.1, 6.2**) seems a fair assessment although this result may have arisen somewhat fortuitously due to the very large spread between models.

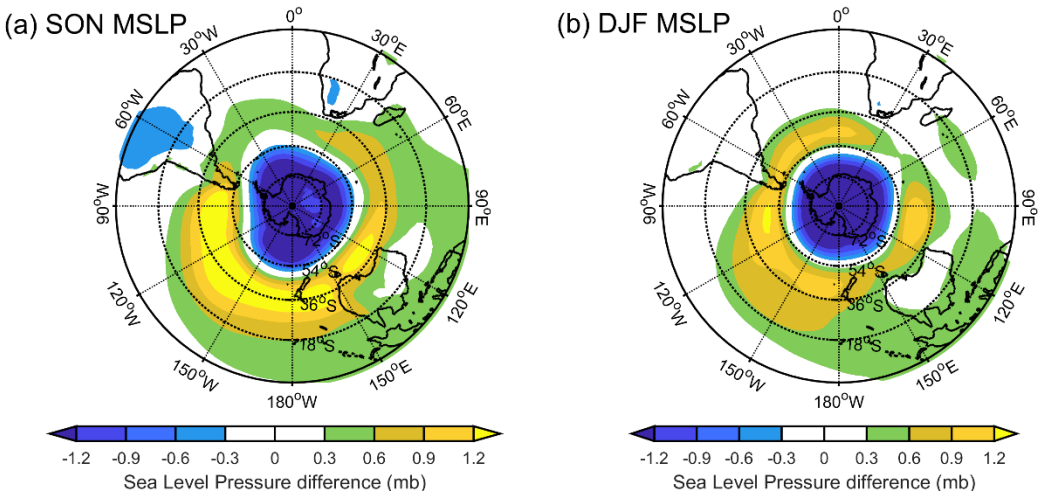

Figure 6.4: Differences in mean sea level pressure (shading: mb) for the **(a)** spring (September - November) and **(b)** summer (December - February) from CMIP5 models mean between the mid-twentieth century (2040–2060) and historic run (1976–2005) under the RCP8.5 scenario. Figures only show areas which are statistically significant at 95%.

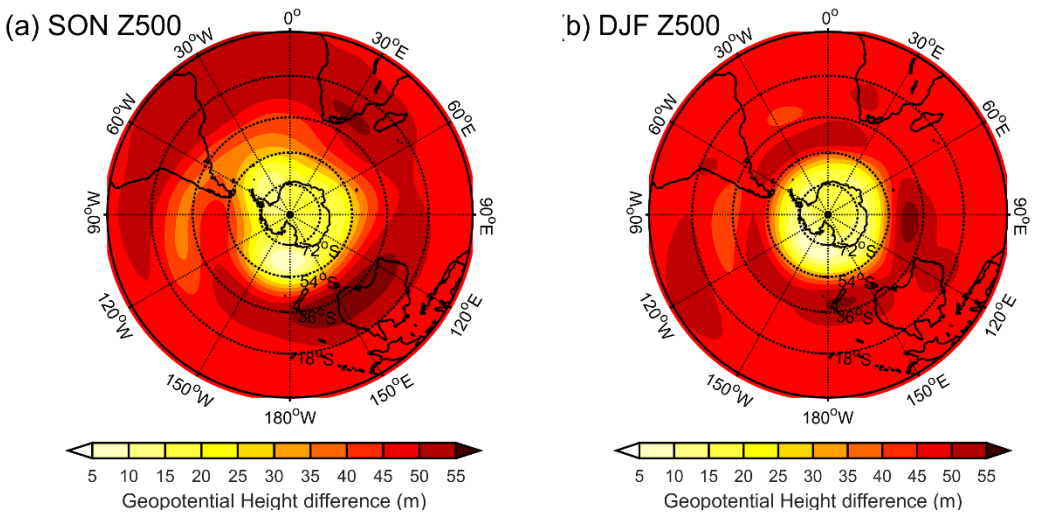

Figure 6.5: Differences in 500 hPa geopotential height (shading: m) for the **(a)** spring (September - November) and **(b)** summer (December - February) from CMIP5 models mean between the mid-twentieth century (2040–2060) and historic run (1976–2005) following the RCP8.5 scenario. Figures only show areas which are statistically significant at 95%.

6.4 Summary

The CMIP5 model ensemble is found to adequately represent the rainfall annual cycle of the Eastern Cape, with the summer half of the year being much wetter than the winter months, as observed. The models, however, only capture one rainfall peak in February, whereas the observed gridded rainfall products (GPCP and CMAP), which use both station and satellite data, exhibit two rainfall peaks (February and November). Furthermore, the multi-model mean indicates that the CMIP5 models have a wet bias in spring, and particularly in summer. They also show far too much rain in winter being almost as wet as the observed summer in terms of totals whereas, in CMAP and GPCP, the winter totals are 2–3 times less wet than spring or summer. These models project (**Fig. 6.1**) that the annual cycle will flatten slightly, with May - July becoming slightly wetter and the extended summer (September - March) becoming drier. The spring months (September-November) are projected to be substantially while summer months (December- February are projected to be drier than spring. However, the spread of the

models in producing this multi-model mean is very large so these results need to be viewed with caution. In the observations (1981–2018), spring shows a significant drying trend across most of the province whereas summer exhibits mixed signals with insignificant drying near the coast and immediately inland but significant wetting much further inland in the central parts. If the observed spring drying trend continues, then substantial impacts on both agricultural production as well as on water supply for local communities are expected at least for this season. This situation could potentially be alleviated to some extent by increased dam construction in wetter parts of the country and piping of stored water towards the Eastern Cape. The Nooitgedacht scheme is supposed to pipe water from the Orange River to the Nelson Mandela Bay region but difficulties between various levels of government have prevented this from properly operating as yet. At the time of writing of this thesis, the Nelson Mandela Bay region remains in a severe water crisis, partly due to poor rainfall in the dam catchments and partly due to government mismanagement. However, at the time of writing, interventions such as water leak reduction programs and water restriction had delayed "Day Zero" and seen a shift in water consumption patterns from local residents.

The large spread in rainfall projections between the various models, with some projecting increases and others decreases over the Eastern Cape region resulted in the multi-model mean showing only a very slight drying (-1%). Since this region is one of strong gradients in topography and vegetation type as well as between cooler coastal waters and the warm Agulhas Current, it is not surprising that such large spreads occur between the various models. A substantial part of the difficulties that such models have with representing the region’s climate may also result from their ability to adequately represent the characteristics of local rainfall systems such as cloud bands, ridging highs and cut-off lows. In the observed climate, Hart et al., (2013) showed that cloud bands on average bring a substantial amount of rainfall to the

Eastern Cape region, particularly in late spring and early summer while Singleton and Reason (2007) found that cut-off lows were important in spring and autumn. The significance of ridging highs to observed rainfall over this part of the country has been highlighted by Engelbrecht et al. (2015) and Ndarana et al. (2020). As previously discussed in this and earlier chapters, changes in the frequency of cloud bands during SON can result in wetter (more cloud bands) or drier (fewer cloud bands) conditions in the Eastern Cape. The models suggest increased subsidence over the subcontinent, which implies strengthening in the Botswana High. A stronger Botswana High has been linked to dry conditions over southern Africa due to how it results in more mid-level subsidence, thereby hindering organised convection and cloud band development in the summer half of the year (Driver and Reason, 2017).

In a comprehensive analysis of the ability of CMIP5 models to represent cloud bands over southern Africa, James et al. (2020) found that there were large variations in the average locations and frequencies of these weather systems between the models even though all models correctly simulate the large-scale generation and evolution of these cloud bands. Since the Eastern Cape is only part of the large area in southern Africa affected by cloud bands, small errors in the model simulations of cloud bands can therefore lead to substantial discrepancies in the resulting model simulation of seasonal rainfall. This result is consistent with earlier findings of climate model limitations attributed to a poor simulation of deep convection (MacKellar et al., 2014, Engelbrecht et al., 2015, Lazenby et al., 2014, Abiodun et al., 2015).

The models also project increased anticyclonic conditions over the midlatitude South Atlantic in both seasons as well as over the South Indian Ocean but much closer to the south coast in spring than in summer. These patterns suggest increased ridging along the south coast in spring which has previously been found to be important for onshore moisture flow into the Eastern

Cape, creating favourable conditions for rainfall (Engelbrecht et al, 2015, Ndarana et al., 2020). In summer, the model projections near the Eastern Cape are less clear. Both seasons show projections of increasing positive SAM phase. SAM is positively correlated with summer rainfall over most of the Eastern Cape in the observed data (**Fig. 5.21b**, consistent with Gillett et al., 2006); however, spring did not show any significant correlations with this mode (**Fig. 5.17b**). A positive trend in SAM is expected to continue into the twenty-first century under high emission scenarios and have been associated with projected drying over southwestern Africa (IPCC, 2021).

Overall, the projected changes in large scale circulation in the mid-21st Century relative to the current climate do not allow robust inferences to be made about future rainfall over the Eastern Cape region with any degree of confidence. Furthermore, the large model spread in seasonal rainfall totals in both the historical and projected future climate means that future projections based on the multi-model mean need to be viewed with caution. It is likely that the complex geography and meteorology of this region will continue to pose significant challenges for climate models. The disagreement among models highlights difficulties in projecting rainfall over meteorologically complex regions like the Eastern Cape and a need for downscaled techniques to better resolve local circulation patterns. Whether the substantially increased model resolution (few tens of km or less) of the latest generation earth system models which will start to resolve the ocean mesoscale or improvements in the parameterisations of sub-grid scale physics in the models will lead to significant improvements for the Eastern Cape region is an important topic for future research.

Chapter seven: Discussion and conclusions

7.1 Introduction

In this study, focus was placed on better understanding rainfall variability and trends over the Eastern Cape province, located on the southeast of South Africa. This region like most of the country has been facing severe pressure with respect to water security. Due to El Niño-induced dry conditions, major supply dams in the region reached dangerously low levels in 2015. The province was designated as a drought disaster region following severe water shortages in many urban and rural areas throughout the region. This is not the only South African province to have experienced such critical water shortages. The Western Cape (a winter rainfall region and located immediate to the west of the EC) also experienced severe water shortages during the "Day Zero" drought of 2015–2018 (Pienaar and Boonzaaier 2018, Sousa et al. 2018, Mahlalela et al. 2019, Burls et al. 2019). These recent drought events have placed immense pressure on local municipalities and society in general to adapt to the ongoing risk of water shortages. It is reminded that the climate is only one factor in the availability of water for the region. Increased water demand due to population growth, limited investment in reservoir infrastructure, poor water management and land management (e.g., alien vegetation, inappropriate farming practices), coupled with persistent dry years have put the Eastern Cape, and particularly the Nelson Mandela Bay municipal area, under severe water stress over the last decade.

At the time of writing this thesis, dam levels[2] in the Eastern Cape region were higher than at the same time the previous season, with local residents spared from complete water cuts. However, with government interventions still in place, the situation remains precarious. This is with some relief for parts of the province (i.e., Nelson Mandela Bay and OR Tambo district) that experienced flood events in April 2022. Floods in particular have been shown to have

[2] Website: https://mygqeberha.com/dam-levels/

devastating socioeconomic consequences for the region, due to infrastructure damages and regional agriculture losses (Singleton and Reason, 2007ab, Weldon and Reason, 2014, Engelbrecht and Landman, 2016). Recent floods in April 2022 affecting the KwaZulu-Natal and Eastern Cape Provinces highlight the devastating socio-economic and environmental impacts of these extreme weather events. The flooding events in these provinces resulted in over 400 deaths, massive infrastructure damage and inundated cropland.

The goal of this study is to better understand the nature of rainfall variability and trends over the Eastern Cape region as well as the associated regional circulation patterns. Improved understanding of the rainfall inputs into the water balance is important for proper water management and planning as well as to help determine how much of the current water shortage might be due to drought. Part of the challenge in understanding rainfall characteristics is that the region forms part of the transition zone between the summer and winter rainfall zones in southern South Africa. As a result, the meteorology here is complex as rainfall is influenced by systems from both the midlatitudes and tropics. Local topography and interactions with the neighbouring warm Agulhas Current also contribute to rainfall spatial variability in this region (Jury et al., 1993, Rouault et al., 2002, Singleton and Reason 2006).

The northeastern part of the Eastern Cape predominantly receives summer rainfall in the core summer months (December – February) while the south coast receives a significant amount of rainfall all year round. Previous studies have therefore either only focused on the summer rainfall region or the all year region (Jury, 1993, Weldon and Reason, 2014, Engelbrecht and Landman, 2016, Blamey et al., 2018, Thoithi et al., 2021). In this study, focus was placed on the spring (September to November; SON) and summer months (December – February; DJF). These months were chosen because of their significant contribution to annual totals, with SON

and DJF contributing approximately 30 and 40 – 45 % to annual totals, respectively. Furthermore, analysis has been restricted by the available station data, resulting in a limited spatial analysis of the region. The increased confidence in satellite-derived rainfall products, such as CHIRPS and GPM, allow for more comprehensive analysis with greater spatial coverage.

This final chapter addresses some of the limitations identified in our analysis of local rainfall characteristics and trends. It also provides an overview of the mechanisms underlying observed interannual variability, as well as how these patterns can be influenced by large scale modes of variability. The chapter concludes with the key findings of the study and their implications for the Eastern Cape.

7.2 Rainfall variability

A challenge experienced across many regions in Africa is the lack of long-term, reliable observations (i.e., station data). This has also been identified as a major constraint for climate research on the continent in the Intergovernmental Panel on Climate Change's sixth Assessment Report (IPCC, 2021). Given this challenge, satellite-derived rainfall products have been used to fill the void. In this analysis, CHIRPS data (Funk et al., 2015), a blended satellite product, that also provides considerable temporal coverage (1981–2018 period) was used. A comparison of CHIRPS and the station data across the Eastern Cape was performed to ensure that the product accurately represented rainfall over the region. Apart from a few stations, there appears to be relatively high correspondence between CHIRPS and station data. Other studies, such as (Thoithi et al., 2021, Moses et al., 2022), have found similar high correspondence for other locations across southern Africa. It is likely that stations that do not correspond well to CHIRPS

could be due to a few factors, namely, strong topographic gradients and satellite rainfall products performing poorly at coastline.

The increased regional coverage provided by CHIRPS allows for the investigation of spatial / temporal differences in rainfall across the province. The seasonality of rainfall varies across the region. For example, the coastal areas each receive approximately 30% of the annual total in spring and summer, whereas summer dominates in the northern interior of the province (40–45%). Autumn rainfall accounts for approximately 20–25% of the province's rainfall, with a small region in the far west accounting for 30% on average, whereas winter rainfall accounts for only 15% of the annual total in the far south. These spatial differences highlight the importance of taking smaller domains into account when analysing rainfall variability across the region.

Rainfall is also found to vary spatially with a strong gradient both along the coast and, particularly in the west, from the coast towards the inland where the southern part of the Great Karoo semidesert is located. Given the spatial differences in rainfall across the province, the analysis takes into account two smaller domains. These two domains are based on the province's main water management areas and are referred to in the text as the east basin (wetter domain), which covers two rivers draining the province's northeastern part, and the west basin (drier domain), which shows the catchment area of the main dams supplying the province's largest municipality (Nelson Mandela Bay) and major cities (i.e., Gqeberha, Makhanda and East London). The difference in rainfall totals between the west and east basins has been attributed to increased sea surface temperatures from the province's south to northeast due to increased proximity to the Agulhas current (Jury et al., 1993) which lies very close to the coast north of about East London, but which moves increasingly seawards of the coast from this

point towards Cape Agulhas on the south coast of the Western Cape. Furthermore, convective processes (i.e., convective storms and cloud bands) are common in the northern parts of the province, bringing heavy rainfall, as opposed to the west basin, where midlatitude processes (i.e., ridging highs and frontal systems) bring light to moderate rainfall (Weldon and Reason, 2014, Engelbrecht et al., 2015, Ndarana et al., 2020).

The interannual variability analysis across stations also shows spatial variations. The El Nino-induced drought in 2015/16 (i.e., Blamey et al., 2018) only occurred over northern and inland stations in the Eastern Cape (i.e., Cwebe Nature Reserve, Port St Johns, and Umtata) (along with many other areas in southern Africa), whereas southwestern stations received above-average rainfall for the same period. There is also a generally an agreement in wet and dry years with similar magnitudes for stations nearby to each other. This spatial variation emphasizes the importance of exercising caution when defining rainfall domains, as definitions based on political boundaries may be ineffective in highlighting local rainfall features such as spatial variability.

Overall, rainfall is found to have a high degree of interannual variability, with multi-year periods of above or below average amounts occurring frequently. The most recent was the 2015–2020 drought, which was visible in both spring and summer. Prolonged dry periods are found to be common not only in Eastern Cape, but also in parts of KwaZulu-Natal (Blamey et al., 2018), and Western Cape province (Pienaar and Boonzaaier, 2018, Sousa et al., 2018, Mahlalela et al., 2019, Burls et al., 2019). In response to global warming, these multi-year droughts are projected to increase by a factor of three over southwestern South Africa (IPCC, 2021). Analysis of rainfall trends reveals a significant decrease in spring rainfall over most of the province, except in the far southwest and far northeast, indicating a weakening of the

rainfall gradient in this region. A decrease in rainfall over the northern part of the province has significant water implications for the province's rural population who rely on rainfed agriculture. Many of the areas showing significant decreasing trends are also important for commercial agriculture (both livestock and fruit). In summer, only the northern interior of the province showed any significant trends (in this case increasing rainfall). Most of the rest of the province showed a decreasing tendency but it was not found to be significant.

Rainfall characteristics are examined in order to better understand observed trends and seasonal anomalies. Station data and CHIRPS are used for the analysis, a comparison of dry days (1 mm/day), light (2 – 9 mm/day), moderate (10 – 30 mm/day), and heavy (> 30 mm/day) highlights disparities between the two datasets. The CHIRPS product is found to record more moderate rainfall days compared to station data, while near the coast stations are found to record more heavy rainfall days compared to CHIRPS. These disparities can be attributed to satellite sensors detecting proxy variables and calculating rainfall estimates based on relationships with gauged rainfall (Tote et al., 2015, Funk et al., 2015, du Plessis and Kibii, 2021). As a result, the rainfall product may be more sensitive to moderate rainfall and less sensitive to light rainfall. Also, the paucity in available station data means there are less data available for assimilation and validation for blended products such as CHIRPS. The available station data was instrumental in the rainfall characteristics analysis. The results suggest that moderate and heavy rainfall days have a stronger influence on seasonal totals compared to light rainfall days for both spring and summer. The observed decrease in spring seasonal rainfall totals is found to be associated with a decrease in light, moderate and heavy rainfall. For the summer, there is a significant decrease in dry day frequency inland and increase in the light and moderate rainfall. This result is consistent with the findings of Thoithi et al. (2021), who discovered a decrease in dry spell frequency and an increase in moderate wet days over an

interior southeast South African region, including the inland Eastern Cape, during the summer. This region was shown by these authors to be part of a NE-SW gradient of high dry spell frequency in the summer. As a result, the observed increasing trend in rainfall indicates a weakening in the dry spell gradient, more consistent rainfall for the season, and thus potentially favourable conditions for crop production. This inland area also corresponds to that where this thesis found an increasing trend in summer rainfall totals. However, near the coast, the results show a decrease in heavy rainfall days which accounts for the observed decline in summer rainfall totals, although the trend is not significant. Investigating different rainfall characteristics (dry spell and rain day numbers) is useful in understanding observed seasonal rainfall patterns and provides more helpful information to user groups (e.g., farmers, water resource managers) for applications.

The complexities of rainfall over the Eastern Cape are reflected in future rainfall projections for this region. Although CMIP6 model projections are now available, computational constraints meant that only CMIP5 data could be utilized. Analysis of mid-century (2040–2060) projections under the RCP8.5 scenario in CMIP5 suggest that there may be a slight flattening of the annual cycle over the Eastern Cape with the winter becoming wetter and the summer drier. Furthermore, the multi-model mean indicates that the CMIP5 models have a wet bias in spring, and particularly in summer. Although many of the 36 models analysed project a spring drying over the Eastern Cape, there is a large spread in the future projections and the multi-model mean indicates only very slight drying in this season. For DJF, models also indicate a slight decrease in rainfall totals, again with a very large spread between the models. As a result, it is difficult to have confidence in future rainfall projections over the region. However, given the strong land and ocean surface gradients in the region and its sensitivity to both tropical and midlatitude circulation, it is not surprising that the models should show a

large spread in projections over the Eastern Cape and have difficulties in accurately representing the local climate. Furthermore, the difficulties relative to observations that CMIP5 models have in simulating the frequency and location of cloud bands (James et al., 2020), a key rainfall-producing system over the region, adds to the uncertainty in future rainfall changes. Caution therefore needs to be taken regarding future projections over this region. Nonetheless, the complex geography and meteorology of this region does provide an interesting test bed for climate models.

7.3 Circulation patterns

To identify circulation features associated with wet (dry) seasons, a composite analysis was used. The composite method has been acknowledged as a simple and effective tool for identifying common conditions observed during specific climate states. However, there are some concerns about using this method because inconsistencies in the design, creation, interpretation, and evaluation of composites can have a significant impact on the conclusions of some studies (Simmonds and Rudeva 2014, Boschat et al., 2016). The results presented here should therefore be interpreted with caution.

This analysis revealed that rainfall variability is linked to the large-scale conditions that are conducive for the formation and development of the major rain bearing systems for the region i.e., cloud bands, ridging high pressures and storm tracking into the domain. Thus, wet (dry) springs are characterised by a weaker (stronger) Botswana High as evident in mid-level geopotential height anomalies. The relationship between Botswana high and rainfall is investigated further for southern Africa using an ERA5 reanalysis-derived Botswana High index. When compared to the coarse resolution provided by NCEP reanalysis (Kanamitsu et al., 2002) data, the higher resolution in ERA5 (Hersbach et al., 2020) data allows for a much

better representation of the Botswana High. This analysis revealed a strong negative relationship between rainfall and the Botswana High; in summer, this relationship is statistically significant across most of southern Africa, including the entire Eastern Cape province, but it is only significant in the province's northern parts (“east basin”) in spring. This strong relationship may result from a stronger (weaker) mid-level Botswana High leading to enhanced (reduced) subsidence over subtropical southern Africa which results to less (more) favourable conditions for cloud bands to develop (Reason, 2016, Driver and Reason, 2017). Cyclonic (anticyclonic) circulation anomalies over the southwest Indian Ocean associated with divergence (convergence) over the Agulhas Current region also indicate unfavourable (favourable) conditions for ridging and cloud bands during dry (wet) springs. It was found that there were approximately 1–2 fewer (more) cloud band days than average over much of South Africa, including the majority of the Eastern Cape during these dry (wet) springs (N. Hart, 2020 Per comm.). Note that cloud bands have been found to be significant for rainfall production in early summer over the Eastern Cape (Hart et al., 2013).

During the summer months, ridging over the south coast appears to play a significant role in rainfall changes, in addition to the Botswana High influence. This season is characterised by equatorward (poleward) shift in the westerly wind belt during dry (wet) seasons. Summer conditions suggest negative (positive) SAM conditions during dry (wet) summers. Ridging highs tend to decrease (increase) as the mid-latitude circulation patterns push equatorward (retreat poleward), causing rainfall to decrease (increase) along the south coast of South Africa and neighbouring inland. Ridging highs involve the onshore flow of moisture across the warm Agulhas Current region and onto the landmass (Weldon and Reason 2013, Engelbrecht and Landman, 2016, Ndarana et al., 2020). Furthermore, SST composites indicate cooler (warmer) SST anomalies over southwest Atlantic a key cyclogenesis region in the Southern Hemisphere

(Jones and Simmonds, 1993, Hoskins and Hodges, 2005) suggesting more unfavourable (favourable) conditions for mid-latitude cyclogenesis during dry (wet) summers. Ridging days have also been found to have a significant positive relationship with storm tracks at specific bands, implying less (more) ridging along the south coast as storm tracks are located further south (north) across the South Atlantic.

7.4 Influence of large-scale modes of variability on rainfall

Previous work has shown that large-scale modes of variability such as the El Niño Southern Oscillation (ENSO), the South Indian Ocean Subtropical Dipole (SIOD), and the Southern Annular Mode (SAM) influences summer rainfall over many parts of southern Africa (Lindesay, 1986, 1988, Nicholson and Kim, 1997, Reason et al., 2000, Behera and Yamagata, 2001, Reason, 2001, 2002, Gillett et al., 2006). However, in spring, the influence of any of these modes on Eastern Cape rainfall is unclear. For anomalously wet springs, the SST composite indicates La Niña-like conditions. However, an examination of the correlations between southern African rainfall and the Niño 3.4 index reveals only weak and non-significant links with spring rainfall over the Eastern Cape region. Correlations with the Marshal (2003) SAM index produce weak positive correlations, indicating that SAM has little influence in the spring. Similarly, no SIOD relationship was found either although dry (wet) springs exhibited cool (warm) SST anomalies in the greater Agulhas Current region which have previously been associated with dry (wet) summers over eastern South Africa (Reason and Mulenga, 1999). On the other hand, ENSO is known to impact atmospheric circulation over both the South Atlantic and the South Indian Oceans during spring (Reason et al., 2000, Colberg et al., 2004). This thesis showed that changes in the SIHP outer bounds, particularly its eastern extent, have a strong relationship with spring rainfall over the Eastern Cape. Part of the province also showed a significant correlation between spring rainfall and the zonal wavenumber 3 index.

Changes in the SIHP may lead to changes in the easterly moisture fluxes towards subtropical southern Africa from the South Indian Ocean and hence affect rainfall.

A strong ENSO correlation is evident during the summer season. Sea surface temperature anomalies during dry (wet) summers show the typical El Niño (La Niña) pattern in the Pacific and South Atlantic but not the Indian Ocean which shows generally negative anomalies in both composites. Several studies (e.g., Kiladis and Mo, 1986, Ropelewski and Halpert, 1987, Cook, 2000) have shown how ENSO-driven anomalies in the tropical Pacific lead to atmospheric teleconnections to higher latitudes via the propagation of Rossby-wave-like features. One common pattern is the Pacific-South America pattern which is clearly associated with impacts over the South East Atlantic and along the west and south coasts of South Africa (Colberg et al., 2004). During El Niño (La Niña) summers, large scale positive pressure anomalies develop over the Indian Ocean and subtropical southern Africa (Reason et al., 2000), resulting in unfavourable (favourable) conditions for tropical convection and cloud band alignment over the subcontinent (Mulenga et al., 2003, Hart et al., 2018) and typically drier (wetter) conditions. During an El Niño event, the preferred locations of the cloud bands tend to move offshore (Fauchereau et al., 2009, Hart et al., 2018) resulting in below average rainfall over southern Africa (Lindesay, 1998, Reason et al., 2000). The OLR data used in this study suggest decreased (increased) convective cloud over subtropical southern Africa and the neighbouring ocean to the east and the opposite over the northern Mozambique / northern Madagascan region during dry (wet) summers implying shifts in cloud band activity.

A significant correlation between the SAM and rainfall over most of the Eastern Cape in summer was also found consistent with previous work for the Southern Hemisphere as a whole

(Gillett et al., 2006). The mid-level geopotential height for the dry (wet) summers composite shows negative (positive) pressure anomalies over the mid-latitudes and positive (negative) pressure anomalies over Antarctica, reflecting a negative (positive) SAM phase. For dry summers, a strong wavenumber four pattern is also present, but it is less obvious in the wet composite. A positive SAM phase is associated with a southward shift in the subtropical jet, leading to a more equatorward positioned SAHP and more ridging over the south coast (Sun et al., 2017).

In summary, interannual variability in summer rainfall over the Eastern Cape appears related to both ENSO and SAM whereas, in spring, neither of these climate modes appears to clearly influence rainfall totals. Both spring and summer rainfall are related to the Botswana High, but some of the variability in this regional circulation system may result from ENSO (Driver and Reason, 2017). The summer connection with the SAM is particularly important because it is expected that SAM will continue to shift towards an increasingly positive phase in the future (e.g., Fyfe et al. 1999, Thompson and Solomon, 2002, Cai et al. 2003, Gillett and Fyfe, 2013, Zheng et al. 2013, Lim et al. 2016). Other global signals are that the Hadley circulation (or tropics) will continue to expand (e.g., Lu et al., 2007, Seidel et al., 2008, Nguyen et al., 2013, 2015) and extra-tropical weather systems will shift further poleward (e.g., Fyfe, 2003). It is possible that such trends may also reflect in future changes in the Botswana High found here to be significantly related to both spring and summer rainfall in the current climate. The CMIP5 projections presented in Chapter 6 are consistent with a stronger Botswana High in the mid-21st Century compared to recent decades. At the surface, these CMIP5 differences suggested more anticyclonic conditions over the entire mid-latitude South Atlantic and part of the South Indian Ocean in both seasons which has implications for ridging along the south and east coasts of the country as well as the mid-latitude inputs into the cloud bands.

7.5 Thesis conclusion

The Eastern Cape province of South Africa lies in the transition zone between the winter rainfall (western South Africa) and the summer rainfall (rest of subtropical southern Africa) regions which makes it an interesting but complex region to study. It is characterised by strong topographic; soil moisture and vegetation gradients and its northern (southern) coast is close to (more distant from) the highly variable Agulhas Current, (the most intense western boundary current in the global oceans. Given its latitudinal range of about 30–34°S, the Eastern Cape is influenced by both tropical and midlatitude weather systems and their interactions further adding to the complexity of its meteorology. Severe droughts and flooding events are frequently experienced in the Eastern Cape which cause substantial socioeconomic impacts, including loss of life in some cases. Recently, the province experienced an intense drought (which started in 2015) with several urban areas under stringent water restrictions and having been close to have run out of piped water from the corresponding dams. The impacts of the below average rainfall were significantly impacted by poor local and provincial management of water resources so the lack of piped water cannot be solely blamed on poor rainfall. Although the 2015-drought has manifest itself throughout all seasons, the spring (September – November) shows the strongest and most coherent signal. On average, the spring (summer) contributes between 25 and 35% (30 and 45%) of the annual total rainfall.

While ENSO and SAM seem to be important for summer rainfall over the Eastern Cape, this does not appear to be the case for spring. Although other modes of variability, such as the Benguela Niño (Rouault et al., 2003, Hansingo and Reason, 2009), the SIOD (Behera and Yamagata, 2001, Reason, 2001, 2002) have been identified as having an influence on summer rainfall over various parts of subtropical southern African rainfall, this study found no obvious

links with these modes of variability for the Eastern Cape in either season. Nor were any relationships found with the Indian Ocean Dipole, known to strongly influence East African rainfall in austral spring (Saji et al., 1999).

Another difference between the spring and summer rainfall over the Eastern Cape is that the former showed a significant decreasing trend over most of the province whereas the latter showed a significant increasing trend but only over a relatively small interior region. Overall, the findings indicate that the rainfall gradient across the province is weakening in the spring. The observed spring rainfall decline is concerning because this season marks the start of the rainy season and the first opportunity for surface and groundwater resources to begin replenishing, especially if the previous summer was drier than average. The majority of rural communities in the northern Eastern Cape rely on rain-fed agriculture, and current trends indicate a need for a shift in the planting season, as an early start may result in crop failure due to rainfall shortfalls.

Summer rainfall trends are mixed; some inland areas show a significant increase in rainfall totals whereas the coast and northeast of the region show a decrease, but it is not statistically significant. The observed increase in rainfall inland is associated with an increase in light and moderate rainfall days, whereas the observed (but not significant) decrease along the coast in summer rainfall is associated with a significant decrease in heavy rainfall days. Persistent dry conditions throughout the summer season have implications for water storage during the summer, particularly in coastal towns such as Port Elizabeth and East London, given that the summer and spring contribute a significant portion of annual rainfall totals. Furthermore, these results emphasize the need for analysis to take into account rain day characteristics in order to better understand observed seasonal patterns and for seasonal forecasters to consider providing

more detailed information than simply whether seasonal totals are likely to be near, below, or above average.

Although there appear to be some robust signals in projected large-scale circulation changes over the southern African region, as models improve future work needs to consider the implications for dominant rain-producing systems such as cloud bands and ridging anticyclones. For example, CMIP5 models have varying degrees of success in adequately representing cloud bands in the current climate (James et al., 2020). Improved understanding of the relationships between these weather systems and large-scale climate modes is needed, particularly as these modes are themselves projected to change in future (IPCC, 2021).

Analysis of the CMIP5 models presented here, using the RCP8.5 scenario, shows a slight drying, with a large model spread in seasonal rainfall for both spring and summer during the mid-twenty-first century. The CMIP5 model spread highlights the difficulties of projecting rainfall over meteorologically complex regions like the Eastern Cape with strong local gradients in surface conditions. It is unclear whether downscaling techniques may provide any significant advantages or whether the new generation of global Earth System models with resolutions able to capture the ocean mesoscale may allow more robust rainfall projections for this region to be developed. Although there is little certainty about future rainfall changes, if observed rainfall trends continue, there is a need for increased investment in water reservoir infrastructure over the province, particularly given the national government aim to develop special industrialized zones at Coega.

References

ABIODUN, B. J., ABBA OMAR, S., LENNARD, C. & JACK, C. 2016. Using regional climate models to simulate extreme rainfall events in the Western Cape, South Africa. *International Journal of Climatology,* 36**,** 689-705.

ABIODUN, B. J., ADEGOKE, J., ABATAN, A. A., IBE, C. A., EGBEBIYI, T. S., ENGELBRECHT, F. & PINTO, I. 2017. Potential impacts of climate change on extreme precipitation over four African coastal cities. *Climatic Change,* 143**,** 399-413.

ABRAM, N. J., MULVANEY, R., VIMEUX, F., PHIPPS, S. J., TURNER, J. & ENGLAND, M. H. 2014. Evolution of the Southern Annular Mode during the past millennium. *Nature Climate Change,* 4**,** 564-569.

ADELEKAN, I. O., SIMPSON, N. P., TOTIN, E. & TRISOS, C. H. 2022. IPCC Sixth Assessment Report (AR6): Climate Change 2022-Impacts, Adaptation and Vulnerability: Regional Factsheet Africa.

ADLER, R. F., HUFFMAN, G. J., CHANG, A., FERRARO, R., XIE, P.-P., JANOWIAK, J., RUDOLF, B., SCHNEIDER, U., CURTIS, S. & BOLVIN, D. 2003. The version-2 global precipitation climatology project (GPCP) monthly precipitation analysis (1979–present). *Journal of hydrometeorology,* 4**,** 1147-1167.

ANGHILERI, D., BOZZINI, V., MOLNAR, P., JAMALI, A. A. & SHEFFIELD, J. 2022. Comparison of hydrological and vegetation remote sensing datasets as proxies for rainfed maize yield in Malawi. *Agricultural Water Management,* 262**,** 107375.

ARCHER, C. L. & CALDEIRA, K. 2008. Historical trends in the jet streams. *Geophysical Research Letters,* 35.

ARIAS, P. A., BELLOUIN, N., COPPOLA, E., JONES, R. G., KRINNER, G., MAROTZKE, J., NAIK, V., PALMER, M. D., PLATTNER, G.-K. & ROGELJ, J. 2021. Technical summary. *Climate Change***,** 33-144.

BARIMALALA, R., DESBIOLLES, F., BLAMEY, R. C. & REASON, C. 2018. Madagascar Influence on the South Indian Ocean Convergence Zone, the Mozambique Channel Trough and Southern African Rainfall. *Geophysical Research Letters,* 45.

BARRUCAND, M. G., ZITTO, M. E., PIOTRKOWSKI, R., CANZIANI, P. & O'NEILL, A. 2018. Historical SAM index time series: linear and nonlinear analysis. *International Journal of Climatology,* 38**,** e1091-e1106.

BEHERA, S. K., LUO, J. J., MASSON, S., RAO, S. A., SAKUMA, H. & YAMAGATA, T. 2006. A CGCM study on the interaction between IOD and ENSO. *Journal of Climate,* 19**,** 1688-1705.

BEHERA, S. K. & YAMAGATA, T. 2001. Subtropical SST dipole events in the southern Indian Ocean. *Geophysical Research Letters,* 28**,** 327-330.

BENGTSSON, L., HODGES, K. I. & ROECKNER, E. 2006. Storm tracks and climate change. *Journal of climate,* 19**,** 3518-3543.

BLAMEY, R., KOLUSU, S., MAHLALELA, P., TODD, M. & REASON, C. 2018. The role of regional circulation features in regulating El Niño climate impacts over southern Africa: A comparison of the 2015/2016 drought with previous events. *International Journal of Climatology,* 38**,** 4276-4295.

BLAMEY, R., MIDDLETON, C., LENNARD, C. & REASON, C. 2017. A climatology of potential severe convective environments across South Africa. *Climate Dynamics,* 49**,** 2161-2178.

BLAMEY, R. C. & REASON, C. 2012. Mesoscale convective complexes over southern Africa. *Journal of Climate,* 25**,** 753-766.

BOSCHAT, G., SIMMONDS, I., PURICH, A., COWAN, T. & PEZZA, A. B. 2016. On the use of composite analyses to form physical hypotheses: An example from heat wave–SST associations. *Scientific reports,* 6**,** 1-10.

BURLS, N. J., BLAMEY, R. C., CASH, B. A., SWENSON, E. T., AL FAHAD, A., BOPAPE, M.-J. M., STRAUS, D. M. & REASON, C. J. 2019. The Cape Town "Day Zero" drought and Hadley cell expansion. *Npj Climate and Atmospheric Science,* 2**,** 1-8.

CHAMBERS, D., TAPLEY, B. & STEWART, R. 1999. Anomalous warming in the Indian Ocean coincident with El Niño. *Journal of Geophysical Research: Oceans,* 104**,** 3035-3047.

COLBERG, F., REASON, C. & RODGERS, K. 2004. South Atlantic response to El Niño–Southern Oscillation induced climate variability in an ocean general circulation model. *Journal of Geophysical Research: Oceans,* 109.

COOK, C., REASON, C. J. & HEWITSON, B. C. 2004. Wet and dry spells within particularly wet and dry summers in the South African summer rainfall region. *Climate Research,* 26**,** 17-31.

COOK, K. H. 2000. The South Indian convergence zone and interannual rainfall variability over southern Africa. *Journal of Climate,* 13**,** 3789-3804.

COOK, K. H. & VIZY, E. K. 2013. Projected changes in East African rainy seasons. *Journal of Climate,* 26**,** 5931-5948.

CRÉTAT, J., POHL, B., DIEPPOIS, B., BERTHOU, S. & PERGAUD, J. 2019. The Angola Low: relationship with southern African rainfall and ENSO. *Climate Dynamics,* 52**,** 1783-1803.

CRÉTAT, J., RICHARD, Y., POHL, B., ROUAULT, M., REASON, C. & FAUCHEREAU, N. 2012. Recurrent daily rainfall patterns over South Africa and associated dynamics during the core of the austral summer. *International Journal of Climatology,* 32**,** 261-273.

D'ABRETON, P. & LINDESAY, J. 1993. Water vapour transport over southern Africa during wet and dry early and late summer months. *International Journal of Climatology,* 13**,** 151-170.

D'ABRETON, P. & TYSON, P. 1996. Three-dimensional kinematic trajectory modelling of water vapour transport over Southern Africa. *Water sA,* 22**,** 297-306.

DIEPPOIS, B., POHL, B., CRÉTAT, J., EDEN, J., SIDIBE, M., NEW, M., ROUAULT, M. & LAWLER, D. 2019. Southern African summer-rainfall variability, and its teleconnections, on interannual to interdecadal timescales in CMIP5 models. *Climate Dynamics,* 53**,** 3505-3527.

DINKU, T., FUNK, C., PETERSON, P., MAIDMENT, R., TADESSE, T., GADAIN, H. & CECCATO, P. 2018. Validation of the CHIRPS satellite rainfall estimates over eastern Africa. *Quarterly Journal of the Royal Meteorological Society,* 144**,** 292-312.

DOSIO, A., LENNARD, C. & SPINONI, J. 2022. Projections of indices of daily temperature and precipitation based on bias-adjusted CORDEX-Africa regional climate model simulations. *Climatic Change,* 170**,** 1-24.

DRIVER, P. & REASON, C. 2017. Variability in the Botswana High and its relationships with rainfall and temperature characteristics over southern Africa. *International Journal of Climatology,* 37**,** 570-581.

DU PLESSIS, J. & KIBII, J. 2021. Applicability of CHIRPS-based satellite rainfall estimates for South Africa. *Journal of the South African Institution of Civil Engineering,* 63**,** 43-54.

DUNNING, C. M., BLACK, E. & ALLAN, R. P. 2018. Later wet seasons with more intense rainfall over Africa under future climate change. *Journal of Climate,* 31**,** 9719-9738.

DYSON, L. & VAN HEERDEN, J. 2002. A model for the identification of tropical weather systems over South Africa. *Water SA,* 28**,** 249-258.

DYSON, L. L., VAN HEERDEN, J. & SUMNER, P. D. 2015. A baseline climatology of sounding-derived parameters associated with heavy rainfall over Gauteng, South Africa. *International Journal of Climatology,* 35**,** 114-127.

ENDRIS, H. S., OMONDI, P., JAIN, S., LENNARD, C., HEWITSON, B., CHANG'A, L., AWANGE, J., DOSIO, A., KETIEM, P. & NIKULIN, G. 2013. Assessment of the performance of CORDEX regional climate models in simulating East African rainfall. *Journal of Climate,* 26**,** 8453-8475.

ENGELBRECHT, C. J. & LANDMAN, W. A. 2016. Interannual variability of seasonal rainfall over the Cape south coast of South Africa and synoptic type association. *Climate dynamics,* 47**,** 295-313.

ENGELBRECHT, C. J., LANDMAN, W. A., ENGELBRECHT, F. A. & MALHERBE, J. 2015a. A synoptic decomposition of rainfall over the Cape south coast of South Africa. *Climate Dynamics,* 44**,** 2589-2607.

ENGELBRECHT, F., ADEGOKE, J., BOPAPE, M.-J., NAIDOO, M., GARLAND, R., THATCHER, M., MCGREGOR, J., KATZFEY, J., WERNER, M. & ICHOKU, C. 2015b. Projections of rapidly rising surface temperatures over Africa under low mitigation. *Environmental Research Letters,* 10**,** 085004.

FAUCHEREAU, N., POHL, B., REASON, C., ROUAULT, M. & RICHARD, Y. 2009. Recurrent daily OLR patterns in the Southern Africa/Southwest Indian Ocean region, implications for South African rainfall and teleconnections. *Climate Dynamics,* 32**,** 575-591.

FAUCHEREAU, N., TRZASKA, S., ROUAULT, M. & RICHARD, Y. 2003. Rainfall variability and changes in southern Africa during the 20th century in the global warming context. *Natural hazards,* 29**,** 139-154.

FAVRE, A., HEWITSON, B., LENNARD, C., CEREZO-MOTA, R. & TADROSS, M. 2012. Cut-off Lows in the South Africa region and their contribution to precipitation. *Climate Dynamics,* 41**,** 2331-2351.

FOGT, R. L. & MARSHALL, G. J. 2020. The Southern Annular Mode: variability, trends, and climate impacts across the Southern Hemisphere. *Wiley Interdisciplinary Reviews: Climate Change,* 11**,** e652.

FOGT, R. L., PERLWITZ, J., MONAGHAN, A. J., BROMWICH, D. H., JONES, J. M. & MARSHALL, G. J. 2009. Historical SAM variability. Part II: Twentieth-century variability and trends from reconstructions, observations, and the IPCC AR4 models. *Journal of Climate,* 22**,** 5346-5365.

FUNK, C., PETERSON, P., LANDSFELD, M., PEDREROS, D., VERDIN, J., SHUKLA, S., HUSAK, G., ROWLAND, J., HARRISON, L., HOELL, A. & MICHAELSEN, J. 2015. The climate hazards infrared precipitation with stations--a new environmental record for monitoring extremes. *Sci Data,* 2**,** 150066.

GEBRECHORKOS, S. H., HÜLSMANN, S. & BERNHOFER, C. 2018. Evaluation of multiple climate data sources for managing environmental resources in East Africa. *Hydrology and Earth System Sciences,* 22**,** 4547-4564.

GILLETT, N. P., KELL, T. D. & JONES, P. 2006. Regional climate impacts of the Southern Annular Mode. *Geophysical Research Letters,* 33.

GONG, D. & WANG, S. 1999. Definition of Antarctic oscillation index. *Geophysical research letters,* 26**,** 459-462.

GOSLING, S. N., DUNN, R., CARROL, F., CHRISTIDIS, N., FULLWOOD, J., GUSMAO, D.D., GOLDING, N., GOOD, L., HALL, T., KENDON, L. AND KENNEDY, J., .. 2011. Climate: Observations, projections and impacts. *Climate: Observations, projections and impacts*.

GRAMCIANINOV, C., CAMPOS, R., DE CAMARGO, R., HODGES, K., SOARES, C. G. & DA SILVA DIAS, P. 2020. Analysis of Atlantic extratropical storm tracks characteristics in 41 years of ERA5 and CFSR/CFSv2 databases. *Ocean Engineering,* 216**,** 108111.

GULEV, S. K., THORNE, P. W., AHN, J., DENTENER, F. J., DOMINGUES, C. M., GERLAND, S., GONG, D., KAUFMAN, D. S., NNAMCHI, H. C. & QUAAS, J. 2021. Changing state of the climate system. *Climate change***,** 287-422.

HARRISON, M. 1984. A generalized classification of South African summer rain-bearing synoptic systems. *Journal of Climatology,* 4**,** 547-560.

HART, N., REASON, C. & FAUCHEREAU, N. 2010. Tropical–extratropical interactions over southern Africa: Three cases of heavy summer season rainfall. *Monthly weather review,* 138**,** 2608-2623.

HART, N. C., REASON, C. J. & FAUCHEREAU, N. 2013. Cloud bands over southern Africa: seasonality, contribution to rainfall variability and modulation by the MJO. *Climate dynamics,* 41**,** 1199-1212.

HART, N. C., WASHINGTON, R. & STRATTON, R. A. 2018. Stronger local overturning in convective-permitting regional climate model improves simulation of the subtropical annual cycle. *Geophysical Research Letters,* 45**,** 11,334-11,342.

HART, N. C. G., REASON, C. J. C. & FAUCHEREAU, N. 2012. Cloud bands over southern Africa: seasonality, contribution to rainfall variability and modulation by the MJO. *Climate Dynamics,* 41**,** 1199-1212.

HARTMANN, D. L. & LO, F. 1998. Wave-driven zonal flow vacillation in the Southern Hemisphere. *Journal of the Atmospheric Sciences,* 55**,** 1303-1315.

HERSBACH, H., BELL, B., BERRISFORD, P., HIRAHARA, S., HORÁNYI, A., MUÑOZ-SABATER, J., NICOLAS, J., PEUBEY, C., RADU, R. & SCHEPERS, D. 2020. The ERA5 global reanalysis. *Quarterly Journal of the Royal Meteorological Society,* 146**,** 1999-2049.

HOELL, A., FUNK, C., ZINKE, J. & HARRISON, L. 2017. Modulation of the southern Africa precipitation response to the El Niño Southern Oscillation by the subtropical Indian Ocean dipole. *Climate Dynamics,* 48**,** 2529-2540.

HOERLING, M., HURRELL, J., EISCHEID, J. & PHILLIPS, A. 2006. Detection and attribution of twentieth-century northern and southern African rainfall change. *Journal of climate,* 19**,** 3989-4008.

HOSKINS, B. J. & HODGES, K. I. 2005. A new perspective on Southern Hemisphere storm tracks. *Journal of Climate,* 18**,** 4108-4129.

HOWARD, E. & WASHINGTON, R. 2018. Characterizing the synoptic expression of the Angola low. *Journal of Climate,* 31**,** 7147-7165.

HOWARD, E. & WASHINGTON, R. 2019. Drylines in southern Africa: Rediscovering the Congo air boundary. *Journal of Climate,* 32**,** 8223-8242.

HOWARD, E., WASHINGTON, R. & HODGES, K. I. 2019. Tropical lows in southern Africa: Tracks, rainfall contributions, and the role of ENSO. *Journal of Geophysical Research: Atmospheres,* 124**,** 11009-11032.

HUANG, X., HU, C., HUANG, X., CHU, Y., TSENG, Y.-H., ZHANG, G. J. & LIN, Y. 2018. A long-term tropical mesoscale convective systems dataset based on a novel objective automatic tracking algorithm. *Climate dynamics,* 51**,** 3145-3159.

JAMES, R., HART, N. C., MUNDAY, C., REASON, C. J. & WASHINGTON, R. 2020. Coupled climate model simulation of tropical–extratropical cloud bands over southern Africa. *Journal of Climate,* 33**,** 8579-8602.

JAMES, R. & WASHINGTON, R. 2013. Changes in African temperature and precipitation associated with degrees of global warming. *Climatic change,* 117**,** 859-872.

JONES, D. A. & SIMMONDS, I. 1993. A climatology of Southern Hemisphere extratropical cyclones. *Climate Dynamics,* 9**,** 131-145.

JURY, K. 1993. The eastern Cape drought. *Water SA,* 19**,** 133-137.

JURY, M. R. & LEVEY, K. 1993. The climatology and characteristics of drought in the eastern Cape of South Africa. *International journal of climatology,* 13**,** 629-641.

JURY, M. R., LEVEY, K. & MAKARAU, A. 1996. Mechanisms of short term rainfall variability over southern Africa. *WRC Rep,* 436.

KANAMITSU, M., EBISUZAKI, W., WOOLLEN, J., YANG, S.-K., HNILO, J., FIORINO, M. & POTTER, G. 2002. Ncep–doe amip-ii reanalysis (r-2). *Bulletin of the American Meteorological Society,* 83**,** 1631-1644.

KENDALL, M. 1975. Rank correlation measures, Vol. 202. *Charles Griffin, London***,** 15.

KILADIS, G. N. & MO, K. C. 1998. Interannual and intraseasonal variability in the Southern Hemisphere. *Meteorology of the Southern Hemisphere.* Springer.

KLEIN, S. A., SODEN, B. J. & LAU, N.-C. 1999. Remote sea surface temperature variations during ENSO: Evidence for a tropical atmospheric bridge. *Journal of climate,* 12**,** 917-932.

KRUGER, A. 2006. Observed trends in daily precipitation indices in South Africa: 1910–2004. *International Journal of Climatology: A Journal of the Royal Meteorological Society,* 26**,** 2275-2285.

L'HEUREUX, M. L. & THOMPSON, D. W. 2006. Observed relationships between the El Niño–Southern Oscillation and the extratropical zonal-mean circulation. *Journal of Climate,* 19**,** 276-287.
LAZENBY, M. J., TODD, M. C. & WANG, Y. 2016. Climate model simulation of the South Indian Ocean Convergence Zone: Mean state and variability. *Climate Research,* 68**,** 59-71.
LEVEY, K. M. & JURY, M. R. 1996. Composite intraseasonal oscillations of convection over southern Africa. *Journal of Climate,* 9**,** 1910-1920.
LINDESAY, J. 1988. South African rainfall, the Southern Oscillation and a Southern Hemisphere semi-annual cycle. *Journal of climatology,* 8**,** 17-30.
LINDESAY, J., HARRISON, M. & HAFFNER, M. 1986. The Southern Oscillation and South-African Rainfall. BUREAU SCIENTIFIC PUBL PO BOX 1758, PRETORIA 0001, SOUTH AFRICA.
LYON, B. & MASON, S. J. 2007. The 1997–98 summer rainfall season in southern Africa. Part I: Observations. *Journal of Climate,* 20**,** 5134-5148.
MACKELLAR, N., NEW, M. & JACK, C. 2014. Observed and modelled trends in rainfall and temperature for South Africa: 1960-2010. *South African Journal of Science,* 110**,** 1-13.
MAHLALELA, P., BLAMEY, R., HART, N. & REASON, C. 2020. Drought in the Eastern Cape region of South Africa and trends in rainfall characteristics. *Climate Dynamics,* 55**,** 2743-2759.
MAHLALELA, P., BLAMEY, R. & REASON, C. 2019. Mechanisms behind early winter rainfall variability in the southwestern Cape, South Africa. *Climate Dynamics,* 53**,** 21-39.
MALHERBE, J., ENGELBRECHT, F. A. & LANDMAN, W. A. 2013. Projected changes in tropical cyclone climatology and landfall in the Southwest Indian Ocean region under enhanced anthropogenic forcing. *Climate dynamics,* 40**,** 2867-2886.
MANHIQUE, A., REASON, C., RYDBERG, L. & FAUCHEREAU, N. 2011. ENSO and Indian Ocean sea surface temperatures and their relationships with tropical temperate troughs over Mozambique and the Southwest Indian Ocean. *International Journal of Climatology,* 31**,** 1-13.
MANN, H. B. 1945. Nonparametric tests against trend. *Econometrica: Journal of the econometric society***,** 245-259.
MANZANAS, R., FIWA, L., VANYA, C., KANAMARU, H. & GUTIÉRREZ, J. M. 2020. Statistical downscaling or bias adjustment? A case study involving implausible climate change projections of precipitation in Malawi. *Climatic Change,* 162**,** 1437-1453.
MARSHALL, G. J. 2003. Trends in the Southern Annular Mode from observations and reanalyses. *Journal of climate,* 16**,** 4134-4143.
MATARIRA, C. H. 1990. Drought over Zimbabwe in a regional and global context. *International Journal of Climatology,* 10**,** 609-625.
MAVUME, A. F., RYDBERG, L., ROUAULT, M. & LUTJEHARMS, J. R. 2009. Climatology and landfall of tropical cyclones in the south-west Indian Ocean. *Western Indian Ocean Journal of Marine Science,* 8.
MAWREN, D., HERMES, J. & REASON, C. 2022. Marine heatwaves in the Mozambique Channel. *Climate Dynamics,* 58**,** 305-327.
MEQUE, A. & ABIODUN, B. J. 2015. Simulating the link between ENSO and summer drought in Southern Africa using regional climate models. *Climate Dynamics,* 44**,** 1881-1900.
MIDGLEY, G., CHAPMAN, R., HEWITSON, B., JOHNSTON, P., DE WIT, M., ZIERVOGEL, G., MUKHEIBIR, P., VAN NIEKERK, L., TADROSS, M. & VAN WILGEN, B. 2005. A status quo, vulnerability and adaptation assessment of the physical and socio-economic effects of climate change in the Western Cape.
MO, K. C. & PAEGLE, J. N. 2001. The Pacific–South American modes and their downstream effects. *International Journal of Climatology: A Journal of the Royal Meteorological Society,* 21**,** 1211-1229.
MOLEKWA, S., ENGELBRECHT, C. J. & RAUTENBACH, C. D. 2014. Attributes of cut-off low induced rainfall over the Eastern Cape Province of South Africa. *Theoretical and applied climatology,* 118**,** 307-318.

MORAKE, D., BLAMEY, R. & REASON, C. 2021. Long-lived mesoscale convective systems over eastern South Africa. *Journal of Climate,* 34**,** 6421-6439.
MOSES, O., BLAMEY, R. C. & REASON, C. J. 2022. Relationships between NDVI, river discharge and climate in the Okavango River Basin region. *International Journal of Climatology,* 42**,** 691-713.
MOUNKAILA, M. S., ABIODUN, B. J. & BAYO OMOTOSHO, J. 2015. Assessing the capability of CORDEX models in simulating onset of rainfall in West Africa. *Theoretical and applied climatology,* 119**,** 255-272.
MULENGA, H., ROUAULT, M. & REASON, C. 2003. Dry summers over northeastern South Africa and associated circulation anomalies. *Climate Research,* 25**,** 29-41.
MULENGA, H. M. 1999. Southern African climate anomalies, summer rainfall and the Angola low.
MUNDAY, C. & WASHINGTON, R. 2017. Circulation controls on southern African precipitation in coupled models: The role of the Angola low. *Journal of Geophysical Research: Atmospheres,* 122**,** 861-877.
NASH, D. J., PRIBYL, K., KLEIN, J., ENDFIELD, G. H., KNIVETON, D. R. & ADAMSON, G. C. 2015. Tropical cyclone activity over Madagascar during the late nineteenth century. *International Journal of Climatology,* 35**,** 3249-3261.
NDARANA, T., MPATI, S., BOPAPE, M. J., ENGELBRECHT, F. & CHIKOORE, H. 2021. The flow and moisture fluxes associated with ridging South Atlantic Ocean anticyclones during the subtropical southern African summer. *International Journal of Climatology,* 41**,** E1000-E1017.
NDARANA, T., RAMMOPO, T. S., CHIKOORE, H., BARNES, M. A. & BOPAPE, M.-J. 2020. A quasi-geostrophic diagnosis of the zonal flow associated with cut-off lows over South Africa and surrounding oceans. *Climate Dynamics,* 55**,** 2631-2644.
NICHOLSON, S. E. & GRIST, J. P. 2003. The seasonal evolution of the atmospheric circulation over West Africa and equatorial Africa. *Journal of climate,* 16**,** 1013-1030.
NICHOLSON, S. E. & KIM, J. 1997. The relationship of the El Niño–Southern oscillation to African rainfall. *International Journal of Climatology: A Journal of the Royal Meteorological Society,* 17**,** 117-135.
PEPLER, A. S., DOWDY, A. J. & HOPE, P. 2021. The differing role of weather systems in southern Australian rainfall between 1979–1996 and 1997–2015. *Climate Dynamics,* 56**,** 2289-2302.
PHILIPPON, N., ROUAULT, M., RICHARD, Y. & FAVRE, A. 2012. The influence of ENSO on winter rainfall in South Africa. *International Journal of Climatology,* 32**,** 2333-2347.
PIENAAR, L. & BOONZAAIER, J. 2018. Drought policy brief Western Cape Agriculture. *Western Cape Department of Agriculture (WCDoA) and the Bureau for Food and Agricultural Policy (BFAP), Elsenburg*.
POHL, B., FAUCHEREAU, N., REASON, C. & ROUAULT, M. 2010. Relationships between the Antarctic Oscillation, the Madden–Julian oscillation, and ENSO, and consequences for rainfall analysis. *Journal of Climate,* 23**,** 238-254.
POHL, B., MACRON, C. & MONERIE, P.-A. 2017. Fewer rainy days and more extreme rainfall by the end of the century in Southern Africa. *Scientific Reports,* 7**,** 1-7.
POHL, B., ROUAULT, M. & ROY, S. S. 2014. Simulation of the annual and diurnal cycles of rainfall over South Africa by a regional climate model. *Climate dynamics,* 43**,** 2207-2226.
RAPHAEL, M. 2004. A zonal wave 3 index for the Southern Hemisphere. *Geophysical Research Letters,* 31.
RAPOLAKI, R., BLAMEY, R., HERMES, J. & REASON, C. 2020. Moisture sources associated with heavy rainfall over the Limpopo River Basin, southern Africa. *Climate Dynamics,* 55**,** 1473-1487.
RAPOLAKI, R., BLAMEY, R., HERMES, J. & REASON, C. 2021. Moisture sources and transport during an extreme rainfall event over the Limpopo River Basin, southern Africa. *Atmospheric Research,* 264**,** 105849.

RAPOLAKI, R. S., BLAMEY, R. C., HERMES, J. C. & REASON, C. J. C. 2019. A classification of synoptic weather patterns linked to extreme rainfall over the Limpopo River Basin in southern Africa. *Climate Dynamics,* 53**,** 2265-2279.

RAPOLAKI, R. S. & REASON, C. J. C. 2018. Tropical storm Chedza and associated floods over south-eastern Africa. *Natural Hazards,* 93**,** 189-217.

REASON, C. 1999. Interannual warm and cool events in the subtropical/mid-latitude South Indian Ocean Region. *Geophysical Research Letters,* 26**,** 215-218.

REASON, C. 2001a. Evidence for the influence of the Agulhas Current on regional atmospheric circulation patterns. *Journal of Climate,* 14**,** 2769-2778.

REASON, C. 2001b. Subtropical Indian Ocean SST dipole events and southern African rainfall. *Geophysical Research Letters,* 28**,** 2225-2227.

REASON, C. 2002. Sensitivity of the southern African circulation to dipole sea-surface temperature patterns in the south Indian Ocean. *International Journal of Climatology: A Journal of the Royal Meteorological Society,* 22**,** 377-393.

REASON, C. 2007. Tropical cyclone Dera, the unusual 2000/01 tropical cyclone season in the South West Indian Ocean and associated rainfall anomalies over Southern Africa. *Meteorology and Atmospheric Physics,* 97**,** 181-188.

REASON, C. 2016. The Bolivian, Botswana, and Bilybara Highs and Southern Hemisphere drought/floods. *Geophysical Research Letters,* 43**,** 1280-1286.

REASON, C. 2019. Low-frequency variability in the Botswana High and southern African regional climate. *Theoretical and Applied Climatology,* 137**,** 1321-1334.

REASON, C., ALLAN, R., LINDESAY, J. & ANSELL, T. 2000. ENSO and climatic signals across the Indian Ocean basin in the global context: Part I, Interannual composite patterns. *International Journal of Climatology: A Journal of the Royal Meteorological Society,* 20**,** 1285-1327.

REASON, C. & JAGADHEESHA, D. 2005. A model investigation of recent ENSO impacts over southern Africa. *Meteorology and Atmospheric Physics,* 89**,** 181-205.

REASON, C. & KEIBEL, A. 2004. Tropical cyclone Eline and its unusual penetration and impacts over the southern African mainland. *Weather and forecasting,* 19**,** 789-805.

REASON, C., LANDMAN, W. & TENNANT, W. 2006. Seasonal to decadal prediction of southern African climate and its links with variability of the Atlantic Ocean. *Bulletin of the American Meteorological Society,* 87**,** 941-956.

REASON, C. & MULENGA, H. 1999. Relationships between South African rainfall and SST anomalies in the southwest Indian Ocean. *International Journal of Climatology: A Journal of the Royal Meteorological Society,* 19**,** 1651-1673.

REASON, C. & ROUAULT, M. 2005. Links between the Antarctic Oscillation and winter rainfall over western South Africa. *Geophysical research letters,* 32.

REASON, C., ROUAULT, M., MELICE, J.-L. & JAGADHEESHA, D. 2002. Interannual winter rainfall variability in SW South Africa and large scale ocean–atmosphere interactions. *Meteorology and Atmospheric Physics,* 80**,** 19-29.

REASON, C. J. & SMART, S. 2015. Tropical south east Atlantic warm events and associated rainfall anomalies over southern Africa. *Frontiers in Environmental Science,* 3**,** 24.

REASON, C. J. C. 2017. Climate of Southern Africa. *Oxford Research Encyclopedia of Climate Science.*

REASON, C. J. C., HACHIGONTA, S. & PHALADI, R. F. 2005. Interannual variability in rainy season characteristics over the Limpopo region of southern Africa. *International Journal of Climatology,* 25**,** 1835-1853.

ROFFE, S. J., FITCHETT, J. M. & CURTIS, C. J. 2020. Determining the utility of a percentile-based wet-season start-and end-date metrics across South Africa. *Theoretical and Applied Climatology,* 140**,** 1331-1347.

ROFFE, S. J., FITCHETT, J. M. & CURTIS, C. J. 2021. Investigating changes in rainfall seasonality across South Africa: 1987–2016. *International Journal of Climatology,* 41**,** E2031-E2050.

ROUAULT, M., FLORENCHIE, P., FAUCHEREAU, N. & REASON, C. J. 2003. South East tropical Atlantic warm events and southern African rainfall. *Geophysical Research Letters,* 30.
ROUAULT, M. & RICHARD, Y. 2003. Intensity and spatial extension of drought in South Africa at different time scales. *water SA,* 29**,** 489-500.
ROUAULT, M., WHITE, S., REASON, C., LUTJEHARMS, J. & JOBARD, I. 2002. Ocean–atmosphere interaction in the Agulhas Current region and a South African extreme weather event. *Weather and Forecasting,* 17**,** 655-669.
SAJI, N., GOSWAMI, B., VINAYACHANDRAN, P. & YAMAGATA, T. 1999. A dipole mode in the tropical Indian Ocean. *Nature,* 401**,** 360-363.
SAJI, N. & YAMAGATA, T. 2003. Possible impacts of Indian Ocean dipole mode events on global climate. *Climate Research,* 25**,** 151-169.
SCHNEIDER, D. P. & FOGT, R. L. 2018. Artifacts in century-length atmospheric and coupled reanalyses over Antarctica due to historical data availability. *Geophysical Research Letters,* 45**,** 964-973.
SEN, P. K. 1968. Estimates of the regression coefficient based on Kendall's tau. *Journal of the American statistical association,* 63**,** 1379-1389.
SILVESTRI, G. E. & VERA, C. S. 2003. Antarctic Oscillation signal on precipitation anomalies over southeastern South America. *Geophysical Research Letters,* 30.
SIMMONDS, I. & RUDEVA, I. 2014. A comparison of tracking methods for extreme cyclones in the Arctic basin. *Tellus A: Dynamic Meteorology and Oceanography,* 66**,** 25252.
SINGLETON, A. & REASON, C. 2006. Numerical simulations of a severe rainfall event over the Eastern Cape coast of South Africa: sensitivity to sea surface temperature and topography. *Tellus A: Dynamic Meteorology and Oceanography,* 58**,** 335-367.
SINGLETON, A. & REASON, C. 2007a. A numerical model study of an intense cutoff low pressure system over South Africa. *Monthly weather review,* 135**,** 1128-1150.
SINGLETON, A. & REASON, C. 2007b. Variability in the characteristics of cut-off low pressure systems over subtropical southern Africa. *International Journal of Climatology: A Journal of the Royal Meteorological Society,* 27**,** 295-310.
SOUSA, P. M., BLAMEY, R. C., REASON, C. J. C., RAMOS, A. M. & TRIGO, R. M. 2018. The 'Day Zero' Cape Town drought and the poleward migration of moisture corridors. *Environmental Research Letters,* 13.
SUZUKI, T. 2011. Seasonal variation of the ITCZ and its characteristics over central Africa. *Theoretical and Applied Climatology,* 103**,** 39-60.
TALJAARD, J. 1953. The mean circulation in the lower troposphere over southern Africa. *South African Geographical Journal,* 35**,** 33-45.
TALJAARD, J. J. 1985. *Cut-off lows in the South African region*, Weather Bureau, Department of Transport.
TALJAARD, J. J. 1996. *Atmospheric circulation systems, synoptic climatology and weather phenomena of South Africa. Part 6, Rainfall in South Africa*, Department of Environmental Affairs and Tourism.
TAMOFFO, A. T., AMEKUDZI, L. K., WEBER, T., VONDOU, D. A., YAMBA, E. I. & JACOB, D. 2022. Mechanisms of Rainfall Biases in Two CORDEX-CORE Regional Climate Models at Rainfall Peaks over Central Equatorial Africa. *Journal of Climate,* 35**,** 639-668.
TAYLOR, K. E., STOUFFER, R. J. & MEEHL, G. A. 2012. An overview of CMIP5 and the experiment design. *Bulletin of the American Meteorological Society,* 93**,** 485-498.
THEIL, H. 1950. A rank-invariant method of linear and polynomial regression analysis. *Indagationes mathematicae,* 12**,** 173.
THOITHI, W., BLAMEY, R. C. & REASON, C. J. 2021. Dry spells, wet days, and their trends across Southern Africa during the summer rainy season. *Geophysical Research Letters,* 48**,** e2020GL091041.
THOMPSON, D. W. & WALLACE, J. M. 2000. Annular modes in the extratropical circulation. Part I: Month-to-month variability. *Journal of climate,* 13**,** 1000-1016.

TODD, M. & WASHINGTON, R. 1998. Extreme daily rainfall in Southern Africa and Southwest Indian Ocean tropical-temperate links. *South African Journal of Science (South Africa)*.
TOTÉ, C., PATRICIO, D., BOOGAARD, H., VAN DER WIJNGAART, R., TARNAVSKY, E. & FUNK, C. 2015. Evaluation of Satellite Rainfall Estimates for Drought and Flood Monitoring in Mozambique. *Remote Sensing,* 7**,** 1758-1776.
TRENBERTH, K. E. 1998. Atmospheric moisture residence times and cycling: Implications for rainfall rates and climate change. *Climatic change,* 39**,** 667-694.
TYSON, P. D. & PRESTON-WHYTE, R. A. 2000. *Weather and climate of southern Africa*, Oxford University Press.
USMAN, M. T. & REASON, C. 2004. Dry spell frequencies and their variability over southern Africa. *Climate research,* 26**,** 199-211.
WALKER, N. D. 1990. Links between South African summer rainfall and temperature variability of the Agulhas and Benguela Current systems. *Journal of Geophysical Research,* 95.
WELDON, D. & REASON, C. 2014. Variability of rainfall characteristics over the South Coast region of South Africa. *Theoretical and applied climatology,* 115**,** 177-185.
XIE, P. & ARKIN, P. A. 1997. Global precipitation: A 17-year monthly analysis based on gauge observations, satellite estimates, and numerical model outputs. *Bulletin of the american meteorological society,* 78**,** 2539-2558.
XULU, N. G., CHIKOORE, H., BOPAPE, M.-J. M. & NETHENGWE, N. S. 2020. Climatology of the mascarene high and its influence on weather and climate over Southern Africa. *Climate,* 8**,** 86.
YU, J.-Y., PAEK, H., SALTZMAN, E. S. & LEE, T. 2015. The early 1990s change in ENSO–PSA–SAM relationships and its impact on Southern Hemisphere climate. *Journal of Climate,* 28**,** 9393-9408.

Appendices

A. Analysis of seasonal dry, light, moderate, and heavy wet days at stations

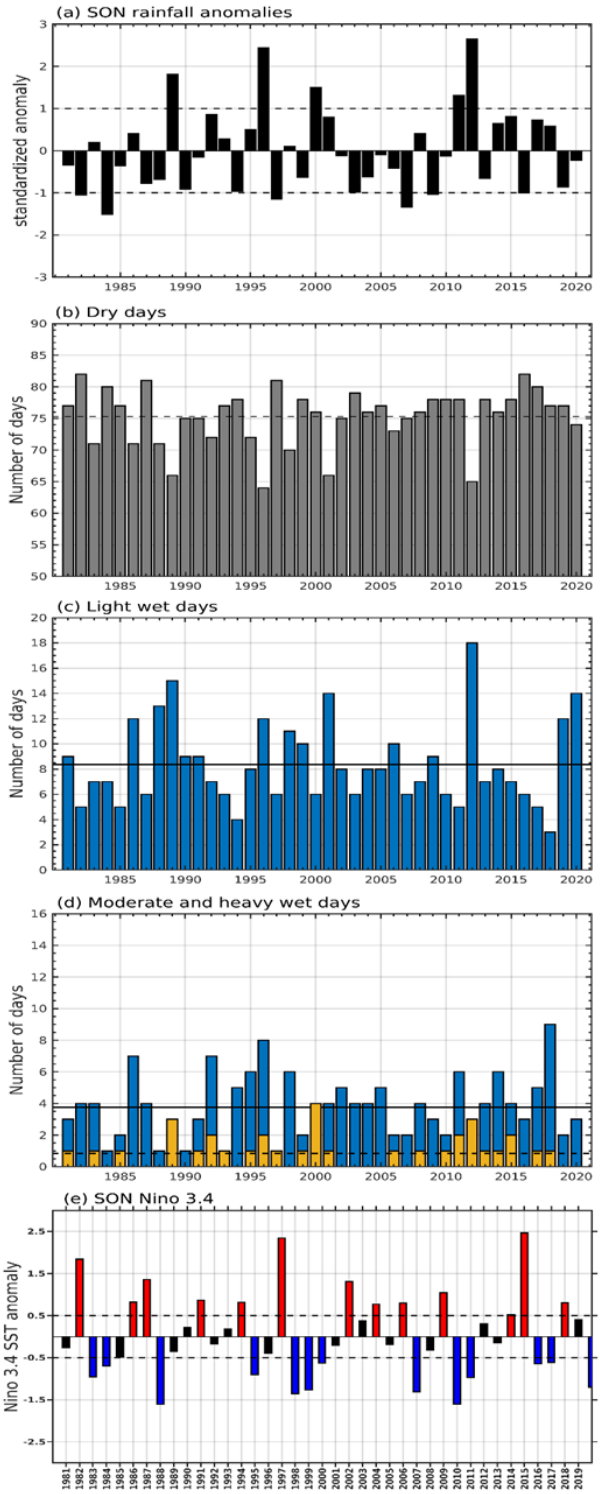

A.1: Spring (SON) **(a)** standardized anomalies for the Humewood Golf Club station (bars), **(b)** dry (σ=4.54) **(c)** light (σ=3.30), **(d)** moderate (blue bars; σ=2.02) and heavy (yellow bars; σ=0.98) wet day totals, solid and dotted lines indicate the seasonal mean for moderate and heavy wet days, respectively. **(d)** Illustrates the corresponding Niño 3.4 SST anomalies.

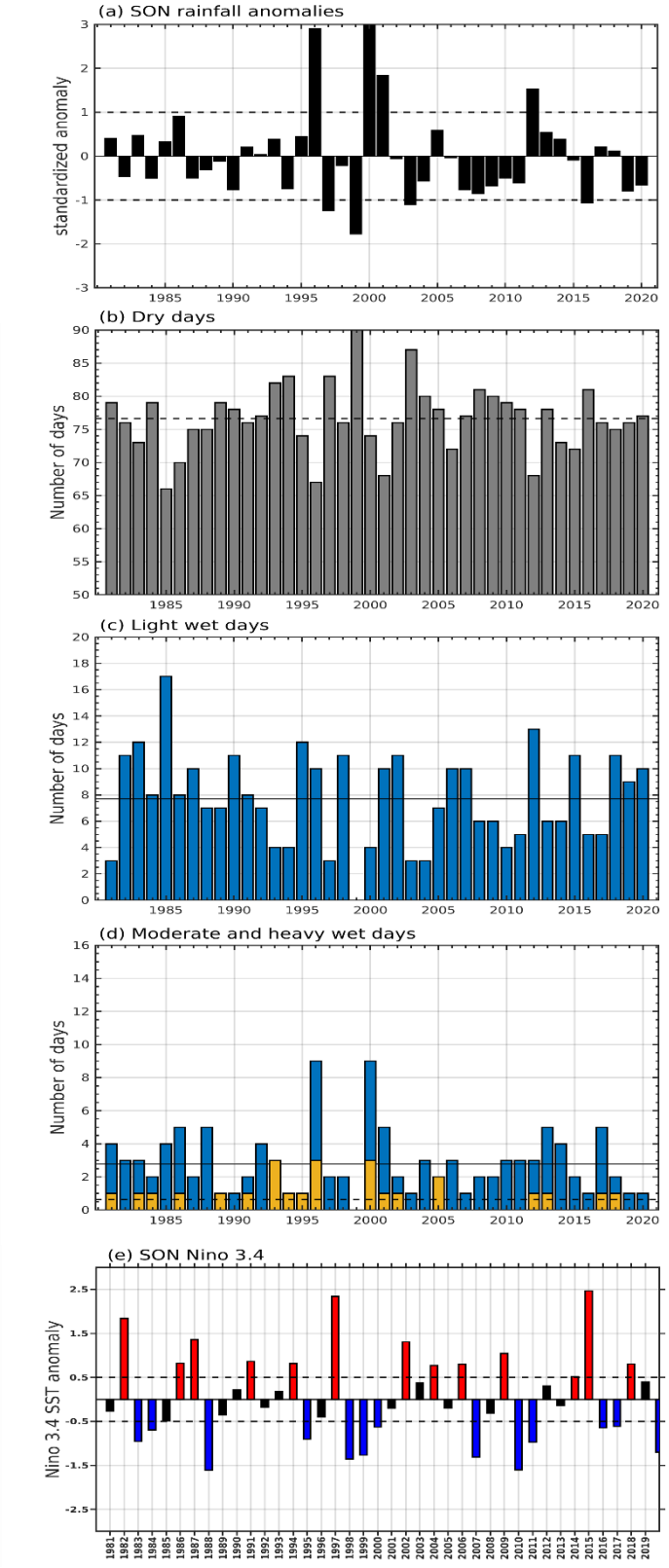

A.2: Same as **A.1**, but for Addo Elephant Park station. **(b)** dry (σ=5.08) **(c)** light (σ=3.54), **(d)** moderate (blue bars; σ=2.00) and heavy (yellow bars; σ=0.87) wet day totals, solid and dotted lines indicate the seasonal mean for moderate and heavy wet days, respectively.

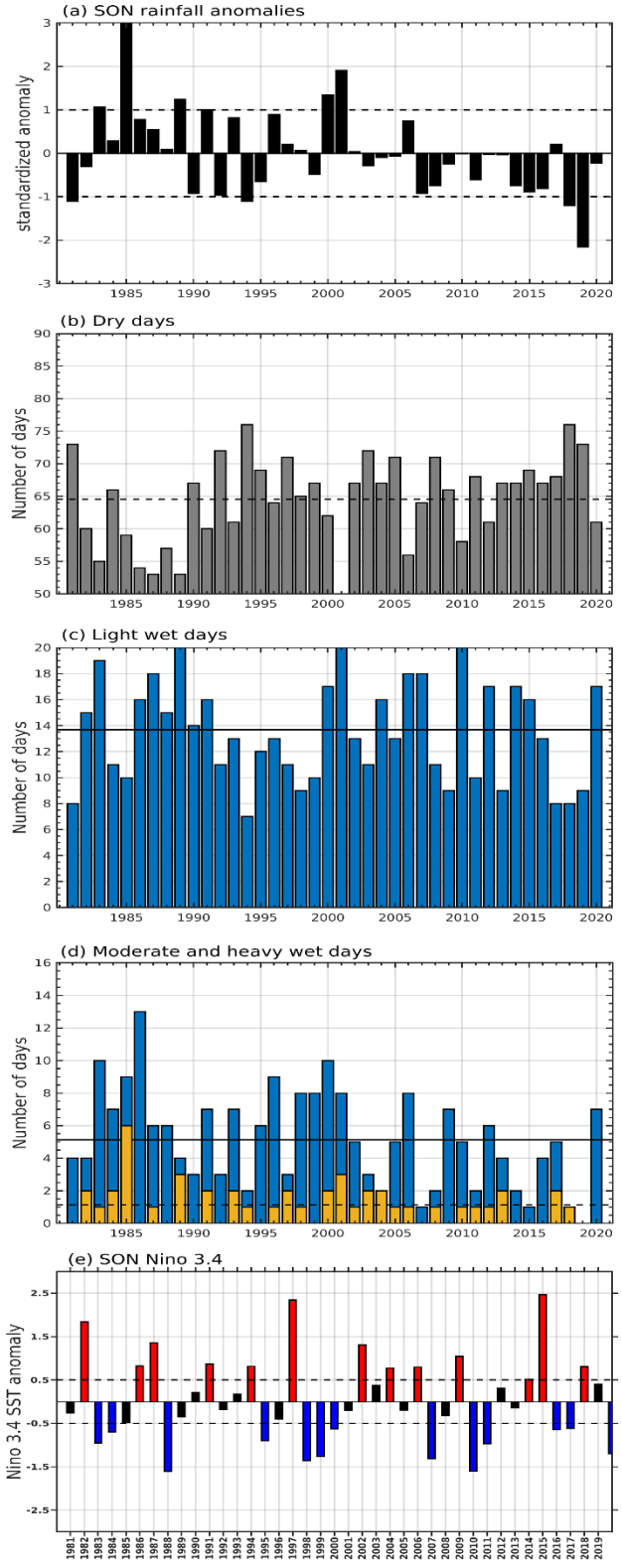

A.3: Same as **A.1**, but for Dohne-AGR station. **(b)** dry (σ=6.76) **(c)** light (σ=4.39), **(d)** moderate (blue bars; σ=3.04) and heavy (yellow bars; σ=1.20) wet day totals, solid and dotted lines indicate the seasonal mean for moderate and heavy wet days, respectively.

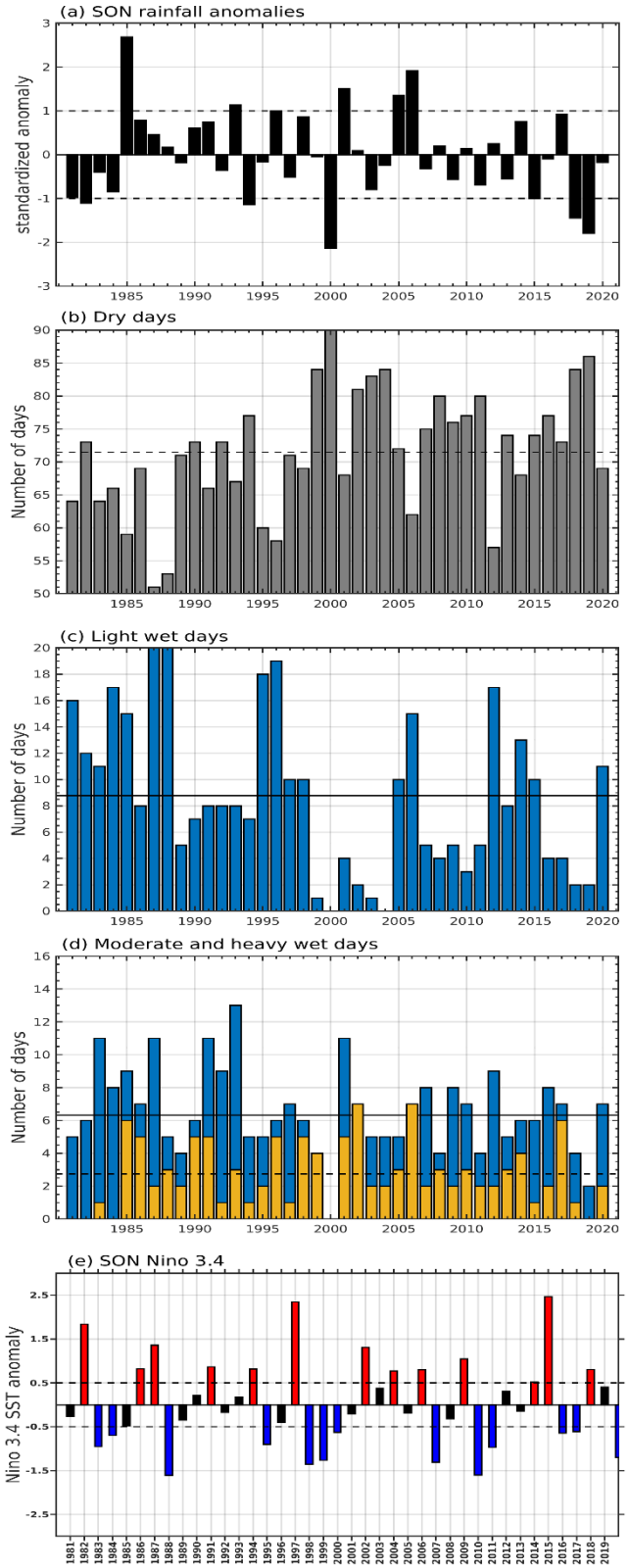

A.4: Same as **A.1**, but for Cwebe Nature Reserve station. **(b)** dry (σ=9.26) **(c)** light (σ=6.22), **(d)** moderate (blue bars; σ=2.82) and heavy (yellow bars; σ=1.98) wet day totals, solid and dotted lines indicate the seasonal mean for moderate and heavy wet days, respectively.

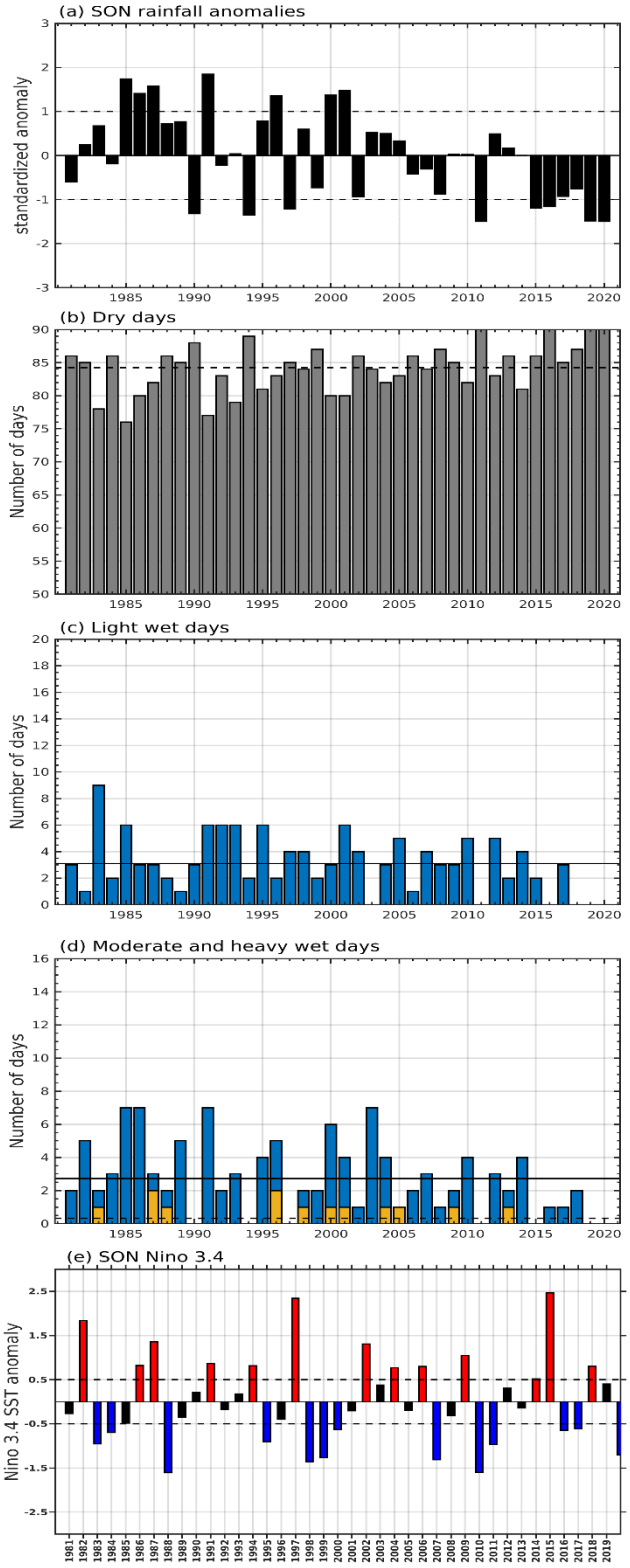

A.5: Same as **A.1**, but for Philadelphia station. **(b)** dry (σ=3.71) **(c)** light (σ=2.15), **(d)** moderate (blue bars; σ=2.14) and heavy (yellow bars; σ=0.57) wet day totals, solid and dotted lines indicate the seasonal mean for moderate and heavy wet days, respectively.

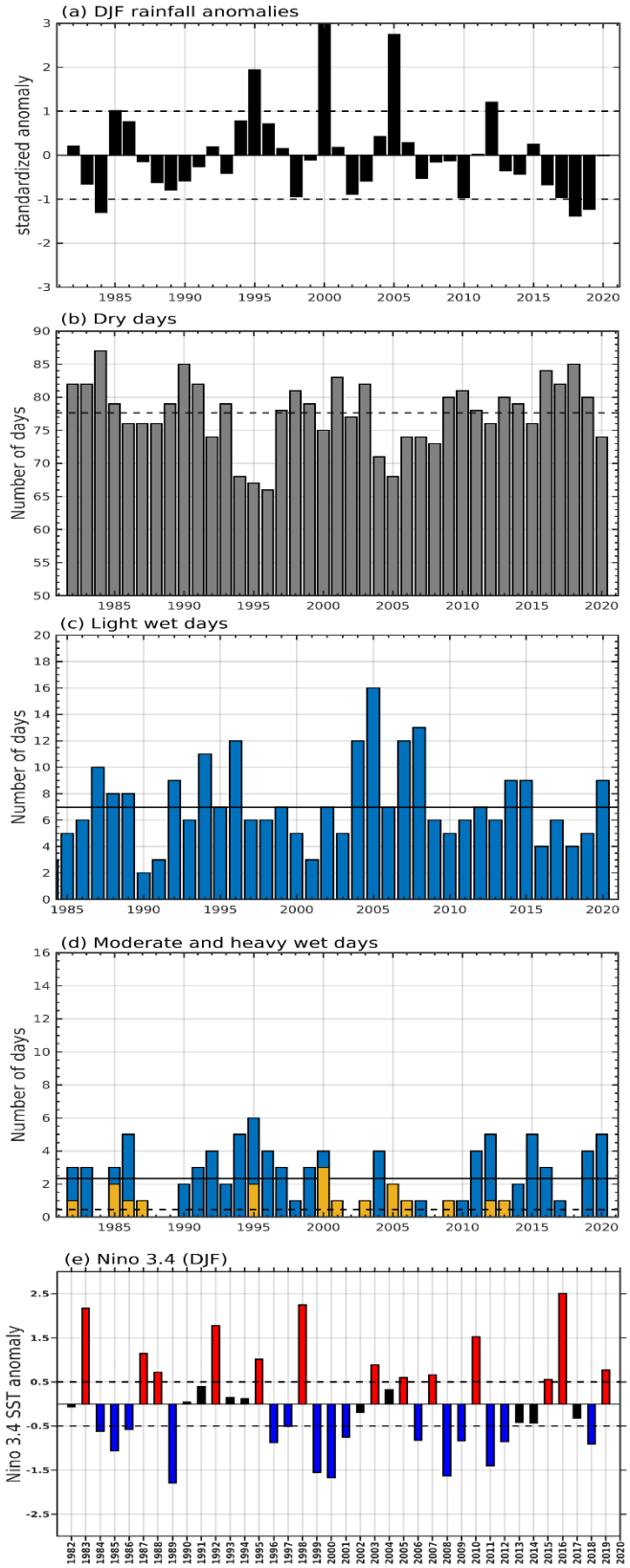

A.6: Summer (DJF) (a) standardized anomalies for the Humewood Golf Club station (bars), **(b)** dry (σ= σ=5.09) **(c)** light (σ=3.16), **(d)** moderate (blue bars; σ=1.84) and heavy (yellow bars; σ=0.76) wet day totals, solid and dotted lines indicate the seasonal mean for moderate and heavy wet days, respectively. **(d)** Illustrates the corresponding Niño 3.4 SST anomalies. Years indicate the last month of the season i.e., 1982 denotes the 1981/82 season.

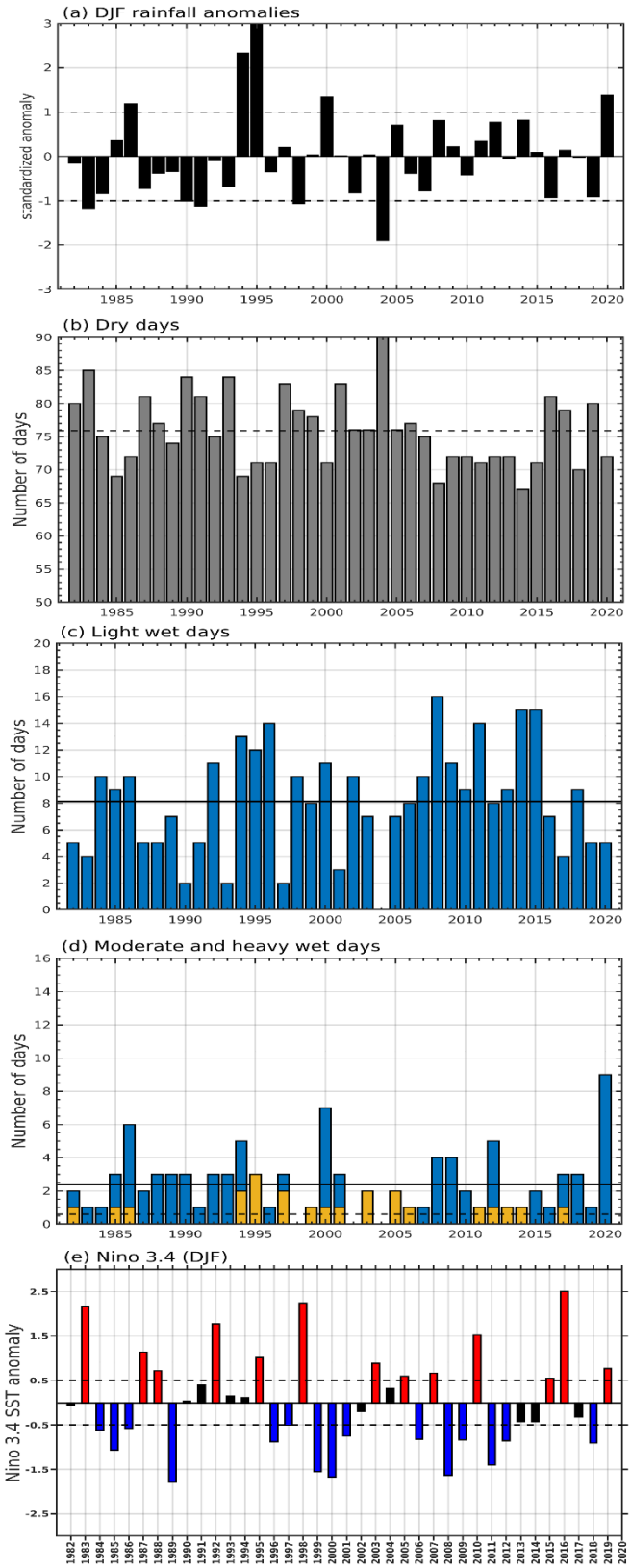

A.7: Same as **A.6** but, for Addo Elephant Park station. **(b)** dry (σ=5.55) **(c)** light (σ=4.01), **(d)** moderate (blue bars; σ=2.02) and heavy (yellow bars; σ=0.79) wet day totals, solid and dotted lines indicate the seasonal mean for moderate and heavy wet days, respectively.

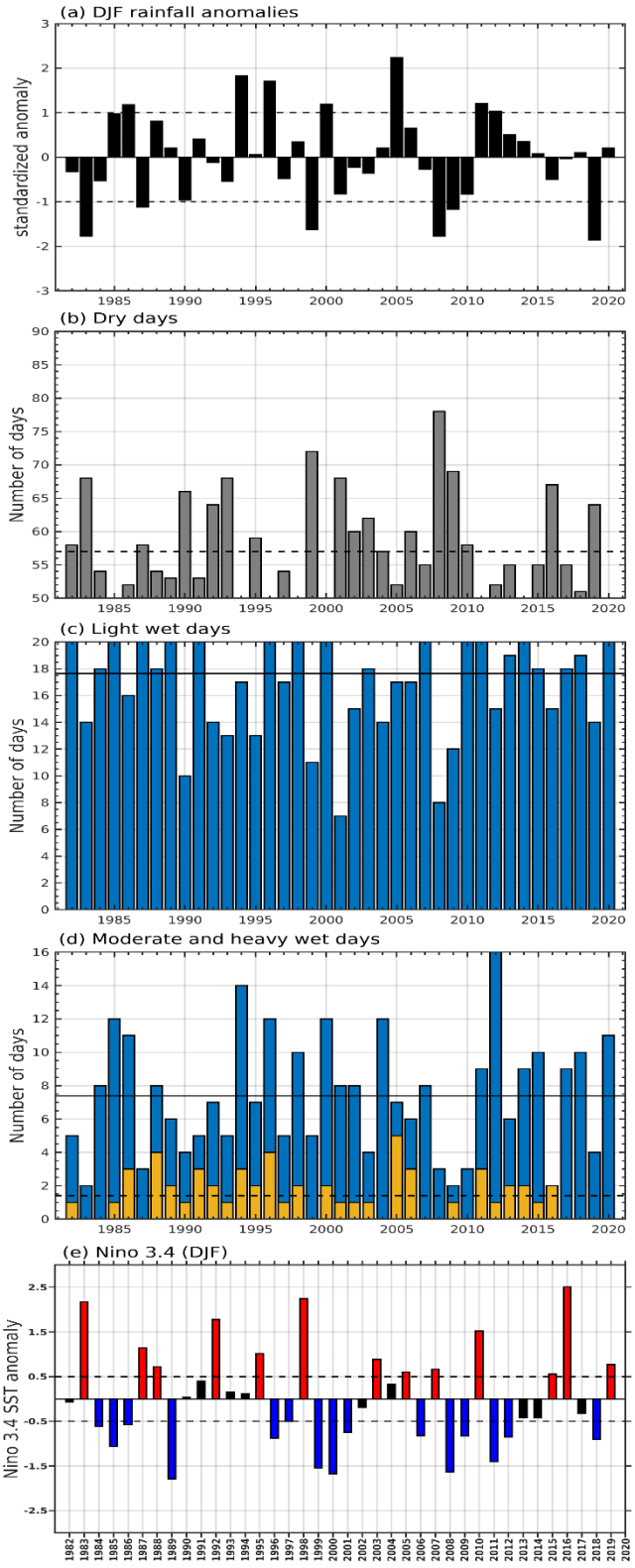

A.8: Same as **A.6** but, for Dohne-AGR station. **(b)** dry (σ=8.41) **(c)** light (σ=5.09), **(d)** moderate (blue bars; σ=3.53) and heavy (yellow bars; σ=1.33) wet day totals, solid and dotted lines indicate the seasonal mean for moderate and heavy wet days, respectively.

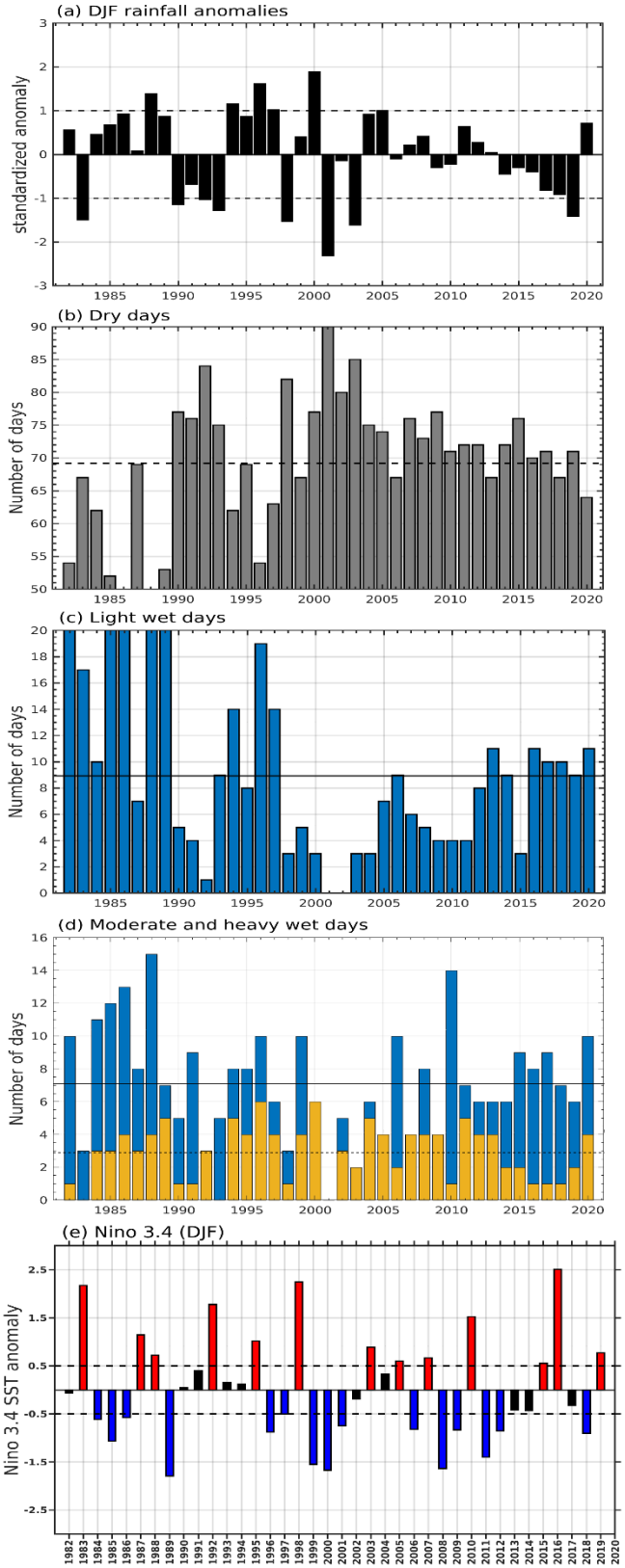

A.9: Same as **A.6** but, for Cwebe Nature Reserve station. **(b)** dry (σ=10.55) **(c)** light (σ=6.18), **(d)** moderate (blue bars; σ=3.51) and heavy (yellow bars; σ=1.70) wet day totals, solid and dotted lines indicate the seasonal mean for moderate and heavy wet days, respectively.

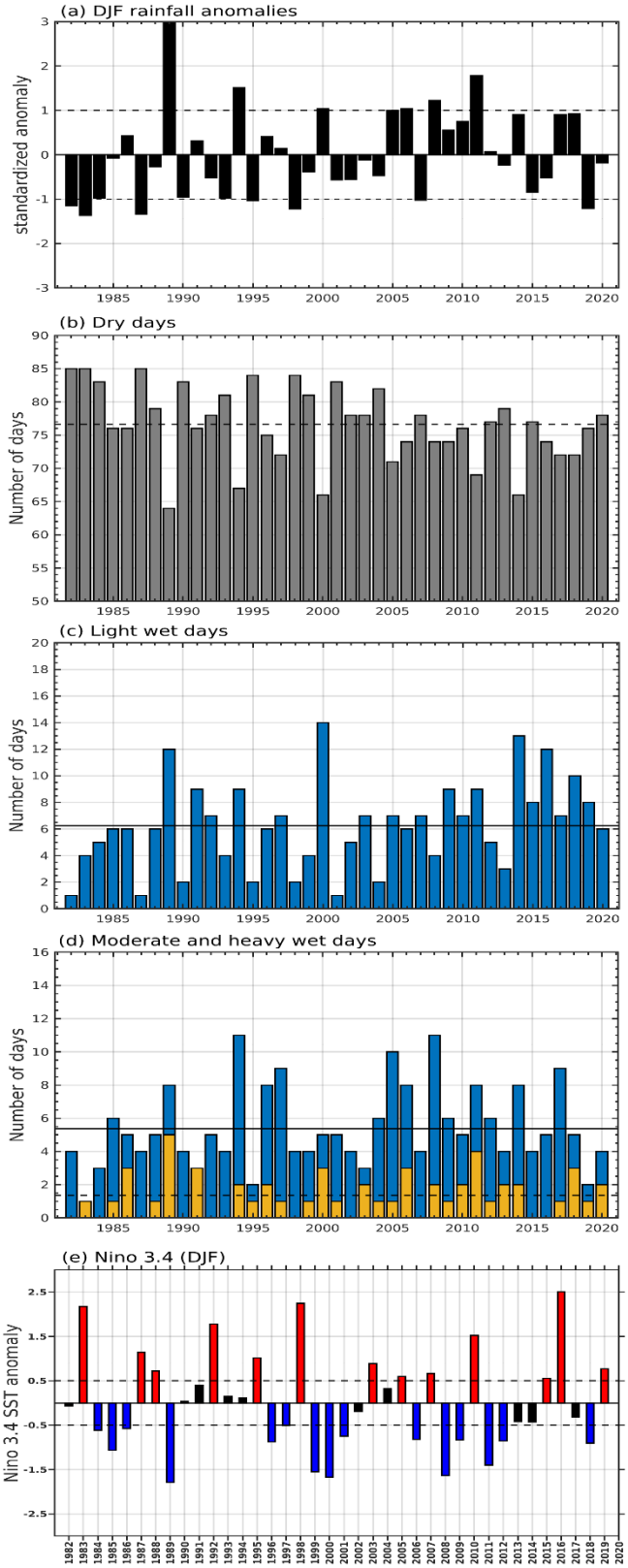

A.10: Same as **A.6** but, for Philadephia station. **(b)** dry (σ=5.60) **(c)** light (σ=3.31), **(d)** moderate (blue bars; σ=2.53) and heavy (yellow bars; σ=1.25) wet day totals, solid and dotted lines indicate the seasonal mean for moderate and heavy wet days, respectively.

B. Spatial CHIRPS seasonal anomalies

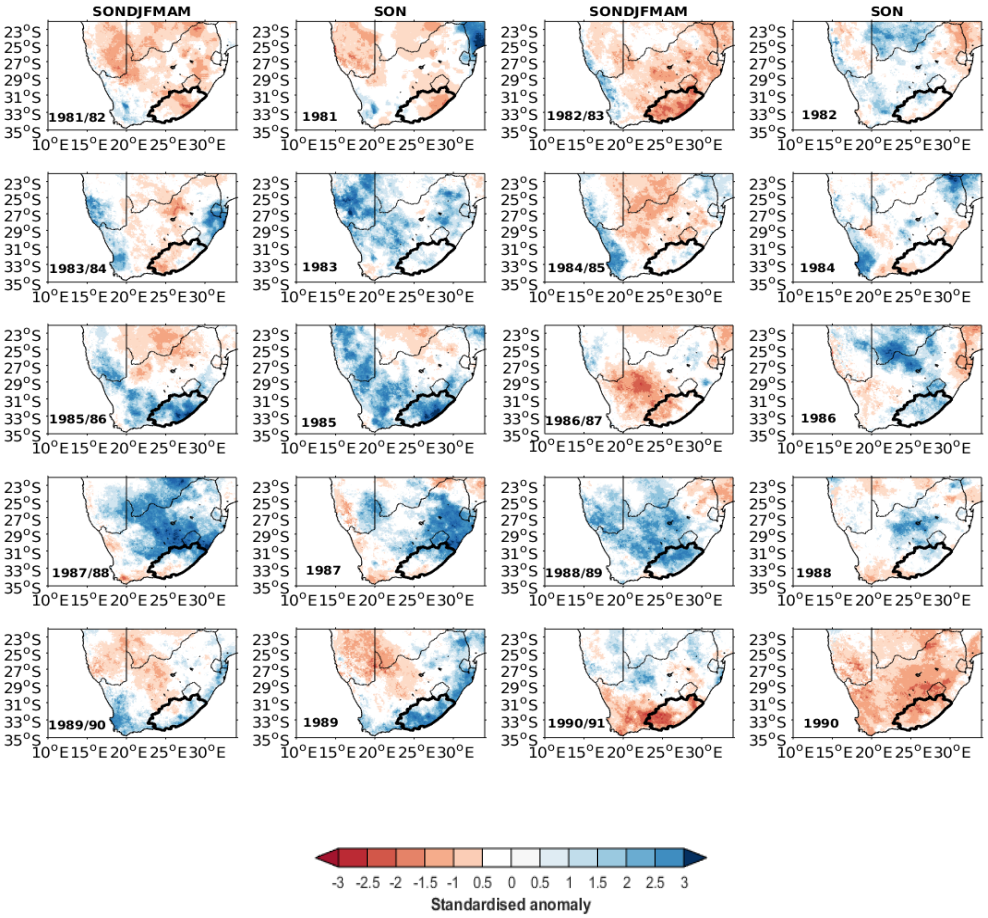

B.1: Spatial standardised anomalies for individual spring seasons. Anomalies for the extended summer; SONDJFMAM and spring; SON are shown for each year between 1981-1990.

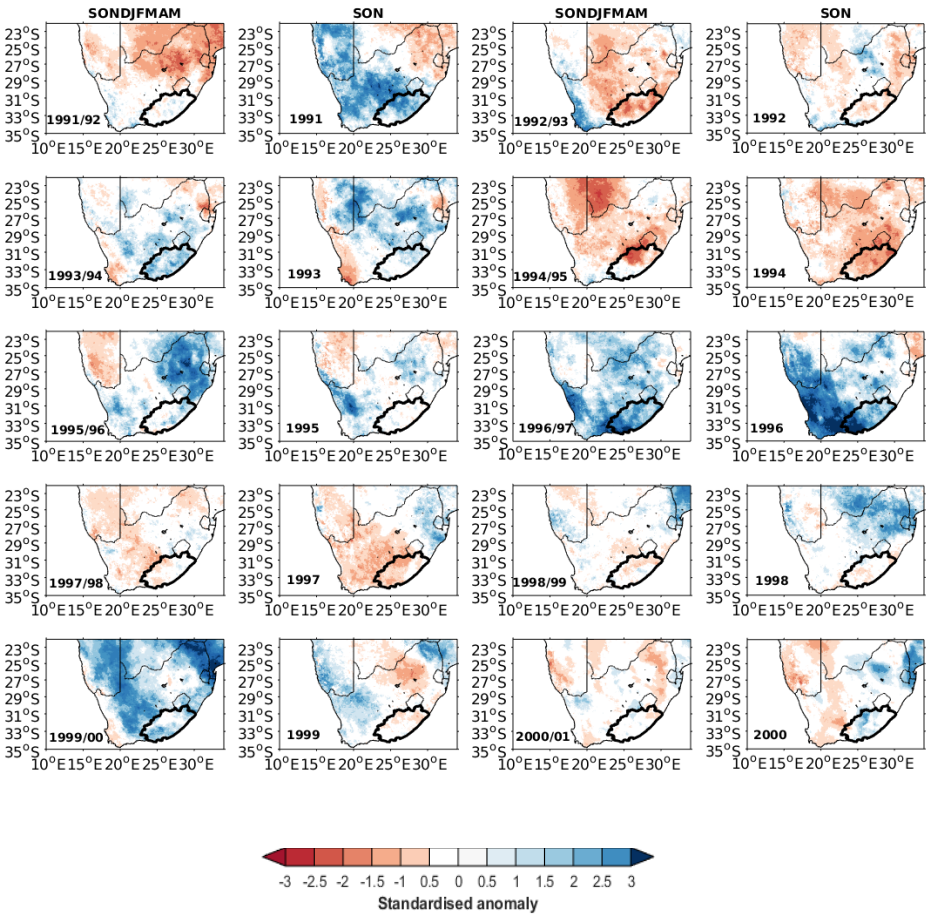

B.2: Same as **B.1**, but for 1991-2000.

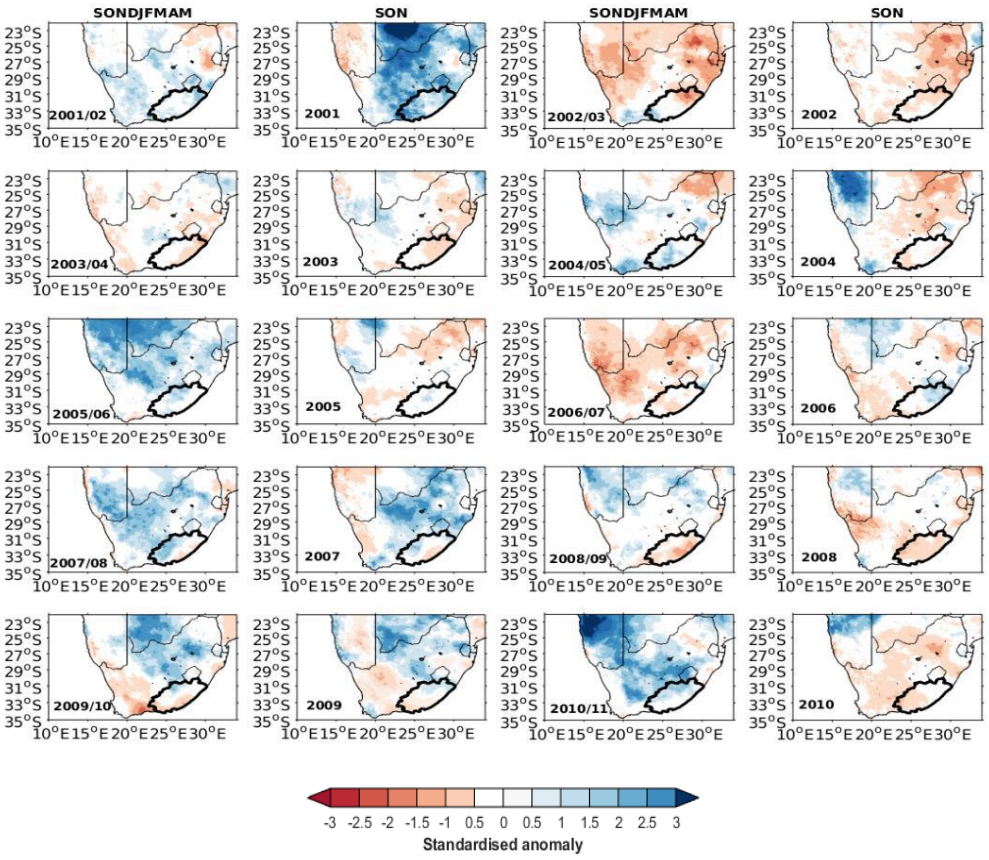

B.3: Same as **B.1**, but for 2001-2010.

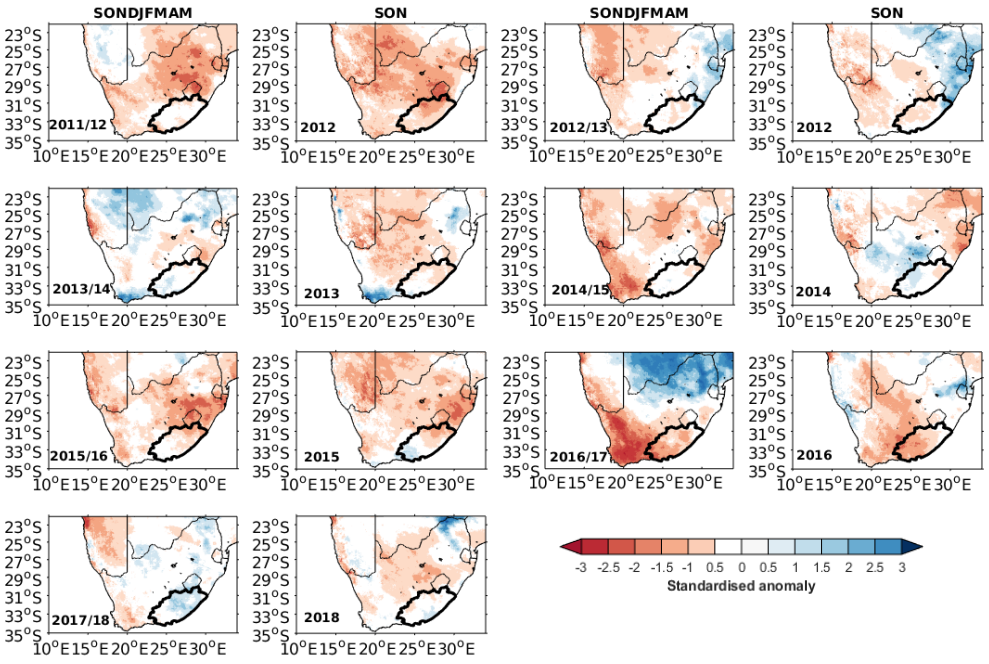

B.4: Same as **B.5**, but for 2012-2018.

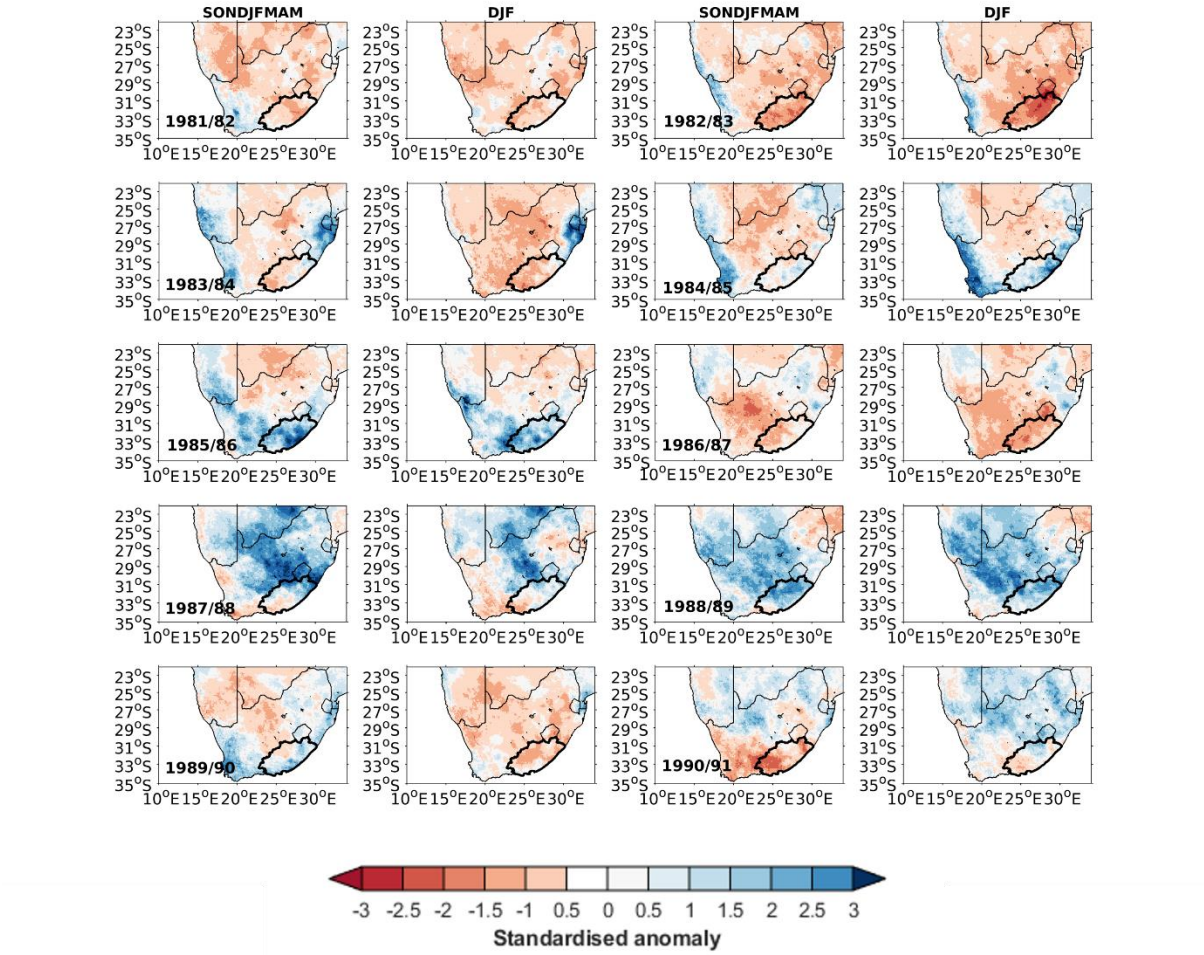

B.5: Spatial standardised anomalies for individual summer seasons. Anomalies for the extended summer; SONDJFMAM and summer; DJF are shown for each year between 1982-1991. Year represents the last month of the season i.e., 1982 indicates the season 1981/82.

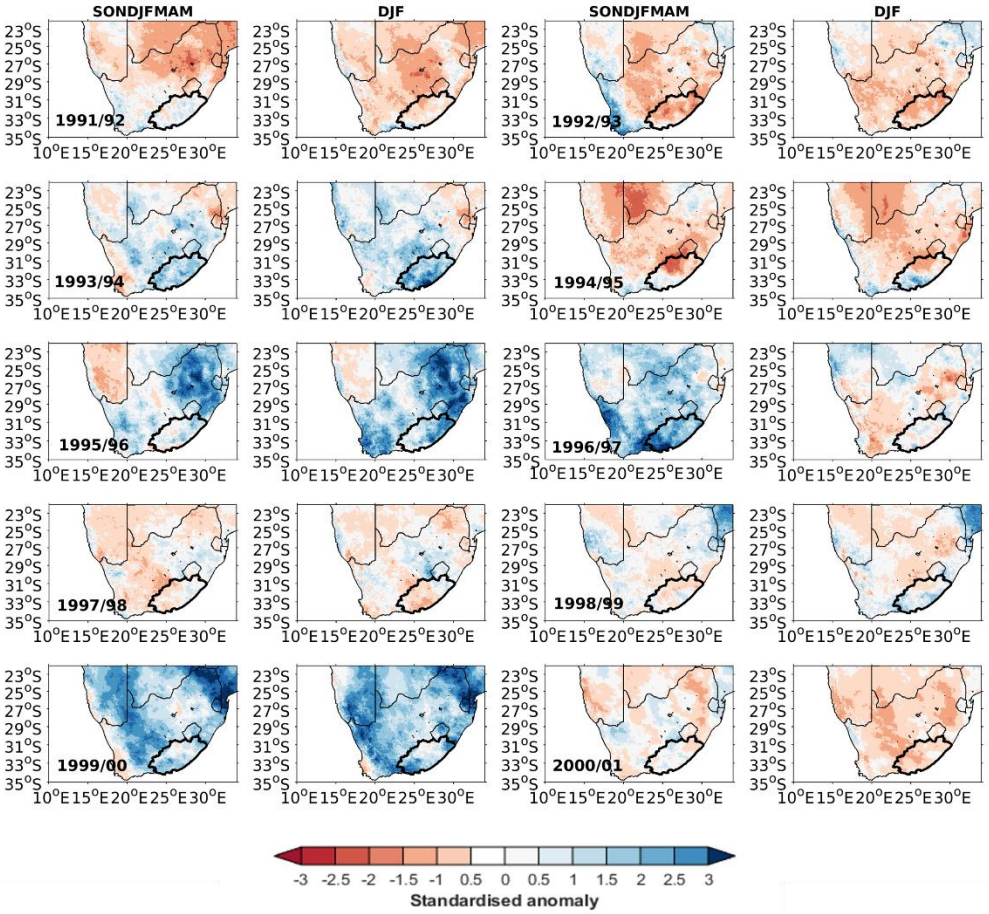

B.6: Same as **B.5**, but for 1992-2001.

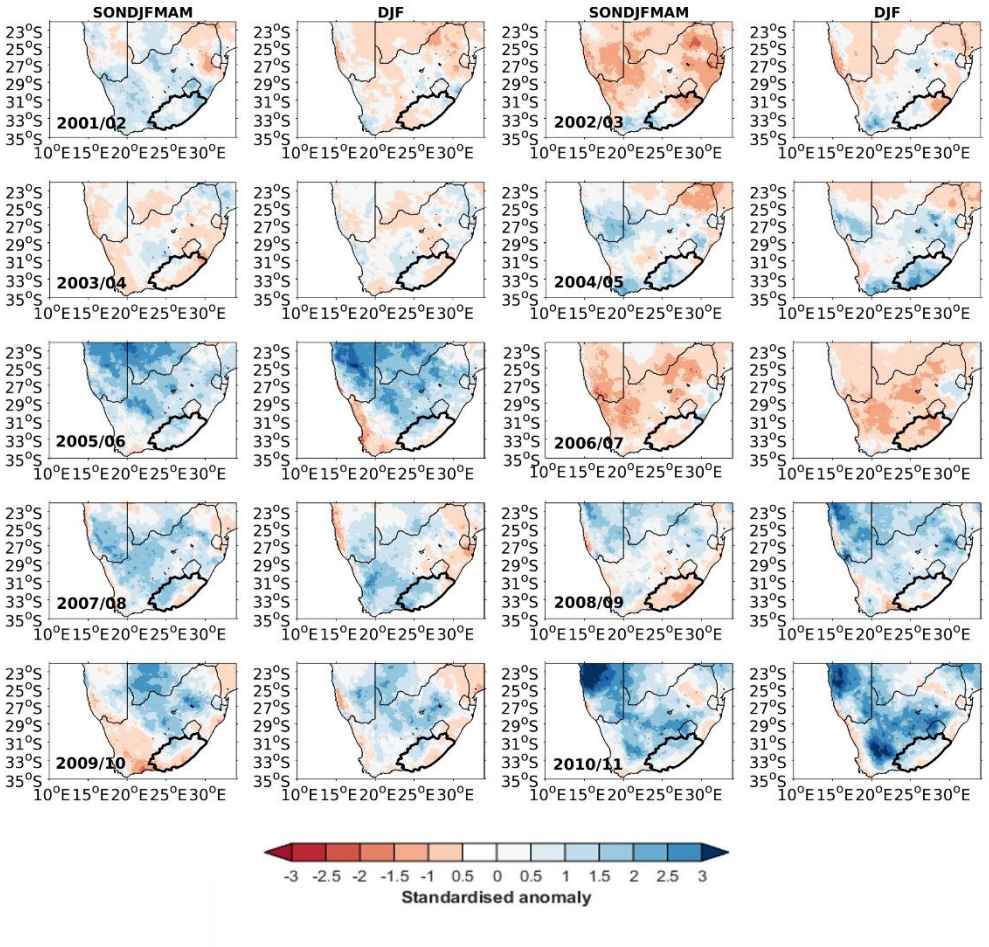

B.7: Same as **B.5**, but for 2002-2011.

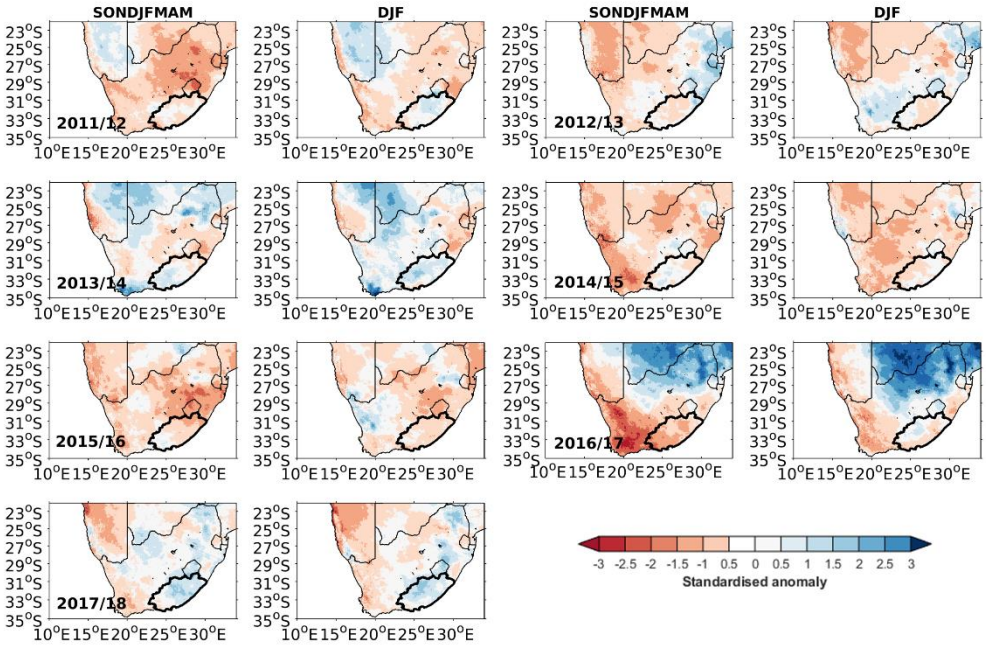

B.8: Same as **B.5**, but for 2012-2018.